

CONDITION-AWARE DISTRIBUTION NETWORK RECONFIGURATION VIA
MULTI-STAGE OPTIMIZATION FRAMEWORK

A THESIS SUBMITTED TO
THE GRADUATE SCHOOL OF NATURAL AND APPLIED SCIENCES
OF
MIDDLE EAST TECHNICAL UNIVERSITY

BY

ARASH MOHAMMADI VANIAR

IN PARTIAL FULFILLMENT OF THE REQUIREMENTS
FOR
THE DEGREE OF MASTER OF SCIENCE
IN
ELECTRICAL AND ELECTRONICS ENGINEERING

MAY 2025

Approval of the thesis:

**CONDITION-AWARE DISTRIBUTION NETWORK RECONFIGURATION
VIA MULTI-STAGE OPTIMIZATION FRAMEWORK**

submitted by **ARASH MOHAMMADI VANJAR** in partial fulfillment of the requirements for the degree of **Master of Science in Electrical and Electronics Engineering Department, Middle East Technical University** by,

Prof. Dr. Naci Emre Altun
Dean, Graduate School of **Natural and Applied Sciences** _____

Prof. Dr. İlkay Ulusoy
Head of Department, **Electrical and Electronics Engineering** _____

Prof. Dr. Murat Göl
Supervisor, **Electrical-Electronics Engineering, METU** _____

Examining Committee Members:

Prof. Dr. Ali Nezih Güven
Department of Electrical and Electronics Engineering, TEDU _____

Prof. Dr. Murat Göl
Department of Electrical and Electronics Engineering, METU _____

Assist. Prof. Dr. Keyvan Firuzi
Department of Electrical and Electronics Engineering, METU _____

Date: 12.05.2025

I hereby declare that all information in this document has been obtained and presented in accordance with academic rules and ethical conduct. I also declare that, as required by these rules and conduct, I have fully cited and referenced all material and results that are not original to this work.

Name, Surname: Arash Mohammadi Vaniar

Signature :

ABSTRACT

CONDITION-AWARE DISTRIBUTION NETWORK RECONFIGURATION VIA MULTI-STAGE OPTIMIZATION FRAMEWORK

Mohammadi Vaniar, Arash

M.S., Department of Electrical and Electronics Engineering

Supervisor: Prof. Dr. Murat Göl

May 2025, 90 pages

Distribution Network Reconfiguration (DNR) is one of the important techniques for enhancing the efficiency and flexibility of electrical distribution networks (DNs). DNR can significantly reduce power losses and improve voltage profiles by dynamically changing the network topology. This thesis presents a three-stage optimization framework for DNR, integrating topology optimization and reactive power compensation to enhance operational efficiency. The first stage, termed Reconfiguration of Tie-Line Switches (RTLS), employs a Particle Swarm Optimization (PSO) algorithm enhanced with Depth-First Search (DFS) algorithm to identify radial network topologies that minimize active power losses. Upon identifying a feasible topology, the network configuration is updated and passed to the second stage, termed Shunt Capacitor Sizing (SCS). In the SCS stage, another PSO algorithm is used to determine the optimal capacitor deployment at predefined locations. Once optimal reactive power injections are determined, the third stage re-applies the RTLS, now considering the updated load model. This final stage evaluates whether a further improvement in active power loss is achievable. If the third stage identifies a better radial topology, its results are adopted; otherwise, the solution from the second stage is finalized. This

stepwise and feedback-driven approach ensures both topological efficiency and voltage support, providing a robust and scalable method for DNR in modern power DNs. This study is validated by using two well-established test cases: the IEEE 33-bus system and the IEEE 123 Feeder system. In addition, the proposed methodology is tested on a 7-bus case for further investigation. Five distinct scenarios were examined to evaluate the robustness and applicability of the proposed methodology under various operating conditions: heavily loaded network, lightly loaded network, normal loading conditions, poor power factor (PF), and good PF cases. Results demonstrate significant reductions in active power losses and enhanced voltage profiles.

Keywords: Distribution Network Reconfiguration (DNR), Multi-Stage Optimization Framework, Particle Swarm Optimization (PSO), Tie-Line Switches, and Shunt Compensation.

ÖZ

ÇOK AŞAMALI OPTİMİZASYON ÇERÇEVESİ ARACILIĞIYLA DURUM FARKINDA DAĞITIM AĞI YENİDEN YAPILANDIRMASI

Mohammadi Vaniar, Arash

Yüksek Lisans, Elektrik ve Elektronik Mühendisliği Bölümü

Tez Yöneticisi: Prof. Dr. Murat Göl

Mayıs 2025 , 90 sayfa

Dağıtım Şebekesi Yeniden Yapılandırması (DNR), elektrik dağıtım şebekelerinin (DN'ler) verimliliğini ve esnekliğini artırmak için önemli tekniklerden biridir. DNR, şebeke topolojisini dinamik olarak değiştirerek güç kayıplarını önemli ölçüde azaltabilir ve voltaj profillerini iyileştirebilir. Bu tez, operasyonel verimliliği artırmak için topoloji optimizasyonu ve reaktif güç kompanzasyonunu entegre eden DNR için üç aşamalı bir optimizasyon çerçevesi sunmaktadır. Bağlantı Hattı Anahtarlarının Yeniden Yapılandırılması (RTLS) olarak adlandırılan ilk aşama, aktif güç kayıplarını en aza indiren radyal ağ topolojilerini belirlemek için Derinlik Öncelikli Arama (DFS) ile geliştirilmiş bir Parçacık Sürüsü Optimizasyonu (PSO) algoritması kullanır. Uygulanabilir bir topoloji belirlendikten sonra, ağ yapılandırması güncellenir ve Şönt Kapasitör Boyutlandırma (SCS) olarak adlandırılan ikinci aşamaya geçilir. SCS aşamasında, önceden tanımlanmış konumlarda optimum kapasitör dağıtımını belirlemek için başka bir PSO algoritması kullanılır. Optimum reaktif güç enjeksiyonları belirlendikten sonra, üçüncü aşama RTLS'yi güncellenmiş yük modelini dikkate alarak yeniden uygular. Bu son aşamada aktif güç kaybında daha fazla iyileşme sağlanıp sağlanamayacağı de-

ğerlendirilir. Üçüncü aşama daha iyi bir radyal topoloji tanımlarsa, sonuçları benimser; aksi takdirde, ikinci aşamadaki çözüm sonlandırılır. Bu aşamalı ve geri bildirim odaklı yaklaşım, modern güç dağıtım sistemlerinde DNR için sağlam ve ölçeklenebilir bir yöntem sağlayarak hem topolojik verimlilik hem de voltaj desteği sağlar. Bu çalışma, iki köklü test örneği kullanılarak doğrulanmıştır: IEEE 33-bus sistemi ve IEEE 123 Feeder sistemi. Buna ek olarak, önerilen metodoloji daha fazla araştırma için 7 baralı bir vaka üzerinde test edilmiştir. Önerilen metodolojinin çeşitli çalışma koşulları altında sağlamlığını ve uygulanabilirliğini değerlendirmek için beş ayrı senaryo incelendi: ağır yüklü ağ, hafif yüklü ağ, normal yükleme koşulları, zayıf güç faktörü (PF) ve iyi PF durumları. Sonuçlar, aktif güç kayıplarında ve gelişmiş gerilim profillerinde önemli azalmalar olduğunu göstermektedir.

Anahtar Kelimeler: Dağıtım Ağının Yeniden Yapılandırılması, Çok Aşamalı Optimizasyon Çerçevesi, Particle Swarm Optimizasyon (PSO), Bağlantı Hattı Anahtarları, Şant Telafisi.

To my beloved family.

ACKNOWLEDGMENTS

I would like to extend my gratitude and respect to Professor Murat Göl, my supervisor, for his guidance, kind support, and encouragement throughout my MSc studies. Also, this study was supported by the Scientific and Technological Research Council of Turkey (TUBITAK) under the Grant Number 221N132. I thank TUBITAK for their support.

TABLE OF CONTENTS

ABSTRACT	v
ÖZ	vii
ACKNOWLEDGMENTS	x
TABLE OF CONTENTS	xi
LIST OF TABLES	xiv
LIST OF FIGURES	xvi
ABBREVIATIONS	xx
CHAPTERS	
1 INTRODUCTION	1
1.1 Literature Review	2
1.2 Contribution of the Thesis	6
1.3 Motivation and Problem Definition	9
1.4 Chapter Summary	12
2 THE PROPOSED METHOD	15
2.1 AC Power Flow Formulation	17
2.2 Depth-First Search (DFS)	20
2.3 Formulation of the Proposed Three-Stage Method	21
2.4 Solution Procedure	24

2.4.1	Data Loading and Initialization	24
2.4.2	First Stage: Reconfiguration of Tie-Line Switching (RTLS)	24
2.4.3	Second Stage: Shunt Capacitor Sizing (SCS)	25
2.4.4	Third Stage: Feedback-Aware Structure	26
2.4.5	Integration of the Three Stages	27
2.5	Chapter Summary	31
3	CASE STUDY AND NUMERICAL RESULTS	33
3.1	Case Study	33
3.2	Numerical Results	35
3.2.1	Case 1 Results	36
3.2.1.1	Normal Loading	36
3.2.1.2	Heavy Loading	38
3.2.1.3	Light Loading	42
3.2.1.4	Extended Light Loading	45
3.2.1.5	Poor PF	45
3.2.1.6	Good PF	50
3.2.2	Case 2 Results	53
3.2.2.1	Normal Loading	54
3.2.2.2	Heavy Loading	56
3.2.2.3	Extended Heavy Loading	58
3.2.2.4	Light Loading	61
3.2.2.5	Poor PF	62
3.2.2.6	Good PF	64

3.2.3	Case 3 - 7-bus system	68
3.2.4	Comparison of the Proposed Method	70
3.3	Chapter Summary	72
4	CONCLUSION	75
	REFERENCES	79
	APPENDICES	89
A	Branch Index for Case 1	89
B	Branch Index for Case 2	90

LIST OF TABLES

TABLES

Table 3.1 Proposed three-stage DNR method's results for Case 1 under normal loading conditions	37
Table 3.2 Proposed three-stage DNR method's results for Case 1 under heavy loading conditions	40
Table 3.3 Proposed three-stage DNR method's results for Case 1 under light loading conditions	45
Table 3.4 Proposed three-stage DNR method's results for Case 1 under light loading conditions - Extended	46
Table 3.5 Proposed three-stage DNR method's results for Case 1 under poor PF conditions	49
Table 3.6 Proposed three-stage DNR method's results for Case 1 under good PF conditions	53
Table 3.7 Summary of results for Case 1 under all loading scenarios	53
Table 3.8 Proposed three-stage DNR method's results for Case 2 under normal loading conditions	56
Table 3.9 Proposed three-stage DNR method's results for Case 2 under heavy loading conditions	58
Table 3.10 Proposed three-stage DNR method's results for Case 2 under light loading conditions	62

Table 3.11 Proposed three-stage DNR method's results for Case 2 under poor PF conditions	64
Table 3.12 Proposed three-stage DNR method's results for Case 2 under good PF conditions	66
Table 3.13 Summary of Results for Case 2 under all loading scenarios	68
Table 3.14 Comparison of the proposed method with recent methods in terms of power loss reduction and minimum voltage for Case 1	72
Table A.1 Branch indexing table for Case 1	89
Table B.1 Branch indexing table for Case 2	90

LIST OF FIGURES

FIGURES

Figure 1.1	Power system model [1]	10
Figure 3.1	Topology of case 1 with specified tie-line switches	35
Figure 3.2	Topology of case 2 with specified tie-line switches	36
Figure 3.3	RTLS stage results under normal loading for Case 1	39
Figure 3.4	SCS stage results under normal loading for Case 1	40
Figure 3.5	Third stage results under normal loading for Case 1	41
Figure 3.6	RTLS stage results under heavy loading for Case 1	42
Figure 3.7	SCS stage results under heavy loading for Case 1	43
Figure 3.8	Third stage results under heavy loading for Case 1	44
Figure 3.9	RTLS stage results under light loading condition for Case 1	46
Figure 3.10	SCS stage results under light loading condition for Case 1	47
Figure 3.11	RTLS stage results under light loading condition for Case 1 - Extended	48
Figure 3.12	SCS stage results under light loading condition for Case 1 - Ex- tended	49
Figure 3.13	RTLS stage results under poor PF condition for Case 1	50
Figure 3.14	SCS stage results under poor PF condition for Case 1	51

Figure 3.15	Third stage results under poor PF condition for Case 1	52
Figure 3.16	RTLS stage results under good PF condition for Case 1	54
Figure 3.17	SCS stage results under good PF condition for Case 1	55
Figure 3.18	RTLS stage results under normal loading for Case 2	57
Figure 3.19	SCS stage results under normal loading for Case 2	58
Figure 3.20	RTLS stage results under heavy loading for Case 2	59
Figure 3.21	SCS stage results under heavy loading for Case 2	60
Figure 3.22	Third stage results under heavy loading for Case 2	61
Figure 3.23	RTLS stage results under light loading for Case 2	63
Figure 3.24	SCS stage results under light loading for Case 2	64
Figure 3.25	RTLS stage results under poor PF condition for Case 2	65
Figure 3.26	SCS stage results under poor PF condition for Case 2	66
Figure 3.27	Third stage results under poor PF condition for Case 2	67
Figure 3.28	RTLS stage results under good PF condition for Case 2	68
Figure 3.29	SCS stage results under good PF condition for Case 2	69
Figure 3.30	Topology of the 7-bus case	70
Figure 3.31	Voltage magnitude and angle profiles for 7 bus case	71

List of Algorithms

1	Pseudo-code for the proposed methodology	30
---	--	----

ABBREVIATIONS

DN	Distribution Network
DNR	Distribution Network Reconfiguration
RES	Renewable Energy Resources
PV	Photovoltaic
PF	Power factor
DSO	Distribution System Operator
PSO	Particle Swarm Optimization
DFS	Depth First Search
RTLS	Reconfiguration of Tie-Line Switch
SCS	Shunt Capacitor Sizing
HC	Hosting Capacity
GA	Genetic Algorithm
LMR	Loss Minimum Reconfiguration
HLF	Harmonic Load Flow

CHAPTER 1

INTRODUCTION

Distribution Network Reconfiguration (DNR) is crucial for enhancing the resilience and efficiency of modern power grids, especially as the integration of small-scale Distributed Energy Resources (DERs) continues to grow. Although DERs-penetrated grids are beneficial in terms of transitioning to net-zero and sustainable grids [2], this integration introduces new complexities to distribution networks (DNs). Traditional centralized generations of the power grids have changed by the intermittent and dispersed allocation of DERs. This geographical change in the power grids can lead to sudden power flow fluctuations, which may exceed the overall capacity of the grid. In addition, the bidirectional power flow capability of various DERs, like solar photovoltaic (PV) systems, corresponds to voltage rise challenges during low demand and high generation intervals. Integrating DERs into DNs is reshaping the modern power grid by ushering in enhanced efficiency, resilience, and sustainability. DERs, typically small-scale generation units installed near consumption points, significantly reduce reliance on traditional centralized power plants, thereby minimizing transmission losses and alleviating stress on transmission infrastructure. Furthermore, their proximity to end-users ensures improved grid reliability and provides essential backup power during outages, significantly reducing service interruptions and enhancing overall power quality [3]. While DERs offer many benefits, their high penetration can negatively impact power quality, presenting challenges to grid reliability. A DN may face higher power losses, reductions in voltage profiles, and unbalanced loads while the power is being transformed from substations to the consumer side [4]. These challenges underscore the need for effective DNR strategies to adapt the network topology to these dynamic operating conditions. DNR, by changing the network topology, provides a flexible and cost-effective solution to mitigate the chal-

lenges posed by DER integration. By changing the switch status of tie-line switches, DNR effectively reduces active and reactive power losses, improves voltage profiles, and ultimately enables smoother DER integration. Also, DNR can effectively enhance the hosting capacity of the network. Therefore, high penetration of renewable energy sources (RESs) can be integrated within the network without violating the operational limits [5].

In addition, implementing DNR arises from its significant potential to enhance flexibility services provided by Distribution System Operators (DSOs). DNs often face dynamic operating conditions, such as periods of dense congestion, unexpected load spikes, or rapid changes in DERs' output. In such scenarios, network operators must quickly and effectively respond to maintain grid stability, power quality, and reliability. DNR can be a solution that can swiftly adapt network topologies to alleviate congestion and redistribute power flows, mitigating the risks of overload conditions and voltage deviations. By utilizing DNR, DSOs gain a robust tool to manage real-time operational challenges without necessarily resorting to expensive grid expansions or investments in additional infrastructure. Thus, DNR not only enhances operational flexibility and network resilience but also provides economic advantages by efficiently managing existing assets and deferring costly upgrades [6].

1.1 Literature Review

DNR is proposed for a meshed DN using the second law of Kirchhoff in 1975 to find an optimal topology that results in minimum active power flow results [7]. A compensation-based power flow technique is proposed in [8] to minimize the line losses in DNs. In [9], a mathematical model is introduced for utilizing feeder reconfiguration to balance load and reduce power losses by using a search method over radial configurations considering power flow approximations [10]. In [11], a genetic algorithm (GA) approach is applied to the loss minimum reconfiguration (LMR) problem for the open-loop radial DNs, where the considered LMR problem is formulated as a mixed integer programming problem, which is validated through numerical examples. In [12], a simulated annealing technique is developed for the network reconfiguration problem (NRP) for loss reduction in DNs by utilizing simplified line

flow equations. A meta-heuristic optimization algorithm, based on heap data structures, is presented in [13] to enhance voltage profiles and minimize power losses in DNs. Reference [14] introduces an approach to optimal NRP for DNs using a moderated Shark Smell optimization algorithm, which seeks to improve system reliability and voltage stability while reducing power losses.

The intermittent nature of RESs becomes more difficult when considering the topology changes of the DNs due to the solutions of the DNR problem since the act of reconfiguration affects the operation parameters of the grid, which include switching status of tie-line switches, ramp-up and down indices for the backup power. To have a reliable and feasible solution for the DNR, AC power flow equations are recommended to be used [15, 16, 17], which reflect physics-based behavior of the electrical grid for real-world applications for the DN operation. Considering the continuous variables inherent in the AC power flow equations and considering the binary variables corresponding to the status of tie-line switches renders the DNR problem a MINLP problem, which makes it difficult to solve. In order to solve this resultant DNR problem, multiple approaches based on mathematical and heuristic methods are proposed in the literature. The optimization techniques involve stochastic optimization [18], deterministic optimization [19], second-order cone programming [20, 21], robust optimization [22], branch-and-bound approach [23], and model predictive control [24]. In addition, various heuristic approaches that are mainly based on search algorithms are developed and proposed in the literature to solve the DNR problem, which includes Genetic Algorithm (GA) [25], modified PSO [26], θ -bat algorithm [27], branch current matrix-based method [28], and Firefly method [29].

In [30], a non-iterative harmonic load flow (HLF) method is implemented to address power quality metrics in DNs. The paper highlights the application of this method to a capacitor-compensated NRP, demonstrating faster and more comprehensive results than traditional HLF approaches. Reference [31] explores the application of DNR to improve power quality metrics and minimize losses of power in DNs by utilizing a discrete PSO to achieve the objectives. In [32], the application of DNR is assessed to resolve power quality metrics arising from variable loads. A discrete PSO approach is employed to formulate the optimization problem that minimizes voltage flicker levels and improves voltage profiles while also considering the objectives of the DNR.

A feeder reconfiguration strategy for RES-integrated DNs is proposed in [33] using Ant Lion optimization method. The approach aims to minimize total operational costs while considering both balanced and unbalanced NRP and uncertainties associated with RESs. In [34], a Selective Bat model is developed for balanced and unbalanced DNR with fluctuating power demands. This method aims to minimize active power losses in DNs. Initial tests on balanced networks demonstrate its effectiveness across varying demand levels, while subsequent trials on unbalanced networks explore the impact of voltage and current imbalances on the DNR solutions. Reference [35] presents an improved PSO method to solve the dynamic DNR problem. This approach optimizes grid performance by considering the integration of energy storage systems, diverse RESs, and fluctuating electricity prices and load demands. The algorithm's effectiveness is demonstrated on the IEEE 95-node test system, comparing its advantages with other evolutionary algorithms.

In [36], a mixed PSO technique is proposed that combines a binary PSO for optimal switching configuration and conventional PSO for DG placement and sizing. A hybrid PSO–ACO algorithm is presented in [37] for optimal DNR considering the time-varying nature of load and the integration of DG resources. The approach, validated on the IEEE 33-bus system, aims to minimize power losses and improve voltage profiles, demonstrating both accuracy and computational efficiency. Authors in [38] addressed the DNR problem by optimizing active power losses and reliability index using PSO, GA, and exhaustive search methods. Applied to the IEEE 33-bus network, the PSO-based method proved effective in improving system reliability and voltage profiles and reducing computational time under operational constraints. The authors develop a PSO-based optimization framework in [39] to jointly determine switching configurations and optimal DG sizes, aiming to reduce active power losses and enhance voltage profiles. Simulation results on the IEEE 33-bus system confirm the effectiveness of the method compared to GA-based approaches. A PSO algorithm for radial network reconfiguration in distribution systems is developed in [40] to reduce active power losses and voltage deviations, which is tested on the IEEE 33-bus network. In [41], a Harmony Search Algorithm (HSA) is developed to optimize both network reconfiguration and DG placement to minimize real power losses and enhance voltage profiles. The method, validated on IEEE 33- and 69-bus systems at

multiple load levels, incorporates voltage and current constraints and demonstrates good performance across various scenarios.

In [42], a stochastic scenario-based framework is proposed to optimize both scheduling problem and DNR in RES-integrated microgrids (MGs). This framework accounts for uncertainties related to generation units and electrical demand patterns. It aims to minimize active power losses and operational costs while maximizing the stability index of voltage. The proposed model is validated on a 33-bus MG, demonstrating its effectiveness in optimizing objective functions. In [43], an optimization approach is advanced for switching of tie-lines in reconfigurable MGs to minimize operational costs. This approach accounts for MG uncertainties for the presence of electric vehicles (EVs). Reference [44] is proposed to implement a framework for simultaneously hourly-based NRP and scheduling problem in advanced DNs using a PSO approach. This framework aims to reduce operational costs by including the demand response program and cost of protection devices. The proposed methodology is validated on the IEEE 33-bus distribution test system, considering different price-based DRP actions and their impact on system load profiles. In [45], a dynamic DNR of DNs is analyzed for cost savings over different time scales using switch replacement to find the optimal frequency of switching.

In [46], authors proposed a multi-objective optimization approach that combines dynamic DNR with power electronic-based switches to maximize HC while accounting for load uncertainty. In [47], an optimization framework is implemented for DNR to maximize HC in DNs, facilitating the integration of RESs while addressing the uncertainties associated with RESs and load variability. The proposed approach is validated on standard IEEE 33-bus and IEEE 69-bus DNs, demonstrating its effectiveness in maximizing HC. In [48], a mathematical framework is presented to enhance the HC of DNs by finding optimized allocation of distributed generation capacity, DNR problem, and control of on-load tap changer for voltage stabilization. The proposed methodology is tested on the IEEE 33-bus test network, and results revealed the effective management of active power across the network. Also, references [49] and [50] investigated the DNR for the unbalanced operation of the DNS, in which 12 and 25% reductions in active power losses are reported, respectively. In [51], the authors presented an optimization framework for the operation of DNs, integrating photovoltaics

with STATCOM devices and network reconfiguration. The methodology was tested only on the IEEE 33-bus system.

1.2 Contribution of the Thesis

Existing approaches to DNR in the literature often suffer from limitations that reduce their applicability in real-world, large-scale DNs. One of the most significant issues is the over-simplification of power flow models. Many DNR formulations rely on linear or approximate models, such as DC power flow or linearized AC models, to improve computational tractability. However, these simplifications neglect the non-linear nature of power flows, particularly in radial DNs where voltage drops, reactive power, and unbalanced loads are significant. As a result, the solutions obtained using such approximations may not be physically feasible or reliable when applied to actual networks. In addition to modeling simplifications, exact optimization methods that incorporate full AC power flow equations—such as Mixed-Integer Nonlinear Programming (MINLP) formulations—face significant scalability issues. These methods are accurate but computationally expensive and often impractical for medium to large-scale networks due to the exponential growth in binary variables and nonlinear constraints. This complexity results in longer computation times, convergence difficulties, and increased sensitivity to solver parameters, limiting their use in time-sensitive or real-time applications. To circumvent these computational barriers, many researchers have turned to heuristic and metaheuristic methods such as GA, PSO, Ant Colony Optimization, and other methods. While these techniques are flexible and capable of handling non-convex problems, they lack a guarantee of global optimality and are inherently stochastic. The quality of the solution often depends heavily on the choice of algorithm parameters, initial conditions, and the structure of the search space. For instance, PSO parameters such as inertia weight and social and behavioral coefficients should be selected with great attention. Moreover, heuristic-based solutions are not always reproducible and may lead to sub-optimal or inconsistent results, particularly under strict operational constraints or changing network conditions. Another fundamental limitation lies in the use of single-stage optimization frameworks. In these formulations, the search for an optimal network topology and the satisfaction

of operational objectives, such as loss minimization or voltage profile improvement, are attempted simultaneously. This coupling of topology identification with complex objective functions often leads to infeasible or sub-optimal solutions, especially when the objectives conflict with topological constraints like radiality. Ensuring radial operation, a critical requirement for DNs, is a non-trivial challenge that is either oversimplified or overconstrained in many single-stage models, further compounding the problem.

These limitations highlight the need for a more robust and scalable approach. This thesis proposes a robust and scalable three-stage optimization framework for DNR, integrating network topology optimization with reactive power support to achieve significant improvements in operational efficiency and voltage quality. The first stage, termed Reconfiguration of Tie-Line Switches (RTLS), focuses on identifying an optimal radial network topology that minimizes active power losses. This is accomplished through a PSO algorithm combined with a DFS mechanism. The DFS is integrated into the PSO process to ensure that only radial configurations are considered feasible, thereby satisfying the structural requirements of DNs and hence contributing to the computational efficiency. In cases where the generated configurations violate radiality, the fitness function is penalized, and the PSO continues its search until a valid radial topology is found or the iteration limit is reached. Once a feasible and loss-minimizing topology is determined, the network's switch statuses are updated accordingly, forming the input for the subsequent stage. The second stage performs Shunt Capacitor Sizing (SCS) based on the topology obtained from the first stage. This stage aims to further improve voltage profiles and compensate for the reactive power by optimally allocating reactive power support through shunt capacitors. The sizing process is executed using a separate PSO algorithm. To comply with practical deployment constraints, the capacitors are treated in a binary fashion: if the optimized sizing result for a capacitor is equal to or exceeds 50% of its full-rated capacity, the capacitor is fully deployed; otherwise, it is set to zero. This binary logic ensures that the capacitor control strategy remains implementable without relying on complex step-size tuning or partial activation mechanisms. The outcome of this stage updates the reactive power injections across the network and prepares the model for further evaluation. The third stage reinitiates the RTLS process using the

updated reactive power profile from the second stage. This feedback mechanism is implemented to assess whether the new reactive injections enable a more loss-efficient switching configuration. The third stage follows the same DFS-PSO approach used in the first stage, ensuring radiality while seeking additional reductions in active power losses. A comparative evaluation is performed between the total active power losses of the second and third stages. If the third stage identifies a configuration that outperforms the second-stage solution, its result is accepted as the final configuration; otherwise, the model retains the second-stage outcome. This conditional evaluation ensures that no unnecessary switching operations are introduced unless a tangible performance improvement is achieved. Overall, this thesis contributes a practical and technically grounded framework that unifies topological reconfiguration and reactive power compensation into a sequential, feedback-aware optimization pipeline. In addition, AC power flow equations are incorporated within the optimization process, which ensures realistic results and provides reliable insights applicable to real-world implementations. The proposed methodology is validated using two benchmarks: the IEEE 33-bus and the IEEE 123 Feeder systems. Sometimes, the network topology might be in an optimum state in terms of switch configuration. To this end, a 7-bus case is implemented to evaluate the proposed methodology in such cases. To further assess the applicability and robustness of the proposed method under diverse operating conditions, five distinct scenarios were evaluated: heavily loaded, lightly loaded, normal loading, poor PF, and good PF. These cases simulate practical variations in demand and reactive power conditions that DNs often encounter. The results across these conditions consistently validated the method's adaptability, demonstrating its capability to enhance performance even under stressed or atypical network states. The proposed methodology makes a significant contribution to the DNR problem by providing a robust, automated solution that enhances both the technical and economic performance of DNs. The key contributions of this thesis are summarized as follows:

- Proposed a three-stage optimization framework for the DNR problem.
- Integration of DFS into a binary PSO algorithm in the first stage to efficiently generate and validate feasible radial configurations while minimizing active power losses.

- Established a feedback-aware loop by reapplying RTLS in the third stage after updating the reactive power profile from the SCS stage to evaluate whether further active power loss reduction can be achieved.
- Demonstrated the applicability of the proposed methodology under diverse operating conditions by testing five practical scenarios: heavily loaded, lightly loaded, normal loading, poor PF, and good PF.
- Implemented extended cases for light loading and heavy loading scenarios for further analysis.
- Ensured modeling accuracy by incorporating full AC power flow equations in all stages of the optimization to avoid the inaccuracies introduced by linearized or simplified power flow models.
- Validated the approach using benchmark systems, including both the IEEE 33-bus and 123-bus feeders, demonstrating the scalability and effectiveness of the proposed methodology in practical scenarios.

1.3 Motivation and Problem Definition

Figure 1.1 illustrates a typical power system model involving transmission and distribution sides. The traditional power generation and transmission system can be seen on the left side of the figure, which represents centralized power plants with high-voltage lines delivering electricity over long distances. Contingencies can be a threat that could lead to a potential disruption of power delivery to the DN. These contingencies include short-circuit faults, open-circuit faults, ground faults, and over-voltage faults. These faults can originate from lightning strikes, equipment failure (e.g., insulator flashover, transformer failure, blown fuse), weather conditions (e.g., trees falling on lines, ice accumulation), animal contact, and faults in other parts of the system [52]. In addition, the right side of the figure showcases a DN equipped with multiple DERs like solar panels and mini-wind turbines. The depicted DN has multiple switches represented by red circles. Control signals for managing the DN operation are marked with blue dashed lines originating from the control center. The red lines indicate communication links that inform the control center about the status

of the switches. As it can be seen, once there is a fault in the transmission network, electrical power can no longer be distributed to the DN.

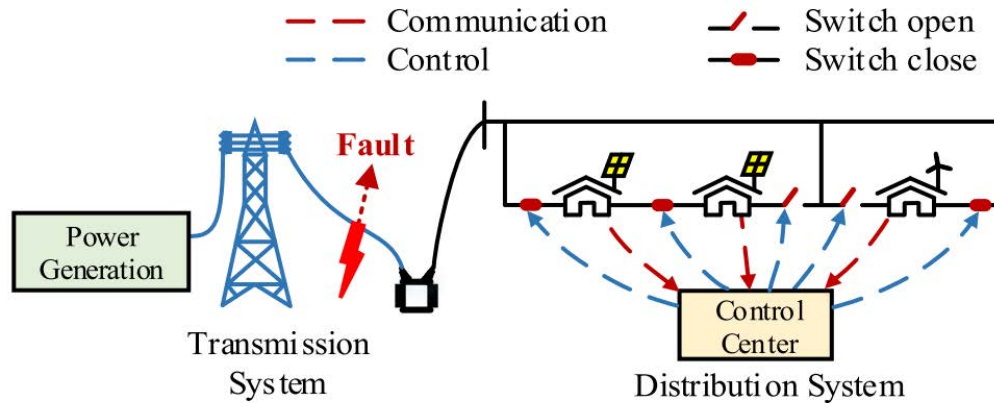


Figure 1.1: Power system model [1]

The ability to remotely control the status of tie-line switches, open or close, is the essence of DNR within a DN. The control center can effectively send commands to open or close the switches to have an optimal topology in the event of disruptions or contingencies in order to satisfy the pre-defined objectives of the distribution operator. Having isolated faulty sections, restoring the power to the affected areas, and optimizing power flow to minimize the active and reactive power losses and maintain voltage stability are some of the major benefits of DNR. DER integration brings an additional layer of complexity and opportunity to the utilization of DNR, in which control signals can manage the coordination of DERs by considering the resultant network topology from the DNR [53]. Also, the hosting capacity of the network can be increased in this approach, which translates to more greener and net-zero power generation from renewables.

A solid understanding of the fundamentals of power systems is essential for implementing effective DNR strategies. DNR primarily aims to reduce active power losses and improve voltage profiles by altering the topology of DNs through tie-line switching, which is also considered as one of the flexibility services by the DSO. While the main focus of this thesis is the optimization of these aspects, it is important to highlight that DNR can also contribute positively to reactive power compensation and voltage support as indirect benefits of the reconfiguration process. Although volt-

age stability is not the central focus of this research, it is worth noting that enhancing voltage profiles—achieved through optimal network topology and reactive power support—can indirectly improve the overall voltage stability of the DNs. For instance, voltage stability is closely linked to the ability of a power system to maintain acceptable voltage levels across all buses during normal operation and after disturbances. One of the key outcomes of DNR is a better-distributed load across the network, which can reduce stress on specific branches and improve voltage regulation throughout the grid. This, in turn, mitigates conditions that could otherwise lead to voltage instability and degraded system performance [54].

Reactive power deficiencies and voltage drops are often addressed in practice by deploying shunt capacitors, synchronous condensers, or static VAR compensators (SVCs) [55, 56, 57]. In the proposed two-stage DNR methodology, shunt capacitor sizing is integrated as the second optimization stage. Although its primary objective is to further reduce active power losses and enhance voltage profiles, it also contributes to reactive power balance and supports local voltage levels—both of which are crucial for system reliability. The importance of such capabilities has been underscored by past large-scale blackouts, including the 2019 South America blackout and the 2021 Texas power crisis. These events, while largely related to transmission-level or generation-side failures, underscore the broader motivation to enhance distribution system resilience and prevent widespread outages [58, 59]. Though such blackouts are beyond the scope of this thesis, they emphasize the value of tools like DNR in contributing to a more resilient, flexible, and robust grid. Ultimately, while the direct focus of this thesis remains on loss minimization and voltage profile improvement, the secondary benefits—including improved voltage support and reactive power distribution—highlight the broader relevance of DNR in supporting modern grid requirements. As power systems continue to evolve to accommodate DERs, smart control technologies, and carbon neutrality goals [60], methodologies like the one proposed here provide a scalable and practical solution to ensure efficient and resilient distribution network operation.

Additionally, During high peak power demand, lower generation, and contingencies in the distribution networks, DNR is considered one of the effective approaches for DSOs to take in order to have a resilient network operation. The status of on/off of the

tie-line switches are determined by solving the DNR problem. DNR problem is often treated as a mixed-integer non-linear programming (MINLP) since it does include binary and continuous variables corresponding to the status of switches, closed when it is 0, and 1 if it is open [1]. Hence, the DNR solution specifies which switches are to be opened/closed while satisfying the grid constraints and radiality of the network. The objectives of DNR include minimizing the active and reactive power, cost of load interruption, or often called Value of Lost Load (VoLL), cost of operating backup generators, and cost of the switching actions [61]. Furthermore, remote-control switches enable the DNR to be performed in an efficient manner. Even though current DNs do not benefit from these remote-control switches, in recent years, industry-based companies have their attention on developing these switches, like Siemens [62], S&C Electric Company [63], Schnieder Electric [64], Hublle Power Systems [65], G&W Electric [66], and Switched Source [67]. The proposed remote-control switches by these companies have common characteristics that include remote monitoring and control, high-speed fault isolation, and voltage regulation. By considering the impact of utilizing remote-control switches in future DNs, the adaptability, flexibility, and resiliency of the DNs are expected by considering the high penetration of DERs.

1.4 Chapter Summary

According to the above discussion, DNs face significant operational challenges due to rapidly increasing electricity demand, aging infrastructure, and the integration of intermittent DERs such as solar PV and wind generation. Traditional radial configurations of DNs, while simple, often lead to suboptimal operation, resulting in higher power losses, voltage violations, limited flexibility, and reduced reliability. Furthermore, the uncertain and variable nature of renewable generation exacerbates operational difficulties, making voltage management and power flow control increasingly challenging for DSOs. DNR aims to achieve various operational benefits, including improving voltage profiles, minimizing active and reactive power losses, balancing load among feeders, enhancing system reliability, and maintaining radial network structures. This can be achieved by modifying the topological structure of the DN by changing the status of open/close tie-line switches. Technically, minimizing active

power loss is crucial, as electrical energy losses in DNs due to conductor resistance lead to inefficiencies and higher operational costs. High active power losses reduce the efficiency of the power delivery and necessitate additional energy generation to meet demand. One of the technical approaches that DSOs take is to change the network topology to have an alternative path for electrical power flow that results in lower active power losses. This approach is done by experienced staff in a DSO organization, which has its own drawbacks. Furthermore, in heavily loaded or long lines of a DN, voltage profiles of the buses experience a drop as power flows from feeders to the load side. In these circumstances, uneven load distribution can also cause the lines and transformers to be overloaded, which ultimately leads to increased active and reactive power losses, reduced equipment lifespan, and potential reliability issues. To overcome these challenges, DNR backed up with shunt capacitors can be a promising solution to redistribute loads and balance the load among feeders and, hence, mitigate power quality metrics as well. To this end, a three-stage optimization framework is proposed in this thesis to address the DNR problem, which will result in reduced active power losses and improved voltage profiles.

CHAPTER 2

THE PROPOSED METHOD

This thesis presents a novel three-stage optimization framework for DNR, designed to enhance the operational efficiency, flexibility, and controllability of modern power DNs. The proposed method supports one of the technical approaches taken by a DSO by enabling a more adaptive and intelligent reconfiguration strategy, which can serve as a flexibility service to address network constraints, reduce losses, and maintain power quality in increasingly dynamic operating environments. The proposed approach addresses the limitations of conventional DNR methods, which often rely on simplified power flow models or heuristic techniques that may produce sub-optimal or infeasible solutions. In the first stage of the framework, a binary PSO algorithm, integrated with a DFS mechanism, is used to identify an optimal radial topology that minimizes active power losses. This combination ensures the generation of feasible radial configurations while maintaining computational efficiency. Once the optimal network topology is determined, the second stage employs another PSO algorithm with the updated topology to optimally size shunt capacitors, targeting the improvement of voltage profiles throughout the system. Following the completion of the second stage, the reactive power injections resulting from the optimized shunt capacitor settings are used to update the network model. The RTLS process is then re-executed in the third stage to search for a new radial topology that may yield lower active power losses than those achieved in the second stage. This feedback-aware structure enhances the robustness of the proposed methodology by enabling an additional layer of optimization. It reduces the likelihood of the solution being trapped in local minima and moves the overall performance closer to a globally optimal result. If the third stage successfully identifies a configuration that outperforms the second stage in terms of active power loss reduction, its results are adopted; otherwise, the

model retains the second-stage outcome as the final solution. To validate the proposed method's performance and reliability across varied operating conditions, five distinct scenarios were tested: heavily loaded, lightly loaded, normal loading, poor PF, and good PF. These cases represent realistic fluctuations in demand and reactive power typical of distribution systems. To this end, AC power flow equations are incorporated in three stages to ensure high modeling accuracy and realistic results.

In this chapter, the AC power flow equations, 2.1, with the formulation of the proposed two-stage methodology, 2.3, are presented. Equations (2.1) to (2.4) denote the AC power flow equations, which represent the system's steady-state operation in terms of voltages and currents. The objective function of the first and second stages of the problem, along with their constraints, are given by equations (2.6) to (2.9), respectively. Prior to problem formulation, the importance of the proposed methodology is outlined in terms of limitations of a single-stage DNR and its drawbacks as follows.

DNR is a critical operation in modern power systems, aiming to improve network performance by adjusting the topology through the changing of tie-line switches. At its core, DNR is performed to minimize power losses, improve voltage profiles, balance loads, and enhance overall system reliability. Traditional methods have approached DNR as a single-stage process, attempting to solve the complete set of technical and operational challenges simultaneously. However, this integrated approach often encounters significant hurdles, primarily due to the complexity of power system models that incorporate non-linear load flow equations, radiality constraints, and discrete switching actions. The inherent combinatorial nature of the reconfiguration problem frequently leads single-stage methods to converge on suboptimal solutions or become computationally burdensome, particularly as the size of the network increases.

In conventional single-stage DNR formulations, the optimization problem is modeled with a comprehensive objective function that typically combines multiple performance indices such as power losses, voltage deviations, and load imbalances. These formulations must respect a series of equality and inequality constraints that represent the physical laws governing power flow, along with operational limitations like thermal limits on feeders and voltage bounds at buses. The integration of these constraints

within a unified optimization framework results in a non-convex and highly complex search space. Consequently, algorithms designed to solve these problems—whether they are based on heuristic, metaheuristic, or exact methods—often suffer from issues related to convergence speed, computational cost, and the risk of getting trapped in local minima. These limitations become especially pronounced in large-scale DNs where the number of potential configurations grows exponentially with the number of switches and feeders.

The two-stage DNR approach proposed in this thesis is designed to overcome these challenges by decoupling the overall problem into two more manageable sub-problems. The first stage focuses on generating a diverse set of candidate configurations using a metaheuristic algorithm, binary-PSO. This method is particularly effective at handling the discrete nature of switching operations and can quickly identify a subset of promising configurations that meet the basic operational criteria, such as maintaining the radial structure of the network and satisfying connectivity requirements. Once a set of candidate configurations is identified by satisfying the networks' constraints, the second stage of the two-stage DNR method takes the updated topology as an input and further improves the voltage profiles. Additionally, the approach can be extended to consider reliability indices, load balancing requirements, and even economic factors such as the cost of switching operations, thereby offering a comprehensive tool for both planning and real-time operation of DNs.

Having the above detailed explanation in mind, the rest of the chapter includes the mathematical formulation for the proposed methodology.

2.1 AC Power Flow Formulation

AC power flow analysis, often simply called "power flow," is an important computational process that reveals the steady-state behavior of an electrical network under specific operating conditions. This analysis is important for power system engineers both in planning and real-time operations. Informed decisions regarding the placement and sizing of the new power plants and required transmission lines, along with additional infrastructure, are made to ensure the power supply of the future load ac-

ording to the power flow results. The current state of the grid is vital when it comes to ensuring the voltage levels of the busbars are in an acceptable range. Identifying the potential issues to prevent outages requires the current state of the grid to be known to the DSO, which can be calculated by solving the AC power flow considering the constraints of the grid. This analysis is the backbone of other analyses, such as generation dispatch, unit commitment, and optimal power flow [68].

The nonlinearity of AC power flow analysis stems from the voltage-current relation of reactive components, non-linear load characteristics, harmonics, power factor variations, transformer behavior, which is highly non-linear, and dynamics of control systems. The relations between various components are expressed in a matrix format for numerical solutions. Also, the complexity of AC power flow adds an additional burden to find optimal global solutions, which normally are represented in mixed integer non-linear programming frameworks. Additionally, linearization techniques are widely used in the literature to solve the resultant AC power flow equations. Due to the nonlinear nature of AC power flow equations, iterative-based methods are often used to solve these equations. Newton-Raphson [69], Gauss-Seidel [70], and fast decoupled power flow [71] methods are some of these iterative-based approaches. The input vector for these methods involves the information regarding network topology, bus-relevant data (e.g., active and reactive loads, generation, and voltage levels), and branch-relevant data (e.g., resistance and reactance impedance of lines, rating of lines to carry current, and etc.).

Voltage magnitudes and voltage angles of the buses, along with active and reactive power flows of the branches, are the result of solving AC power flow equations that provide a set of useful information regarding the system's current state. From the resultant output, active and reactive power losses and stability margins with other operating conditions that are useful for the DSO or transmission system operator (TSO) can be calculated. Some specialized software tools have been developed to ease the utilization of power flow analysis for engineers, like Matpower, PSSE, and OpenDSS. DSO or TSO rely on power flow analysis for operational planning, such as system stability analysis, load forecasting, day-ahead and intra-day scheduling problems, and contingency analysis. Power flow analysis helps these system operators identify and detect anomalies within the network and take preventive steps to avoid the failure of

the network [72]. Understanding the mathematical representation of AC power flow enables power system engineers to better design, operate, and optimize the power grid, which is provided in the following paragraphs.

The power flow problem for DNs can be formulated using the standard AC power flow equations [73]. The complex power injection is given by equation 2.1. Separating the real and imaginary parts, the active and reactive power flows are obtained by equations 2.2 and 2.3, respectively. To ensure safe and reliable operation of the DN, the voltage constraint is given by equation 2.4. The thermal limits of the distribution lines must be satisfied by the maximum allowable current of the lines, which is presented by equation 2.5.

$$S_i = V_i \sum_{k=1}^n V_k (G_{ik} + jB_{ik}) (\cos(\theta_i - \theta_k) + j \sin(\theta_i - \theta_k)) \quad \forall (i, k) \quad (2.1)$$

$$P_i = V_i \sum_{k=1}^n V_k (G_{ik} \cos(\theta_i - \theta_k) + B_{ik} \sin(\theta_i - \theta_k)) \quad \forall (i, k) \quad (2.2)$$

$$Q_i = V_i \sum_{k=1}^n V_k (G_{ik} \sin(\theta_i - \theta_k) - B_{ik} \cos(\theta_i - \theta_k)) \quad \forall (i, k) \quad (2.3)$$

Where, S_i , P_i , and Q_i are the complex power, active power, and reactive power injected at bus i , respectively. G_{ik} and B_{ik} are the conductance and susceptance of the line connecting bus i to bus k . Also, V_i/V_k and θ_i/θ_k are the voltage magnitude and angles at buses i and k , respectively. Furthermore, $|I_{ik}|$ and I_{ik}^{\max} represent the current magnitude and maximum allowable current on the line connecting buses i and k .

$$V_i^{\min} \leq |V_i| \leq V_i^{\max}, \quad \forall i \in \mathcal{B} \quad (2.4)$$

$$|I_{ik}| \leq I_{ik}^{\max} \quad \forall (i, k) \quad (2.5)$$

$$\text{rank}(\mathbf{A}_{ik}) = |\mathcal{N}| - 1 \quad (2.6)$$

For the problem formulation, equations 2.4 to 2.6 present the voltage, current, and radiality constraints that are modeled, where $|V_i|$ is the voltage magnitude at bus i , which is bounded by V_i^{\min} and V_i^{\max} as the lower and upper voltage limits, respectively. \mathcal{B} is the set of all buses in the network. To ensure the network remains radial (i.e., tree structure without loops), constraint 2.6 can be used as the spanning tree constraint to ensure that the number of branches is one less than the number of buses in the network. Where \mathbf{A}_{ik} is the adjacency matrix of the network that is initialized using the connectivity of the topology from branch data.

2.2 Depth-First Search (DFS)

Consider a distribution network represented as a graph $G = (V, E)$, where:

- V denotes the set of buses (nodes),
- E denotes the set of branches (edges).

Let $v_s \in V$ represent the root node (e.g., slack bus) from which the DFS traversal begins. By defining the following sets and indicators:

- Visited status indicator for each node v :

$$\text{Visited}(v) \in \{\text{True}, \text{False}\}, \quad \forall v \in V$$

- The adjacency set of each node v :

$$\text{Adj}(v) = \{u \mid (v, u) \in E\}$$

Initially, all nodes are set as unvisited:

$$\text{Visited}(v) \leftarrow \text{False}, \quad \forall v \in V$$

The DFS algorithm starting from a node v can be defined recursively as follows:

$$\text{DFS}(v) = \begin{cases} \text{Visited}(v) \leftarrow \text{True} \\ \text{For each node } u \in \text{Adj}(v) \text{ such that } \text{Visited}(u) = \text{False}, \\ \quad \text{DFS}(u) \end{cases}$$

DFS is utilized within the binary PSO in the first stage of the problem as a method of ensuring topological feasibility. After each particle within the PSO proposes a candidate network configuration, DFS verifies two crucial conditions: radiality and connectivity, which ensure no loops exist in the network, and confirms that every node in the DN is reachable from a predefined root node.

The DFS algorithm explores each branch of the network to its greatest depth before backtracking. Once the traversal completes, the feasibility check examines the visited status of all nodes. If all nodes are marked as visited exactly once, the configuration satisfies radiality and connectivity constraints. Conversely, if any node remains unvisited or a node is revisited during traversal, the configuration violates these constraints and is considered invalid. Incorporating DFS into PSO ensures that the optimization algorithm consistently explores only feasible, operationally sound solutions, significantly improving the efficiency and reliability of the reconfiguration process.

2.3 Formulation of the Proposed Three-Stage Method

This subsection presents the formulation of the proposed three-stage optimization problem. The goal is to minimize active power losses and enhance voltage profiles in a DN by performing RTLS and SCS. In the first stage of the problem, RTLS is applied using the developed PSO-DFS algorithm. The primary objective of the first stage is to find feasible radial configurations while minimizing the active power losses by determining the optimal switching state of tie-line switches.

The objective of the RTLS is to determine the optimal radial topology that minimizes the total active power losses in the DN. This is achieved by reconfiguring the network through the switching of candidate branches, whose status is encoded in a binary decision vector \mathbf{u} . The objective function of the RTLS stage is formulated as 2.7:

$$\min_{\mathbf{u}} \sum_{(i,j) \in \mathcal{E}_{\text{Lines}}} P_{L,ij}(\mathbf{u}) \quad (2.7)$$

Subject to: Equations (2.1) to (2.5)

Where:

- $\mathbf{u} = [u_1, u_2, \dots, u_n]$ is a binary vector indicating the status of candidate switches:
 - $u_k = 1$ indicates the switch on branch k is closed (line is energized),
 - $u_k = 0$ indicates the switch is open (line is de-energized).
- $P_{L,ij}(\mathbf{u})$ is the active power loss on line (i, j) as a function of the topology determined by \mathbf{u} ,
- $\mathcal{E}_{\text{Lines}}$ is the set of all distribution lines, including those with candidate switches.

The power loss on each branch is calculated using the AC power flow model as:

$$P_{L,ij} = R_{ij} \cdot \frac{P_{ij}^2 + Q_{ij}^2}{V_i^2} \quad (2.8)$$

Where R_{ij} is the resistance of the line (i, j) , P_{ij} and Q_{ij} are the active and reactive power flows on the line, and V_i is the voltage magnitude at node i . The optimization is subject to a set of constraints, which include AC power flow equations, thermal flow limitations of lines, and radiality constraints.

The second stage of the proposed method focuses on SCS, aiming to further improve the network's operational performance after topology reconfiguration. Given the fixed topology from the RTLS stage, this step optimally sizes a set of predefined shunt capacitors installed at candidate buses to minimize total active power losses and enhance the voltage profile across the DN. A binary decision logic is applied for the shunt capacitors: if the optimized sizing is greater than or equal to 50% of the full capacity, the capacitor is fully utilized; otherwise, it is deactivated. The objective function of the SCS is formulated as 2.9

$$\min_{\mathbf{u}, \mathbf{Q}_{\text{cap}}} \sum_{(i,j) \in \mathcal{E}_{\text{Lines}}} P_{L,ij}(\mathbf{u}, \mathbf{Q}_{\text{cap}}) \quad (2.9)$$

Subject to:

$$0 \leq Q_{\text{cap},i} \leq Q_{\text{cap},i}^{\max} \quad \forall i \quad (2.10)$$

and Equations (2.1) to (2.5)

Where:

- $\mathbf{Q}_{\text{cap}} = [Q_{\text{cap},1}, Q_{\text{cap},2}, \dots, Q_{\text{cap},m}]$ is the vector of reactive power injections from shunt capacitors installed at m candidate buses.
- $Q_{\text{cap},i}$ represents the reactive power injected by the capacitor at bus i , and $Q_{\text{cap},i}^{\text{max}}$ is its maximum allowed value.
- \mathbf{u} is the radial topology determined by the RTLS stage and treated as a fixed input in this stage.
- $P_{L,ij}(\mathbf{u}, \mathbf{Q}_{\text{cap}})$ is the power loss on line (i, j) considering the influence of capacitor sizing.

By injecting reactive power into the system, the shunt capacitors reduce the reactive power demand from upstream sources, which in turn decreases the total current in the lines and hence the resistive losses. Additionally, this reactive compensation leads to improved voltage profiles, especially at nodes located far from the substation. This stage ensures that the overall DN performance is enhanced by compensating the reactive power, following the reconfiguration determined in the first stage.

In the third stage, the RTLS process is re-executed using the network updated with the reactive power injections obtained from the second stage. The objective remains identical to that of the first stage, minimizing active power losses while ensuring a radial topology. The same DFS-PSO algorithm and AC power flow constraints are employed as described in Section 2.3. The key distinction in this stage lies in the feedback mechanism: the power flow model now reflects the improved voltage and reactive conditions resulting from the optimized shunt capacitor deployment. The third stage searches for a new switching configuration that yields lower active power losses than those achieved in the second stage. If such a configuration is found, the model proceeds with the third-stage result. Otherwise, the second-stage configuration is retained as the final solution.

2.4 Solution Procedure

This section presents the detailed steps of the two-stage distribution network reconfiguration (DNR) methodology, which is designed to minimize power losses and improve voltage profiles in a distribution system. In what follows, each step of the procedure is explained in detail, including the rationale behind the method, the computational techniques applied, and the expected outcomes at each stage.

2.4.1 Data Loading and Initialization

The optimization process begins by loading the data set that defines the DN under analysis. This includes the full network topology, specifying the connectivity between buses and the configuration of tie-lines (normally open switches). Electrical parameters such as line resistances, reactances, conductances, susceptances, and the active and reactive load demands at each bus are also loaded. Depending on the scenario, loading type and PFs may be modified to reflect varying operating conditions, such as heavy loading, light loading, normal loading, poor PF, and good PF. In addition to line and load data, candidate locations for shunt capacitors are specified based on system design. The algorithm then initializes PSO parameters, including the number of particles, maximum iterations, inertia weight bounds (w_{\max} , w_{\min}), and the social and cognitive acceleration coefficients (c_1 , c_2). These values are carefully tuned to balance exploration and exploitation across the three stages of the optimization. If specific operational constraints exist, such as lines that must remain energized or switches that are restricted from operating, these are incorporated into the initialization step as hard constraints.

2.4.2 First Stage: Reconfiguration of Tie-Line Switching (RTLS)

Once the data is loaded and all constraints are set, the first stage of the procedure, RTLS, begins. The objective of RTLS is to find an optimal radial topology for the considered DN that minimizes the active power losses. This step essentially involves deciding which tie-lines (normally open switches) should be closed and which normally

closed switches might be opened to restructure the network into a loss-minimizing configuration. In most DNs, the system is designed to be radially operated. However, under certain contingency or optimization scenarios, tie-lines can be closed to create temporary loops, allowing the network operator to transfer loads from one feeder to another. The challenge is to ensure that, after any switching action, the network remains in a radial structure. A value of 1 indicates a closed switch, while a value of 0 indicates an open switch. The set of these binary variables across all candidate switches forms the solution space for the DNR problem. During each iteration, the PSO algorithm evaluates the fitness of each candidate by calculating the power losses under the corresponding network topology and network loading type. If the solution violates any constraint, particularly the radiality constraint, the fitness function is penalized to discourage the algorithm from retaining or propagating infeasible topologies. After running the optimization for a specified number of iterations or until a convergence criterion is met, the best feasible solution(s) are extracted. A feasibility check is performed to ensure that the network remains radial and grid constraints are respected. If no feasible radial configurations are found within the maximum allowed iterations, the procedure penalizes the fitness function further or adjusts the algorithmic parameters and re-runs the RTLS step. If no solution is found, which translates to the optimal state of the topology at that time instant, then the model proceeds to the second stage, SCS. To address this, a 7-bus case is implemented and will be provided in the results sections.

2.4.3 Second Stage: Shunt Capacitor Sizing (SCS)

Once a feasible radial configuration with minimized power losses is obtained from RTLS, the algorithm updates the network topology and proceeds to the second stage, SCS. The primary purpose of SCS is to further enhance voltage profiles (and possibly reduce losses further) by optimally sizing capacitor banks at candidate locations. Even with an optimal network configuration from the first stage, certain buses may experience suboptimal voltage levels due to the reactive power demands of the loads. Installing shunt capacitors provides reactive power support locally, thereby improving voltage profiles and potentially reducing feeder currents, which in turn can lead to additional reductions in system losses. The decision on where and how much re-

active power compensation to install is critical to achieving these benefits without overcompensating or causing voltage regulation issues. During the data loading step, a subset of buses is identified as candidate locations for capacitor installation based on practical considerations such as physical space, existing equipment, or historical voltage problems. Each candidate bus can host a capacitor bank of fixed size. The SCS algorithm searches for the optimal size of the shunt capacitors for each candidate bus.

Similar to the first stage, the constraints in the SCS stage include power flow constraints, voltage and current limitations, and capacitor sizing limits. Like RTLS, the SCS problem is typically nonlinear due to the relationship between bus voltages and reactive power injections. Therefore, another PSO method is implemented for the second stage to find the optimal sizing of shunt capacitors to improve the voltage profiles and compensate for the reactive power. A practical binary logic governs the final deployment of shunt capacitors. After determining an optimal reactive power contribution for each potential capacitor location, a threshold rule is applied based on the unit's rated capacity. Capacitors whose optimized value is 50% or more of their rating are switched ON at full capacity. Those falling below the 50% threshold remain OFF according to equation 2.11.

$$Q_{\text{cap},i} = \begin{cases} Q_{\text{rated},i}, & \text{if } Q_{\text{cap},i} \geq 0.5 \times Q_{\text{rated},i} \\ 0, & \text{otherwise} \end{cases} \quad (2.11)$$

2.4.4 Third Stage: Feedback-Aware Structure

In the third and final stage, the RTLS process is executed once more. The input for this execution is the DN model updated with the resultant reactive power injections determined by the capacitor sizing logic in stage two and the topology status found by the first stage. The objective function remains unchanged from the first stage: minimize total active power losses while ensuring the final topology is radial. This is achieved using the identical DFS-PSO algorithm and AC power flow constraints described previously in Section 2.3. The key operational difference in this stage is that the power flow calculations inherently account for the impact of the reactive power

injections by the shunt capacitors. This stage searches for a new switching configuration that may yield lower active power losses than those achieved in the second stage. If such a configuration is found, the model proceeds with the third-stage result. Otherwise, the second-stage configuration is retained as the final solution. A key purpose of re-executing the RTLS in the third stage, incorporating the feedback from the capacitor sizing, is to mitigate the risk of converging to a suboptimal solution inherent in sequential optimization, which is based on heuristic methods. By attempting to refine the topology after reactive power compensation is applied, the algorithm performs a final check. Should the third stage not yield further loss reduction compared to the second stage, it provides increased confidence that the preceding two stages have effectively converged towards a high-quality, if not globally optimal, solution for the compensated network.

2.4.5 Integration of the Three Stages

Although RTLS and SCS are described as separate stages, it is crucial to highlight their interdependence. The network configuration determined in the first stage directly impacts the power flow and voltage profile, which in turn influences how capacitors should be sized. By performing RTLS first, the method ensures that the system topology is already optimized for minimum losses, thereby setting a solid foundation for the capacitor sizing task. In contrast, attempting to solve the proposed three-stage problem in a single integrated step often leads to a highly complex and computationally expensive optimization process, due to the large number of discrete switching variables combined with the continuous variables. The three-stage method thus offers a more tractable and transparent approach, providing clearer insights into how each optimization component contributes to the overall system improvement. After completing the SCS step, the model explores alternative switching configurations that could further reduce active power losses compared to the outcome from the second stage. If a better configuration is identified, it becomes the new solution moving forward; otherwise, the results from the second stage are maintained as the final result. The primary objective of re-running the RTLS process in this third stage, now informed by the results of capacitor sizing, is to address the risk of settling on a suboptimal solution, a common limitation of sequential, heuristic-based optimization

approaches.

Once the optimization process is completed and validated, the final configuration, comprising the selected status of tie-line switches (open or closed) and the optimal capacitor sizes at designated candidate buses, is recorded as the optimal solution. The output results include several performance metrics to evaluate the effectiveness of the proposed methodology. These typically involve a quantitative assessment of system loss reduction, comparing total active and reactive power losses before and after the application of RTLS and SCS stages. Additionally, improvements in the voltage profile are illustrated through graphical representations of voltage magnitudes and angles at each bus, highlighting enhanced voltage regulation across the network.

To wrap up the solution procedure, a pseudo-code is presented in Algorithm 1 to provide a thorough explanation of how the model works. The algorithm outlines a three-stage optimization framework for DNR using PSO to determine an optimal network topology and shunt capacitor sizing. The process begins by selecting the operating condition of the DN, such as heavily loaded, lightly loaded, poor PF, good PF, or normal loading scenario. Then, PSO parameters are initialized like the inertia weight, exploration, and exploitation coefficients. The algorithm then iterates until a specified maximum number of iterations is reached or convergence is achieved. In each iteration, Stage 1, RTLS, is executed to identify a radial network configuration that minimizes the active power losses. If a valid radial topology is found, the network topology is updated based on the RTLS result. The algorithm then proceeds to Stage 2, which involves SCS. Each capacitor is evaluated: if its size is greater than or equal to 50% of its full capacity, it is assigned full capacity; otherwise, it is assigned zero capacity. After updating the reactive power injections in the network, Stage 3 is executed by re-running the RTLS with the updated reactive power injections. If the total active power loss in Stage 3 is lower than in Stage 2, the third-stage configuration is accepted as the final solution; otherwise, the second-stage results are retained as the final configuration. If, however, the RTLS fails to find a radial topology due to having reached its optimal configuration, the algorithm bypasses penalizing the fitness function and directly proceeds to Stage 2 (SCS). In this case, the capacitors are sized as in Stage 2, and the updated reactive power injections are used to finalize the solution. If no radial topology is found and RTLS is not yet at an optimum, the fitness

function is penalized, and the PSO continues to explore alternative configurations. The process continues until either an optimal configuration is found or the maximum iterations are reached. Finally, the algorithm outputs the final network topology and capacitor sizes.

Algorithm 1 Pseudo-code for the proposed methodology

Input : DN data-case; PSO parameters

Output: Optimal switch configuration u and capacitor sizes Q_{cap}

```
1 Select the loading type of the DN and initialize PSO parameters
2 repeat
3   Initialize switch configuration vector  $u_i = [u_1, u_2, \dots, u_n]$ 
4   Run Stage 1, RTLS
5   if radial configuration(s) found then
6     Select  $u^* = \arg \min_{u_i} P_{\text{Loss}}(u_i)$ 
7     Update DN topology according to  $u^*$ 
8     Initialize  $Q_{\text{cap}} = [Q_{\text{cap},1}, Q_{\text{cap},2}, \dots, Q_{\text{cap},m}]$ 
9     Run Stage 2, SCS using  $u^*$  and  $Q_{\text{cap}}$ 
10    foreach  $i = 1$  to  $m$  do
11      if  $Q_{\text{cap},i} \geq 0.5 \cdot Q_{\text{rated},i}$  then
12         $Q_{\text{cap},i} \leftarrow Q_{\text{rated},i}$ 
13      else
14         $Q_{\text{cap},i} \leftarrow 0$ 
15      Update  $Q_{\text{cap}}$  injections
16      Compute  $P_{\text{Loss}}^{(2)} = P_{\text{Loss}}(u^*, Q_{\text{cap}})$ 
17      Run Stage 3, RTLS re-execution, with updated  $Q_{\text{cap}}$ 
18      Compute  $P_{\text{Loss}}^{(3)} = P_{\text{Loss}}(u^{**}, Q_{\text{cap}})$ 
19      if  $P_{\text{Loss}}^{(3)} < P_{\text{Loss}}^{(2)}$  then
20        return  $(u^{**}, Q_{\text{cap}})$ 
21      else
22        return  $(u^*, Q_{\text{cap}})$ 
23    else
24      Initialize  $Q_{\text{cap}} = [Q_{\text{cap},1}, Q_{\text{cap},2}, \dots, Q_{\text{cap},m}]$ 
25      Run Stage 2, SCS
26      foreach  $i = 1$  to  $m$  do
27        if  $Q_{\text{cap},i} \geq 0.5 \cdot Q_{\text{rated},i}$  then
28           $Q_{\text{cap},i} \leftarrow Q_{\text{rated},i}$ 
29        else
30           $Q_{\text{cap},i} \leftarrow 0$ 
31      Inject  $Q_{\text{cap}}$  into the DN model
32      return  $Q_{\text{cap}}$ 
33 until maximum iterations or convergence;
```

2.5 Chapter Summary

The proposed three-stage solution framework, comprising the initial RTLS, followed by SCS, and a final re-execution of RTLS, offers a structured, computationally efficient, and effective approach for minimizing active power losses and enhancing voltage profiles in DNs. By decomposing the overall problem into sequential stages, the method circumvents the complexity associated with a fully integrated optimization involving both discrete and continuous variables. The first stage determines a radial configuration that minimizes losses, while the second stage optimizes reactive power support to improve voltage regulation. The third stage reinforces the near-global optimality of the solution by reapplying the RTLS, now informed by the capacitor sizing results. To further demonstrate the generalizability and practical robustness of the proposed methodology, the complete three-stage framework has been applied under five distinct operating conditions: heavily loaded, lightly loaded, normal loading, good PF, and poor PF. These test scenarios reflect a range of real-world conditions under which DNs are typically operated. This comprehensive evaluation ensures that the proposed approach is not only effective under nominal settings but also adaptable to varying stress levels and load characteristics. When properly implemented and validated, this methodology can substantially enhance the operational efficiency and reliability of modern DNs, meeting the evolving demands of the grid and facilitating the integration of DERs.

CHAPTER 3

CASE STUDY AND NUMERICAL RESULTS

This chapter presents the case studies and numerical results for the proposed methodology. In the following, the chapter is divided into three subsections covering case study, numerical results, and chapter summary.

3.1 Case Study

This subchapter presents the case studies and scenarios used to validate the proposed three-stage optimization methodology for the DNR problem. The methodology is tested on two widely adopted benchmark systems, the IEEE 33-bus distribution system (Case 1) and the IEEE 123 feeder system (Case 2), as well as a small illustrative system, the 7-bus test network (Case 3), which is used to evaluate the algorithm's behavior under minimal reconfiguration potential. Figures 3.1 and 3.2 show the baseline connectivity and tie-line switch locations for Case 1 and Case 2, respectively. For each system, the following configuration details are applied:

- Case 1 includes 5 tie-line switches and 5 shunt capacitors, each rated at 90 kVAR, placed at buses 6, 12, 20, 23, and 29.
- Case 2 includes 11 tie-line switches and 5 shunt capacitors, also each rated at 90 kVAR, located at buses 33, 41, 75, 96, and 114. Additionally, buses 251 and 451 are defined as transmission buses that act as external sources (slack buses) during the RTLS stage, as real-world grid interfacing.
- Case 3 includes three shunt capacitors installed at buses 3, 4, and 5, each with a capacity of 50 KVaR, and is used to test situations where the network topology

is already optimal or offers little opportunity for improvement through reconfiguration.

The simulations are executed on a personal computer with an Intel Core i5-10300H CPU (2.50 GHz) and 8 GB RAM. In addition, detailed branch indexing for Case 1 and Case 2 is presented in Appendices A and B, respectively. These appendices provide an overview of the network topology used in each case study, including the specific numbering and connectivity of each branch. To thoroughly assess the applicability and scalability of the proposed method, each case study is evaluated under five loading conditions: heavily loaded, lightly loaded, normal loading, good PF, and poor PF. These test scenarios represent a wide range of realistic operating conditions that DNs may experience in practice. The parameters used for the developed PSO algorithm in all case studies are as follows: the number of particles is set to 50, and the number of iterations is set to 50 as well. The acceleration coefficients are chosen as $c_1 = 2.0$ and $c_2 = 1.6$, respectively, representing the cognitive and social learning factors. The inertia weight w is dynamically updated during the iterations using a linearly decreasing strategy. The maximum and minimum values of the inertia weight are set to $w_{\max} = 0.93$ and $w_{\min} = 0.4$, and the inertia is calculated at each iteration using the equation 3.1.

$$w = w_{\max} - \left(\frac{w_{\max} - w_{\min}}{\text{num_iterations}} \right) \cdot \text{iter} \quad (3.1)$$

This approach provides a balance between exploration and exploitation over the course of the optimization process. The outcomes from each scenario are categorized into four structures:

- Baseline (original topology with no reconfiguration or capacitor sizing),
- RTLS (radial reconfiguration applied, first stage),
- SCS (capacitor sizing following the reconfiguration from stage 1, second stage),
- RTLS re-applied (third stage based on updated reactive injections from stage 2).

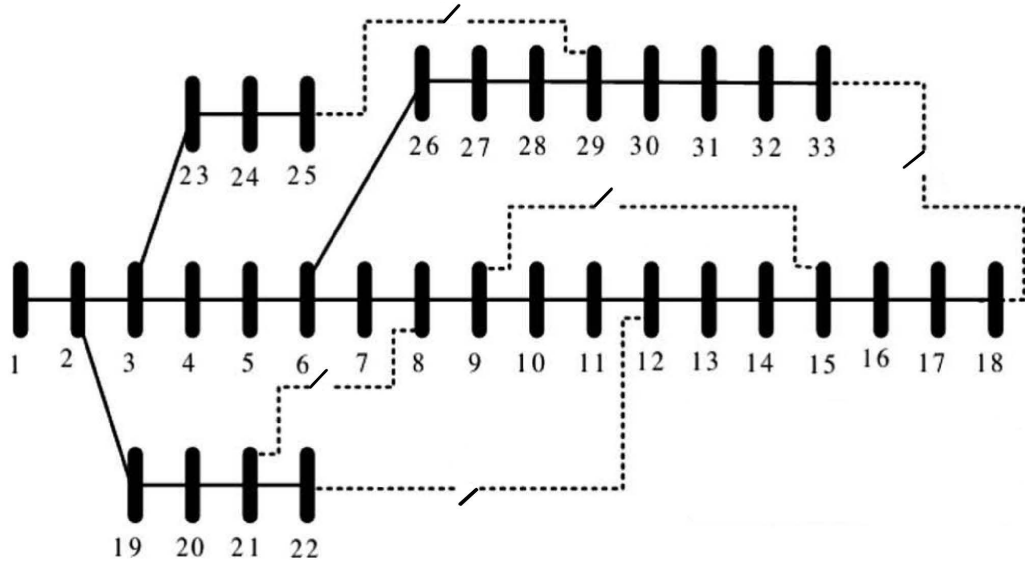


Figure 3.1: Topology of case 1 with specified tie-line switches

Subsection 3.2 provides a detailed breakdown of the numerical results, including performance comparisons across all scenarios and case studies. Each structure, namely as baseline, RTLS, SCS, and third stage, is assessed in terms of power losses, voltage profile, and switching effectiveness to demonstrate the proposed method’s applicability under varying operating conditions.

3.2 Numerical Results

This subsection presents the numerical results obtained from applying the proposed three-stage DNR methodology to two benchmark test systems: Cases 1 and 2. The results are organized by case and loading scenario for clarity and systematic analysis. Specifically, subsection 3.2.1 reports the outcomes for Case 1, while subsection 3.2.2 provides the results for Case 2. Each of these subsections is further divided into five additional subsections based on the loading conditions applied to the network: normal loading, heavy loading, light loading, good PF, and poor PF. For each scenario, comparisons are made between the baseline network, the RTLS stage, the SCS stage, and, where applicable, the final results obtained from the third stage. Voltage magnitudes, voltage angles, active power losses, and reactive power losses are analyzed and visualized to demonstrate the effectiveness and adaptability of the proposed approach

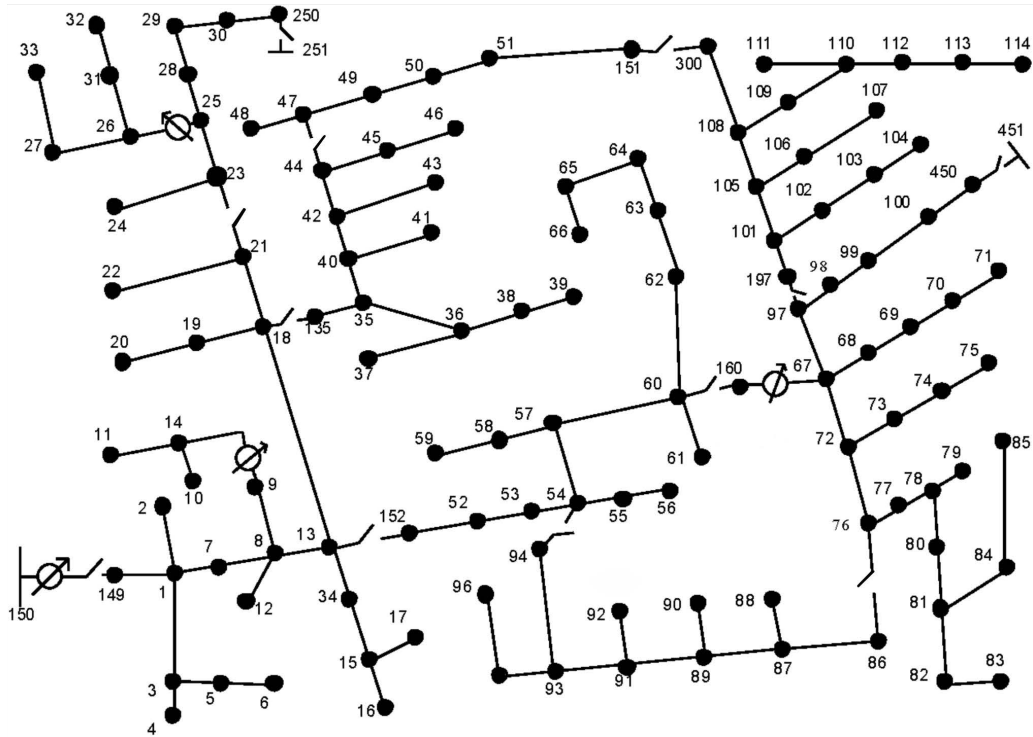


Figure 3.2: Topology of case 2 with specified tie-line switches

under various operational conditions.

3.2.1 Case 1 Results

This subsection presents the numerical results for Case 1, corresponding to the IEEE 33-bus DN. The performance of the proposed three-stage methodology is evaluated under five distinct loading scenarios: normal loading in subsection 3.2.1.1, heavy loading in subsection 3.2.1.2, light loading in subsection 3.2.1.3, poor PF in subsection 3.2.1.5, and good PF in subsection 3.2.1.6.

3.2.1.1 Normal Loading

In this scenario, the proposed three-stage optimization methodology was evaluated under normal loading conditions for Case 1. Normal loading data for Case 1, which includes the initial connectivity of branches, load demand of the various busbars, and resistance and reactance of lines, is loaded in the first step. The first stage, RTLS, is

Table 3.1: Proposed three-stage DNR method’s results for Case 1 under normal loading conditions

Stage	Active Loss (kW)	Reactive Loss (kVaR)	Active Loss Reduction (%)
Baseline	208.28	111.58	–
RTLS (Stage 1)	143.52	104.78	31.10%
SCS (Stage 2)	131.49	96.38	5.76%
Third Stage	130.77	94.20	0.38%

performed to find the radial configurations that satisfy the objectives of the first stage, which is to find a radial configuration that has minimum active power losses compared to the baseline case. The baseline configuration was first analyzed to establish a reference. The network was then optimized using the three-stage framework, comprising RTLS, SCS, and a final RTLS re-execution (ThirdStage) based on updated reactive power profiles. Table 3.1 provides the results of deploying the proposed three-stage DNR at each stage of the methodology. As seen, the first stage (RTLS) reduced the active power loss from 208.28 kW to 143.52 kW, yielding a significant loss reduction. The second stage (SCS), which optimally allocated five shunt capacitors, further reduced the losses to 131.49 kW. The final stage achieved a minor additional reduction, reaching 130.77 kW (almost 0.38%), confirming the near-global optimality of the outcome. All five capacitors were utilized at full capacity. To further evaluate the effectiveness of the proposed methodology under normal loading conditions, it is observed that the third stage identified a configuration that reduces total active power losses by an additional 0.38% compared to the second stage’s result. This marginal improvement highlights the near-global optimality of the proposed methodology, with the third stage offering a fine-tuned enhancement. The decision to adopt the third-stage configuration may depend on the DSO’s operational preferences and switching constraints and costs.

As evident, the initial RTLS stage reduced the active power loss by 31.10%, while the SCS stage further enhanced network performance, achieving a 5.76% reduction compared to the RTLS stage. The final stage, by updating the switching configuration based on the new reactive power profile, yielded a marginal additional improvement,

reducing losses to 130.77 kW or 0.38% below the SCS stage. This result affirms the value of the third stage in fine-tuning the configuration when beneficial. The RTLS stage selected the following tie-line switches to be opened: (7,8), (28,29), (32,33), (9,15), and (8,21). In the final stage, one change was observed in the switch set, where the switch between buses (9,15) was replaced with (14,15). The execution time for the full three-stage process under normal loading was 409.68 seconds, demonstrating the tractability of the proposed approach. Figures 3.3, 3.4, and 3.5 present the voltage magnitude, voltage angle, active power loss, and reactive power loss profiles at each optimization stage. These visualizations highlight the performance improvements and validate the convergence behavior of the method.

Figure 3.5 illustrates the voltage magnitude, voltage angle, and both active and reactive power flows after the third stage. While the improvements over the second stage are relatively minor, they indicate a further refinement of the system's operating condition. The voltage profiles are slightly more stable, and the power flow paths are optimized marginally, which supports the assertion that the configuration found in the second stage is near-globally optimal. These subtle yet measurable improvements provide flexibility for the DSO to decide whether the additional switching actions required for the third stage are justified based on operational priorities.

3.2.1.2 Heavy Loading

This scenario analyzes the Case 1 network under heavy loading conditions, where the active and reactive loads are increased by 50%. The developed methodology's results for the heavy loading condition are presented in Table 3.2. Significant improvements are observed in both active and reactive power losses as the methodology progresses. As shown in Table 3.2, the first-stage RTLS optimization achieves a significant 29.56% reduction in active power losses compared to the baseline case, followed by a 4.46% total reduction after the second stage. The third stage contributes a further enhancement, resulting in an overall reduction of 5.37% compared to the second stage. The reduction in reactive power losses is also notable, improving network stability and efficiency. The optimal switching configuration obtained in the RTLS stage includes the opening of switches located between buses (7,8), (11,12), (32,33),

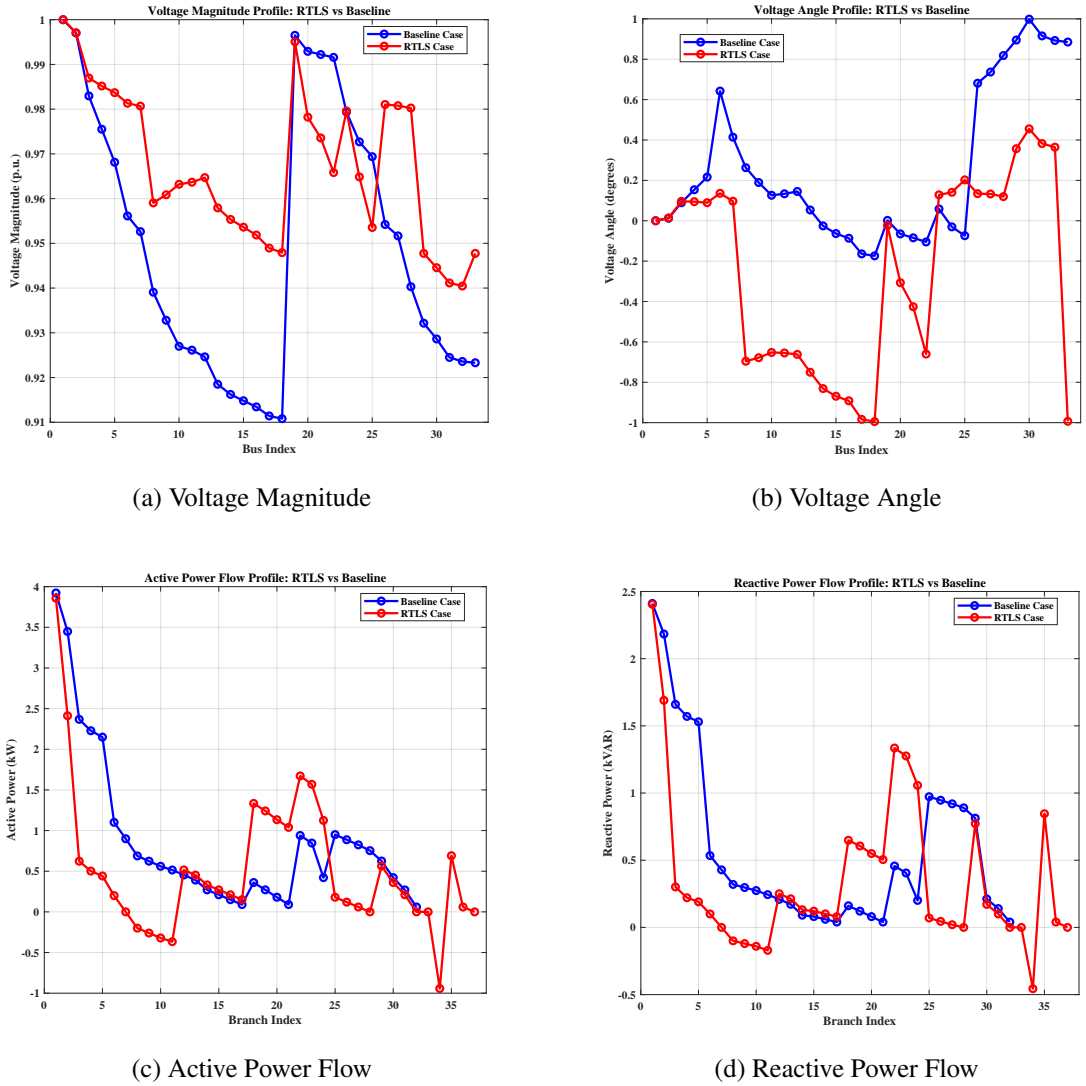
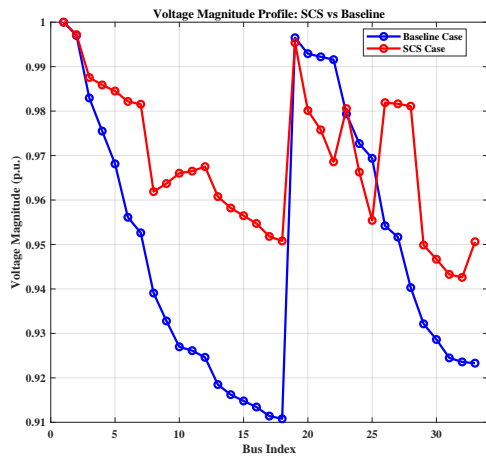


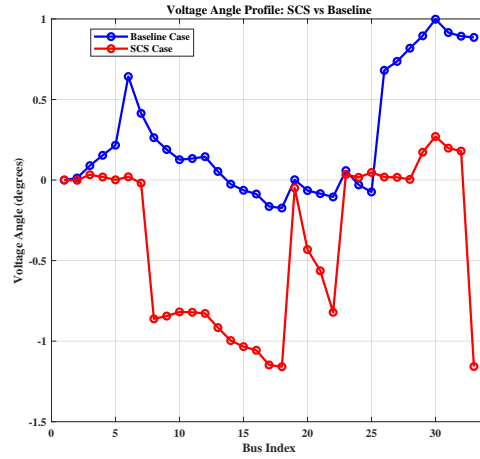
Figure 3.3: RTLS stage results under normal loading for Case 1

(25,29), and (8,21). Following the reactive power compensation in Stage 2 (SCS), the third stage suggests a refined configuration, where the switch between buses (11,12) is replaced by (9,15), indicating a slight topological adjustment for further performance improvement. In addition, five shunt capacitors were utilized at their full-rated capacity found by SCS stage, which contributed to reactive power support and voltage profile enhancement. The total execution time for the complete three-stage optimization process under heavy loading was recorded as 404.07 seconds.

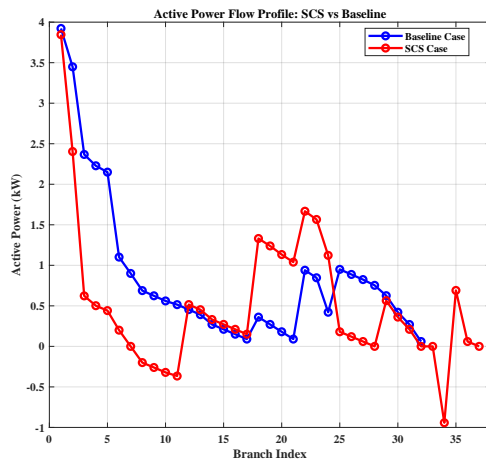
Under heavy loading conditions, there remains significant room for improvement even after the application of the first two stages. The third stage of the proposed



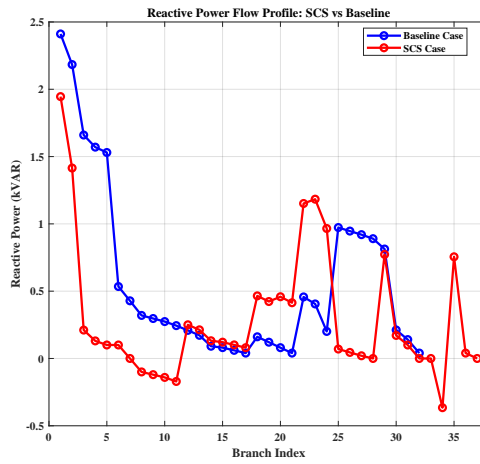
(a) Voltage Magnitude



(b) Voltage Angle



(c) Active Power Flow

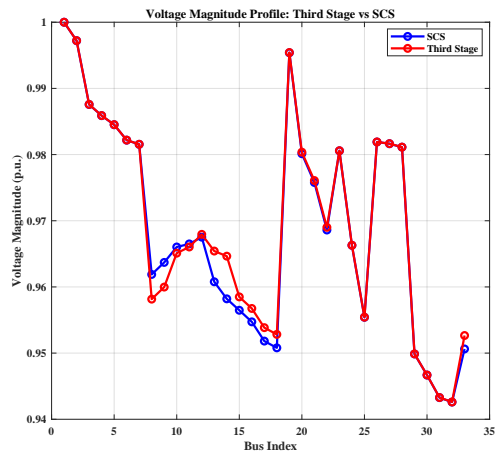


(d) Reactive Power Flow

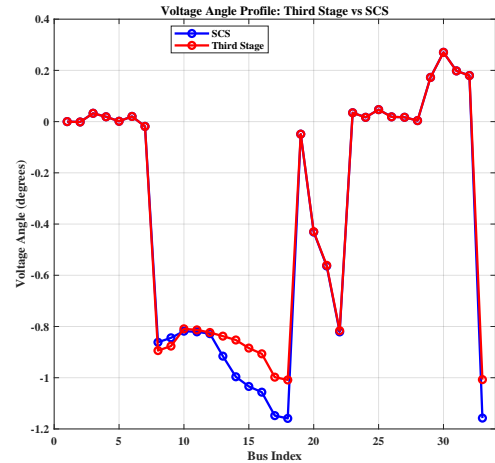
Figure 3.4: SCS stage results under normal loading for Case 1

Table 3.2: Proposed three-stage DNR method's results for Case 1 under heavy loading conditions

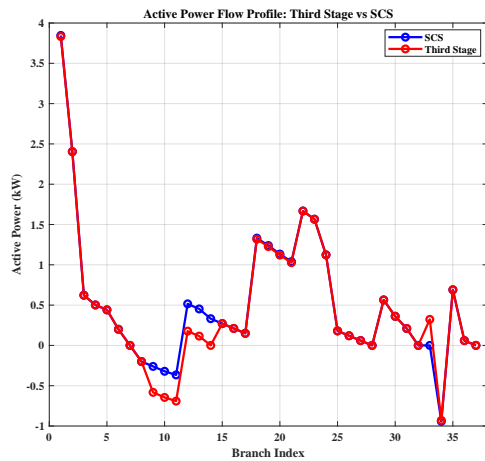
Stage	Active Loss (kW)	Reactive Loss (KVaR)	Active Loss Reduction (%)
Baseline	508.84	272.52	—
RTLS (Stage 1)	358.54	246.19	29.56%
SCS (Stage 2)	335.71	232.17	4.46%
Third Stage	308.37	206.68	5.37%



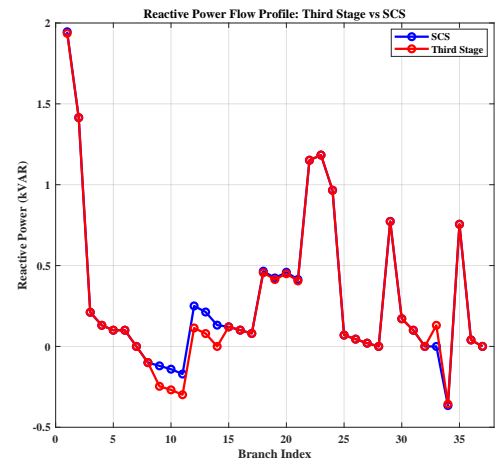
(a) Voltage Magnitude



(b) Voltage Angle



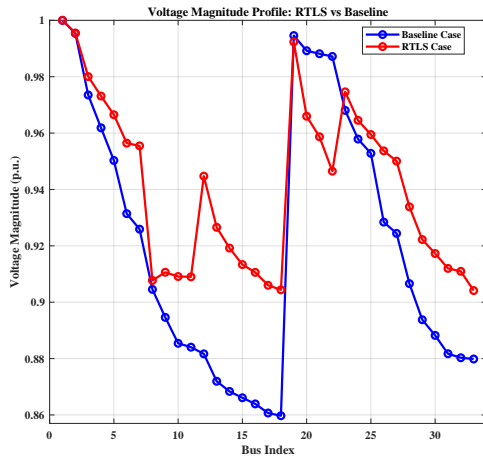
(c) Active Power Flow



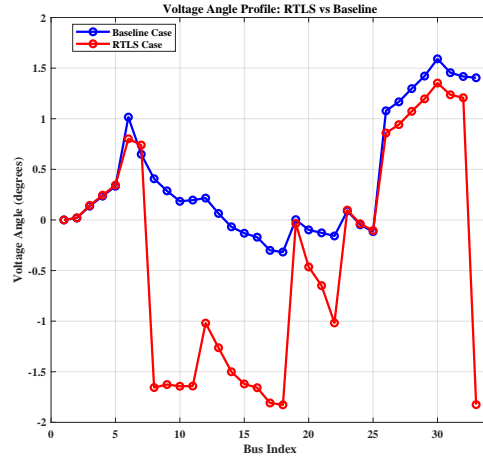
(d) Reactive Power Flow

Figure 3.5: Third stage results under normal loading for Case 1

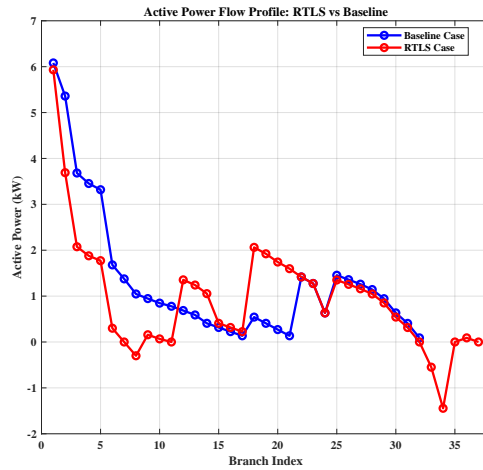
methodology successfully identifies an alternative network topology that yields additional reductions in active power losses. This reinforces the effectiveness and adaptability of the three-stage approach. A DSO may choose to adopt this configuration by balancing the trade-off between the benefit of reduced losses and the potential cost of additional switching operations. The successful application of the third stage in this scenario demonstrates the robustness of the proposed method in high-stress operating conditions. Furthermore, Figures 3.6, 3.7, and 3.8 display the voltage magnitude, voltage angle, and active and reactive power flows profiles for each stage of the methodology. Voltage magnitude improvements and reductions in power flow



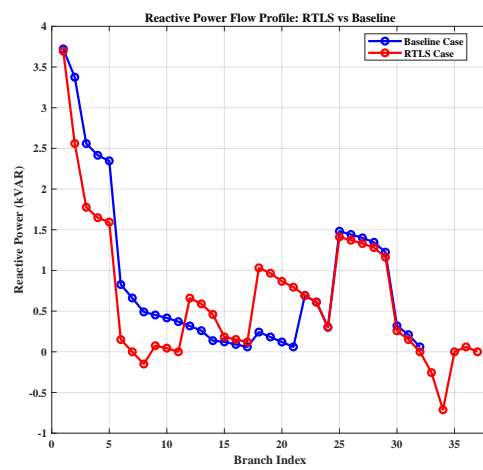
(a) Voltage Magnitude



(b) Voltage Angle



(c) Active Power Flow



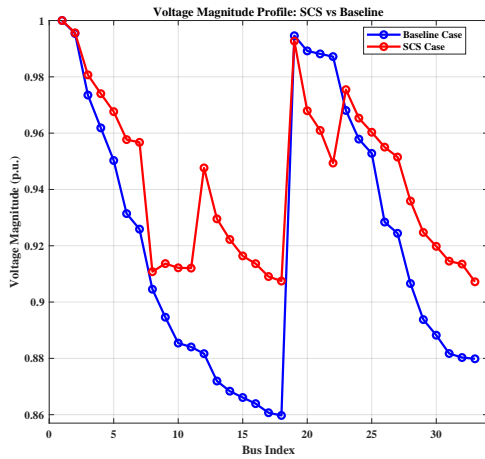
(d) Reactive Power Flow

Figure 3.6: RTLS stage results under heavy loading for Case 1

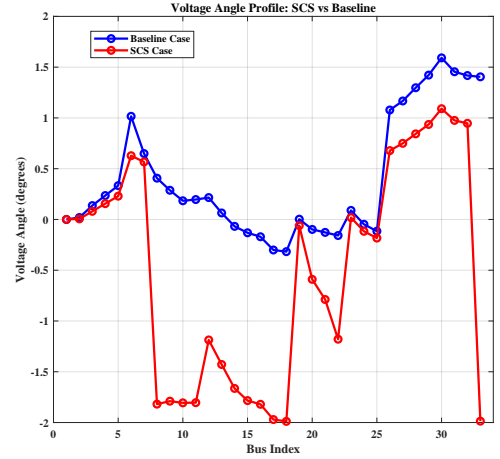
losses are clearly observed as the stages progress.

3.2.1.3 Light Loading

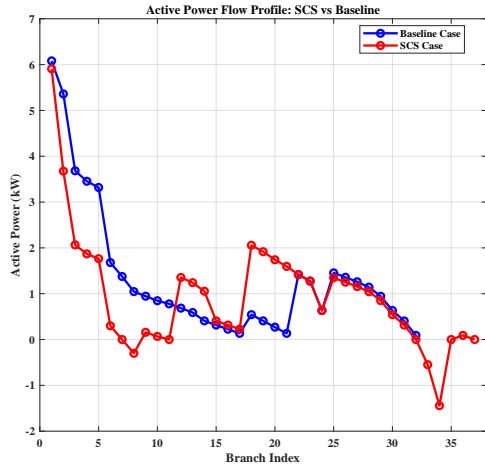
This scenario analyzes the Case 1 network under light loading conditions, where the active and reactive loads are reduced by 50%. Table 3.3 summarizes the results of the proposed methodology at each stage under the light loading condition. Compared to the baseline case, the first stage (RTLS) achieves a 31.08% reduction in active power losses. The second stage (SCS) further improves the loss reduction by



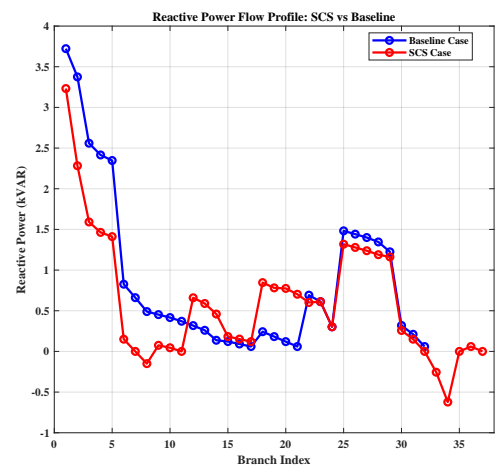
(a) Voltage Magnitude



(b) Voltage Angle



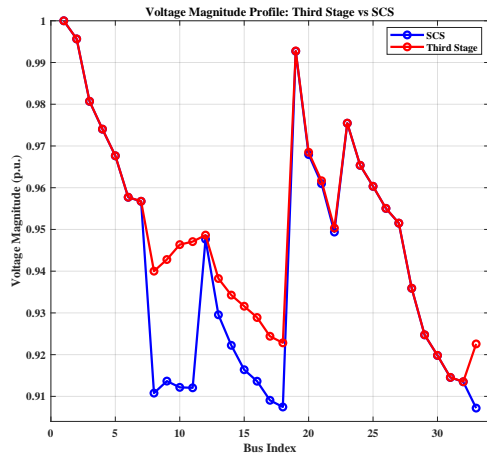
(c) Active Power Flow



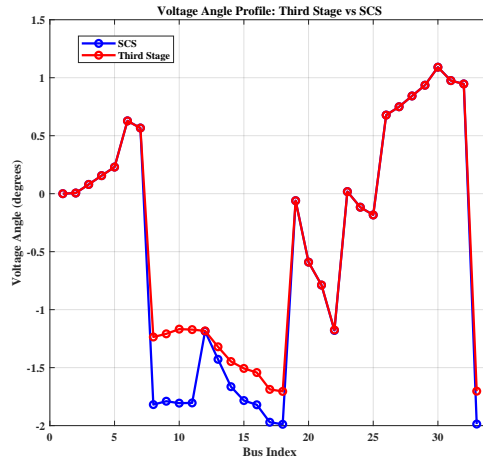
(d) Reactive Power Flow

Figure 3.7: SCS stage results under heavy loading for Case 1

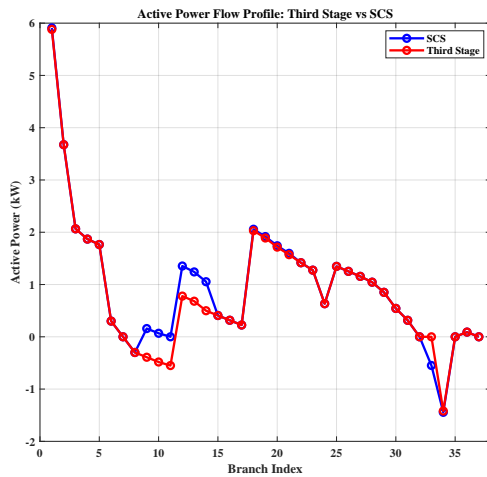
11.64% compared to the RTLS stage output. No third-stage reconfiguration was required in this scenario, indicating that the combination of RTLS and capacitor sizing was sufficient to achieve a near-optimal configuration. The optimal switching configuration obtained during the RTLS stage involved opening the switches between buses (7,8), (9,15), (32,33), (25,29), and (8,21). During the SCS stage, only three out of the five available shunt capacitors, located at buses 12, 20, and 29, were activated at their full capacity according to the binary sizing logic. The total execution time for this simulation was recorded as 381.10 seconds. As anticipated under light loading conditions, the baseline active power losses were relatively low, around 49



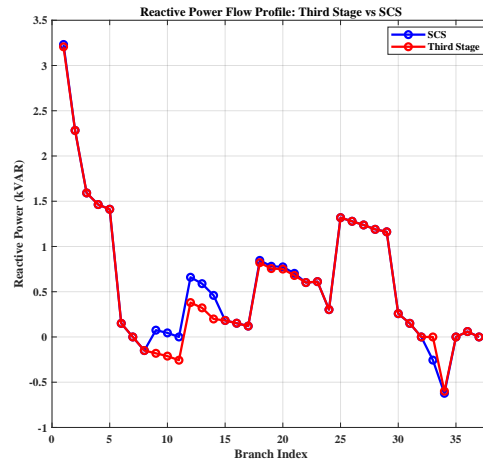
(a) Voltage Magnitude



(b) Voltage Angle



(c) Active Power Flow



(d) Reactive Power Flow

Figure 3.8: Third stage results under heavy loading for Case 1

kW. The first stage successfully identified a reconfigured topology that further reduced these losses, and the second stage provided additional improvements through optimal capacitor compensation. However, the third stage was unable to identify a configuration that outperformed the previous stages in terms of active power loss reduction. This outcome aligns well with expectations, as the network is already operating efficiently under light loading. It also reinforces the validity of the proposed methodology, demonstrating that it does not force unnecessary reconfiguration when no meaningful performance gain can be achieved. Figures 3.9 and 3.10 display the voltage magnitude, voltage angles, and active and reactive power flows profiles for

Table 3.3: Proposed three-stage DNR method's results for Case 1 under light loading conditions

Stage	Active Loss (kW)	Reactive Loss (KVaR)	Active Loss Reduction (%)
Baseline	48.532	26.02	–
RTLS (Stage 1)	33.45	22.29	31.08%
SCS (Stage 2)	27.79	18.89	11.64%
Third Stage	-	-	-

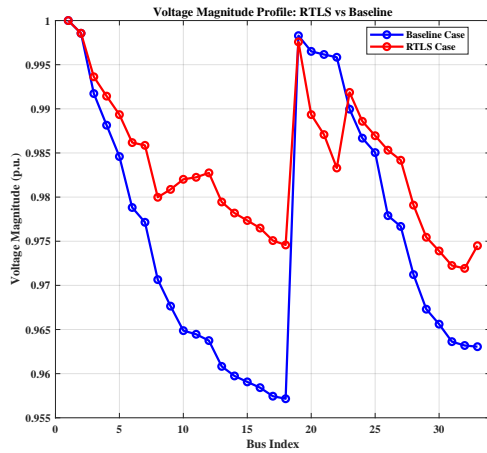
each stage of the methodology. Voltage magnitude improvements and reductions in power flow losses are clearly observed as the stages progress.

3.2.1.4 Extended Light Loading

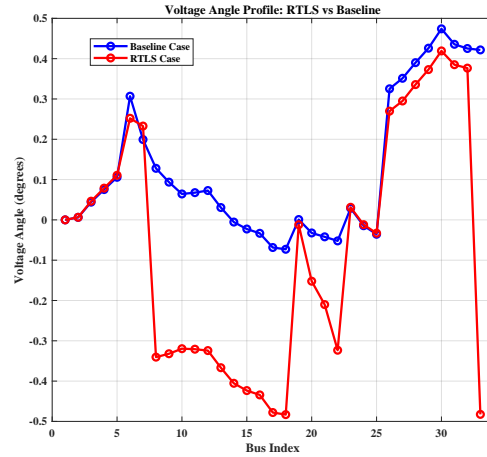
In this subsection, the previous scenario, light loading, has been re-executed with lower and upper voltage bounds of 0.95 and 1.05, respectively. The RTLS stage found the following switches to be opened: (11, 12), (32, 33), (9, 15), (25, 29), (8, 21). Also, the execution time took 374.88 seconds for this extended case of light loading. Table 3.4 provides the results of the proposed three-stage methodology for this extended scenario. Accordingly, the performance of the model is almost the same, with 3.53% deviation in active power losses in comparison with the normal light loading scenario (3.2.1.3). Figures 3.11 and 3.12 depict the voltage magnitude, voltage angle, active and reactive power flow profiles for each stage during the optimization process, respectively. This minor variation indicates that the proposed method consistently identifies high-quality configurations, even when subjected to more restrictive voltage operating limits.

3.2.1.5 Poor PF

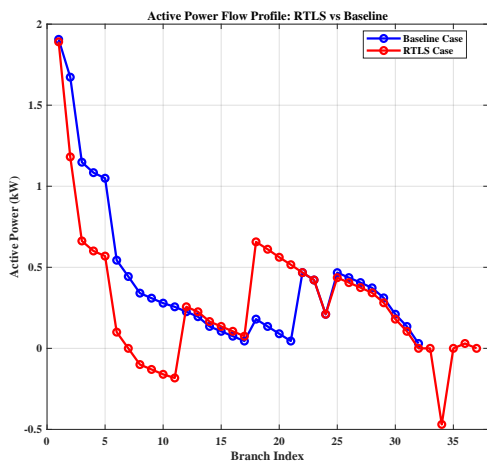
In this scenario, the proposed three-stage optimization framework is applied to the Case 1 under a poor PF condition. A PF value of 0.7 is selected to simulate a less efficient power consumption environment. The results demonstrate the effectiveness of the method in managing both active and reactive power losses while maintaining



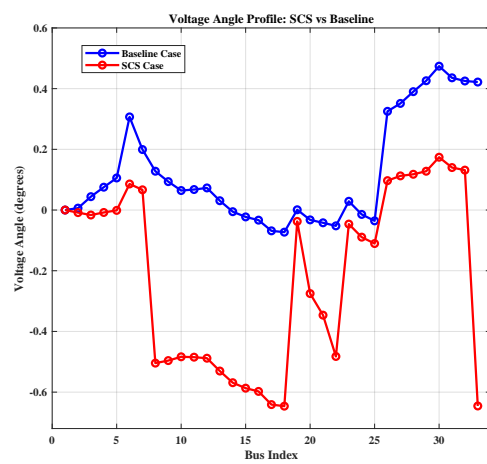
(a) Voltage Magnitude



(b) Voltage Angle



(c) Active Power Flow

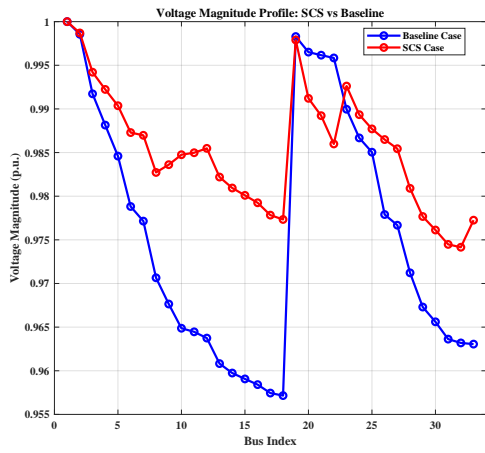


(d) Reactive Power Flow

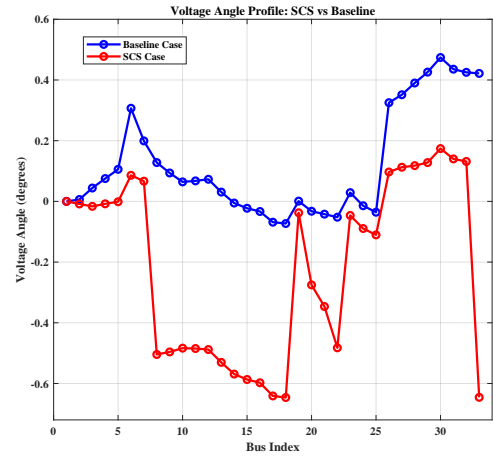
Figure 3.9: RTLS stage results under light loading condition for Case 1

Table 3.4: Proposed three-stage DNR method's results for Case 1 under light loading conditions - Extended

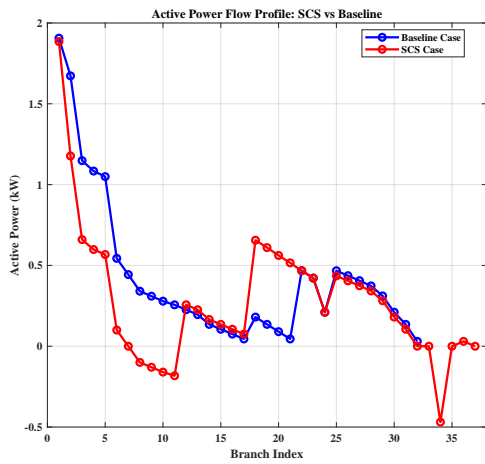
Stage	Active Loss (kW)	Reactive Loss (KVaR)	Active Loss Reduction (%)
Baseline	48.532	26.02	—
RTLS (Stage 1)	35.17	20.71	27.52%
SCS (Stage 2)	29.51	17.61	11.67%
Third Stage	-	-	-



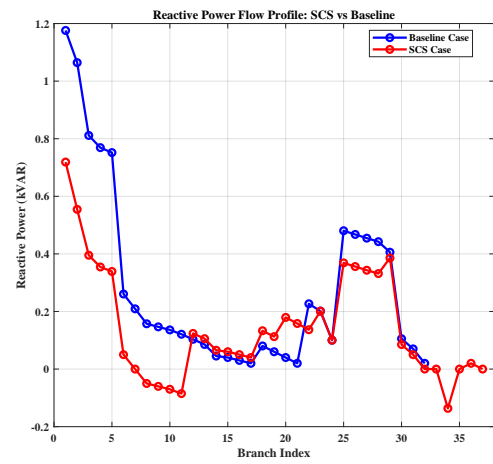
(a) Voltage Magnitude



(b) Voltage Angle



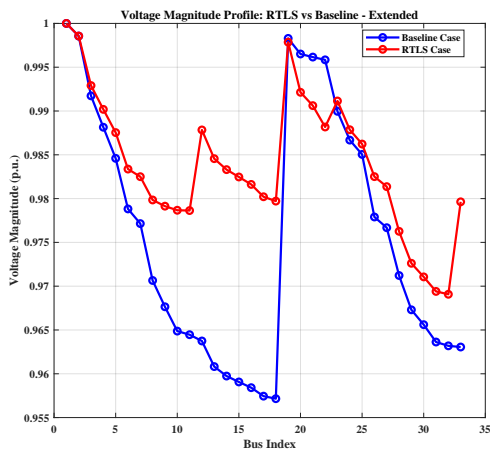
(c) Active Power Flow



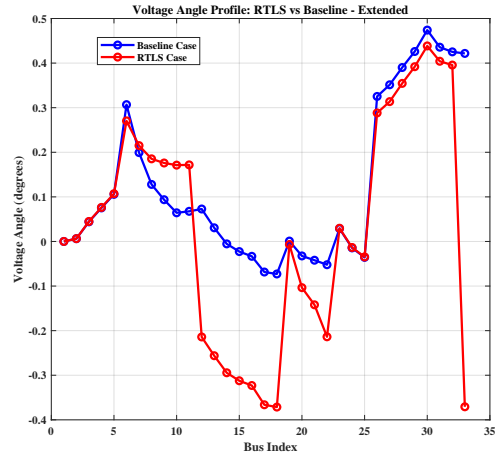
(d) Reactive Power Flow

Figure 3.10: SCS stage results under light loading condition for Case 1

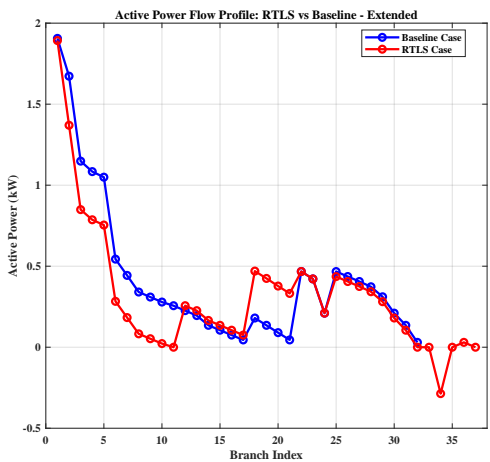
voltage and topological constraints. Table 3.5 presents the active and reactive power losses for the baseline configuration and for each stage of the proposed methodology. Notably, the RTLS stage achieves a 32.5% reduction in active power losses compared to the baseline. Subsequent capacitor sizing in the SCS stage further reduces losses by 6.3% compared to the RTLS stage, and the final third stage provides an additional improvement of 2.7% over the SCS stage. Cumulatively, the proposed approach reduces active power loss by approximately 41.5% from the baseline configuration. In terms of topology changes, the RTLS stage recommends opening switches at buses (11,12), (28,29), (9,15), (18,33), and (8,21). In contrast, the third stage results in a slightly different configuration, opening switches at (7,8), (14,15), (32,33), (25,29),



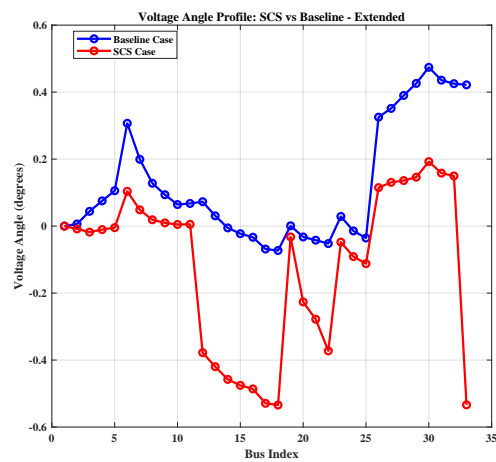
(a) Voltage Magnitude



(b) Voltage Angle



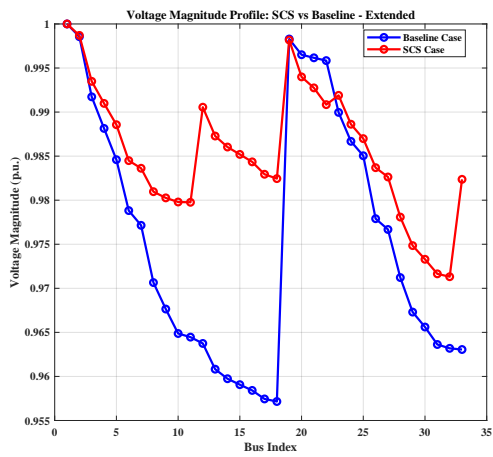
(c) Active Power Flow



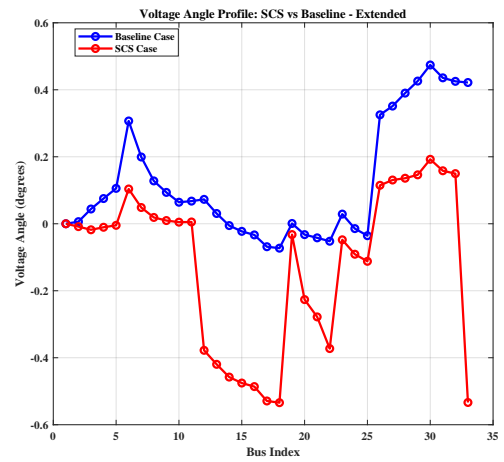
(d) Reactive Power Flow

Figure 3.11: RTLS stage results under light loading condition for Case 1 - Extended

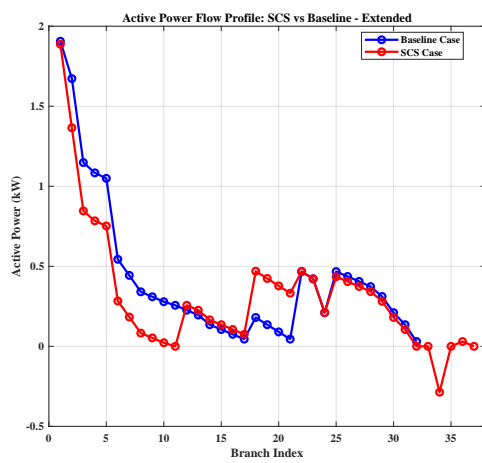
and (8,21), which provides further loss minimization. Notably, all five shunt capacitors were utilized at full capacity in the SCS stage, as expected, since the network's condition is quite ill ($PF=0.7$). Figures 3.13 and 3.14 illustrate the voltage profiles and power losses after the RTLS and SCS stages, respectively, while Figure 3.15 displays the results for the third stage. Significant improvements in voltage magnitude and angle are visible across all buses after the final stage, since the network was ill-conditioned initially. Additionally, the entire optimization process was completed in 411.24 seconds, demonstrating acceptable computational performance given the network complexity.



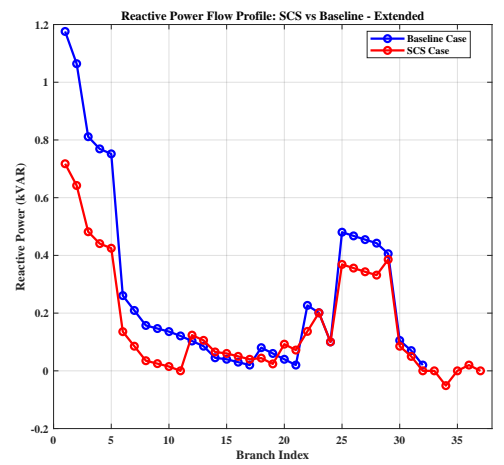
(a) Voltage Magnitude



(b) Voltage Angle



(c) Active Power Flow

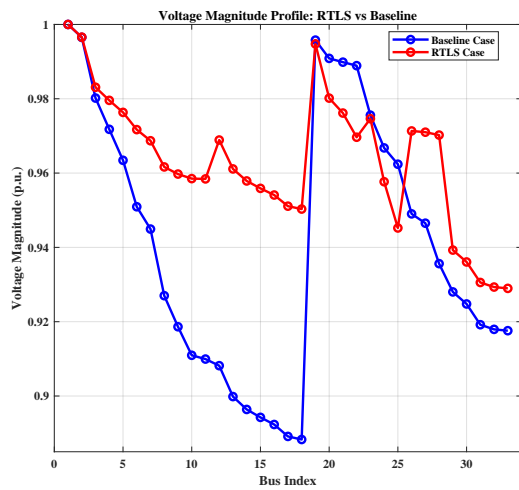


(d) Reactive Power Flow

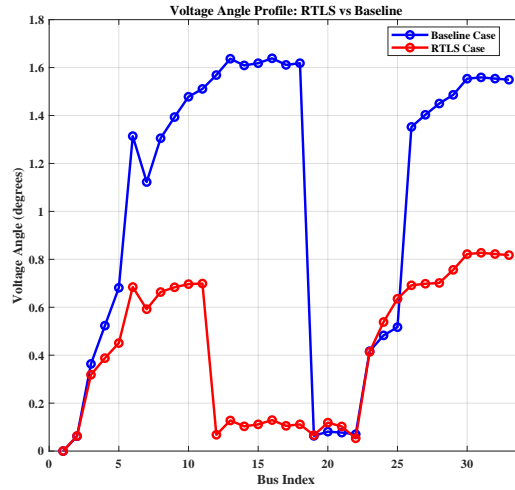
Figure 3.12: SCS stage results under light loading condition for Case 1 - Extended

Table 3.5: Proposed three-stage DNR method's results for Case 1 under poor PF conditions

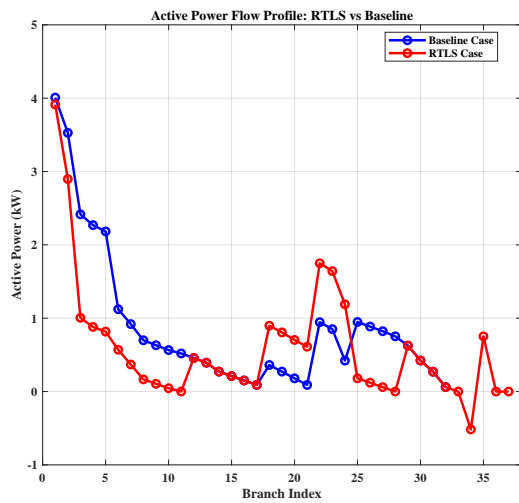
Stage	Active Loss (kW)	Reactive Loss (KVaR)	Active Loss Reduction (%)
Baseline	293.05	158.70	—
RTLS (Stage 1)	197.85	132.358	32.5%
SCS (Stage 2)	179.40	120.21	6.3%
Third Stage	171.43	117.69	2.7%



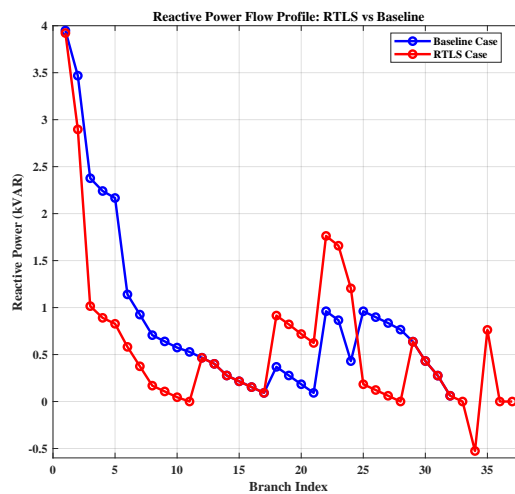
(a) Voltage Magnitude



(b) Voltage Angle



(c) Active Power Losses

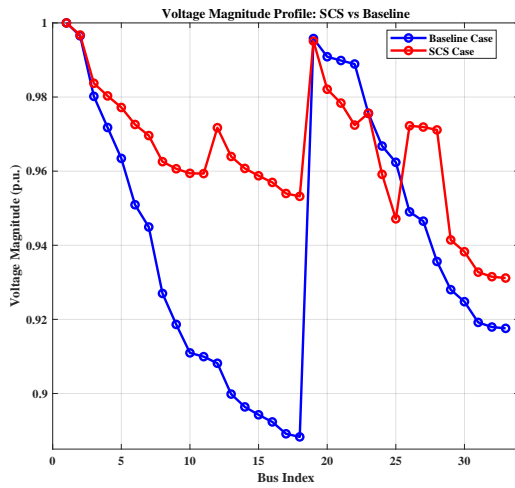


(d) Reactive Power Losses

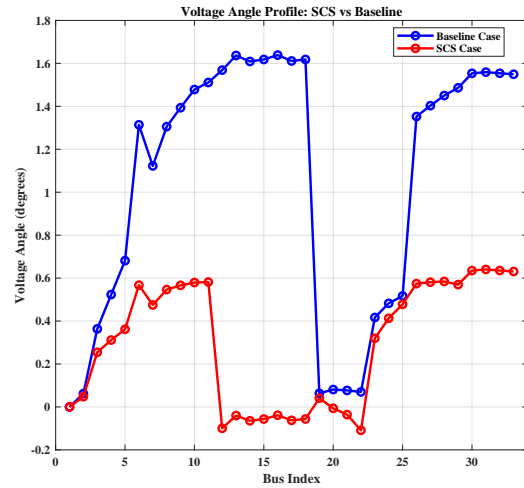
Figure 3.13: RTLS stage results under poor PF condition for Case 1

3.2.1.6 Good PF

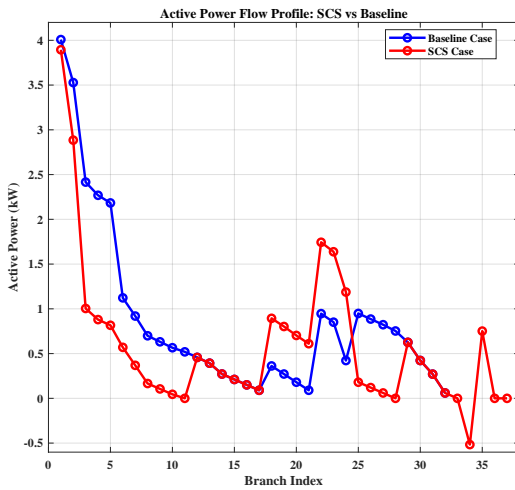
In this final scenario, a power factor of 0.95 is selected to represent a relatively efficient operating condition where active and reactive power demands are well-balanced. The proposed three-stage optimization framework is applied to evaluate its effectiveness under such favorable conditions. As expected, while the improvements are less dramatic than in more stressed scenarios, noticeable gains are still achieved. As presented in Table 3.6, the RTLS stage reduces active power losses by 33.89%, which



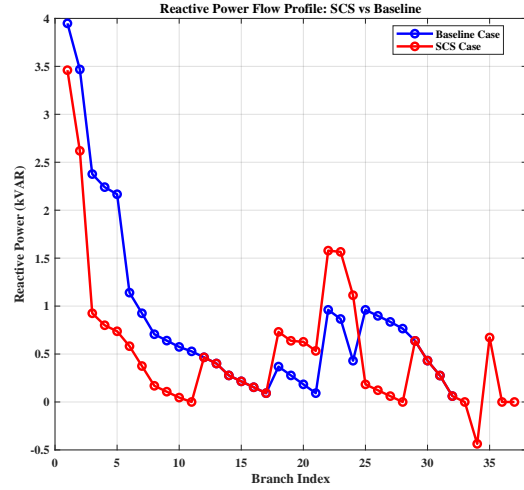
(a) Voltage Magnitude



(b) Voltage Angle



(c) Active Power Losses



(d) Reactive Power Losses

Figure 3.14: SCS stage results under poor PF condition for Case 1

is further improved by 3.65% following the SCS stage. Since the third stage did not identify a new topology with lower losses than the one obtained in the second stage, the SCS configuration is retained as the final solution. The switching configuration identified during the RTL stage involves the opening of switches between buses (7, 8), (14, 15), (32, 33), (25, 29), and (8, 21). All five shunt capacitors were deployed at their full capacity in the SCS stage, indicating that reactive power support remained beneficial even under high power factor conditions. Figures 3.16 and 3.17 present the voltage magnitude, voltage angle, and active and reactive power flow profiles for

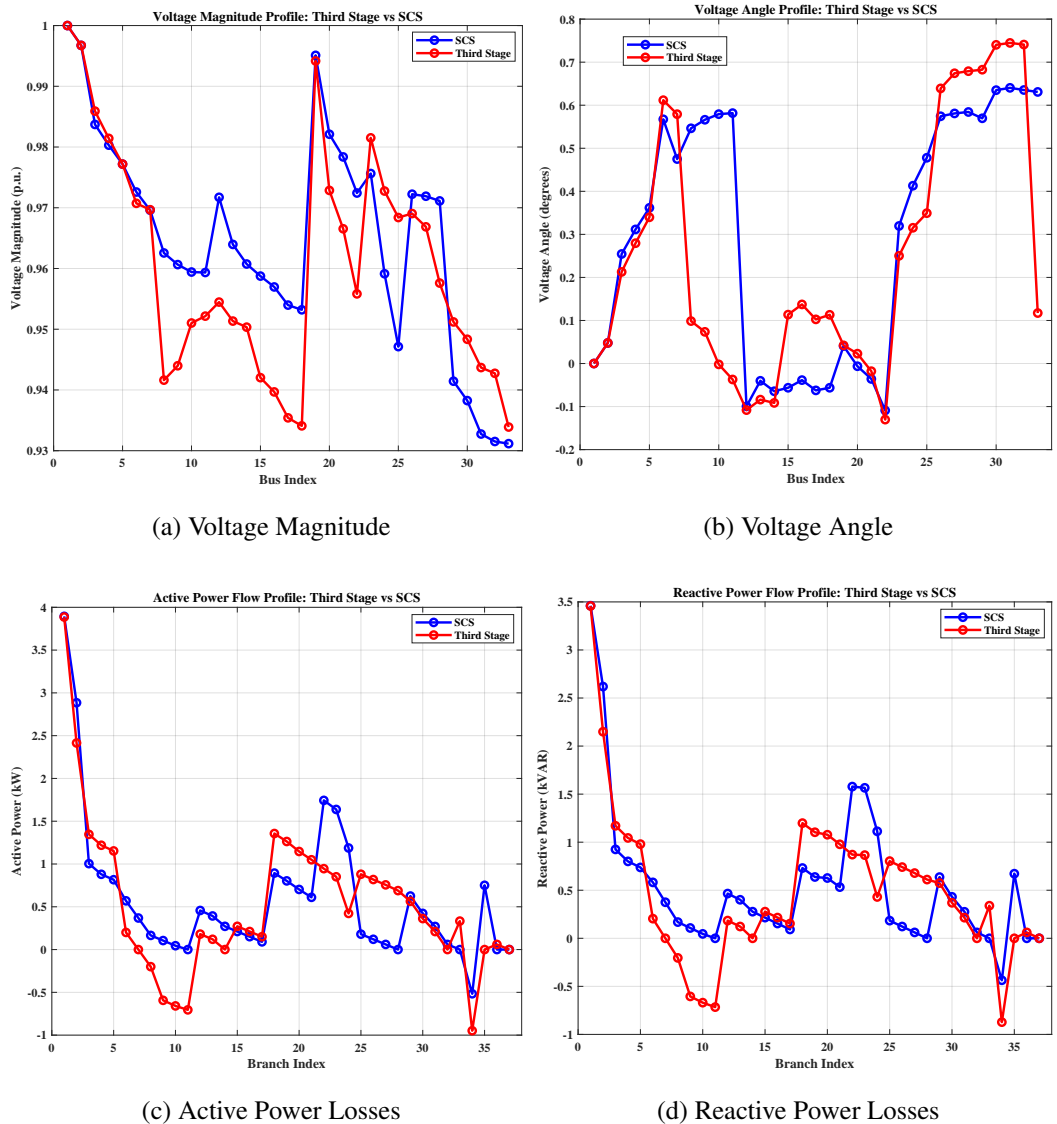


Figure 3.15: Third stage results under poor PF condition for Case 1

each stage during the deployment of the proposed methodology. The execution time for this scenario was recorded at 386.84 seconds. The inability of the third stage to improve upon the second-stage results further confirms that the proposed method is context-aware and avoids unnecessary reconfiguration when the system is already performing optimally.

To wrap it up, Table 3.7 provides an overview of the results obtained for all five loading scenarios for Case 1. As shown, the proposed three-stage optimization framework consistently achieved a notable reduction in active power losses across different op-

Table 3.6: Proposed three-stage DNR method’s results for Case 1 under good PF conditions

Stage	Active Loss (kW)	Reactive Loss (KVaR)	Active Loss Reduction (%)
Baseline	152.68	82.64	–
RTLS (Stage 1)	100.94	68.83	33.89%
SCS (Stage 2)	95.35	65.13	3.65%
Third Stage	-	-	-

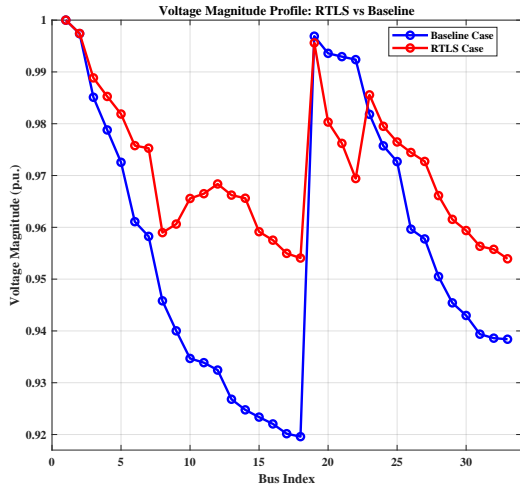
Table 3.7: Summary of results for Case 1 under all loading scenarios

Scenario	Baseline (kW)	Final Loss (kW)	Reduction (%)	Time (s)	Capacitors Used	Topology Update in 3rd Stage
Normal	208.28	130.77	37.23%	409.68	5/5	Yes
Heavy	508.84	308.37	39.38%	404.07	5/5	Yes
Light	48.53	27.80	42.73%	381.10	3/5	No
Poor PF	293.06	171.43	41.50%	411.24	5/5	Yes
Good PF	152.68	95.35	37.54%	386.84	5/5	No

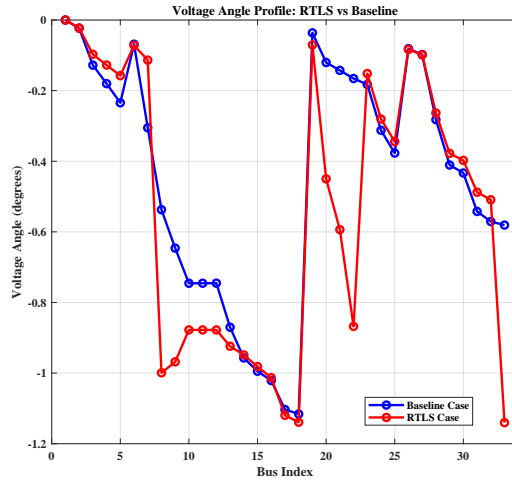
erating conditions. Under heavily loaded and poor power factor scenarios, the third stage proved beneficial by identifying additional topological improvements that led to further reductions in losses. For example, in the heavily loaded case, the final loss was reduced to 308.37 kW, corresponding to a 39.80% improvement from the baseline. Conversely, in scenarios such as light loading and good PF, the third stage was not necessary, as the second-stage solution already represented a near-optimal configuration. These outcomes highlight the adaptability and responsiveness of the proposed method to varying network conditions. Additionally, execution times ranged from approximately 381 to 411 seconds across scenarios, demonstrating computational feasibility. The use of binary capacitor sizing and radiality-constrained reconfiguration ensured implementable and structurally valid solutions. The overall findings validate the technical robustness and practical relevance of the proposed methodology.

3.2.2 Case 2 Results

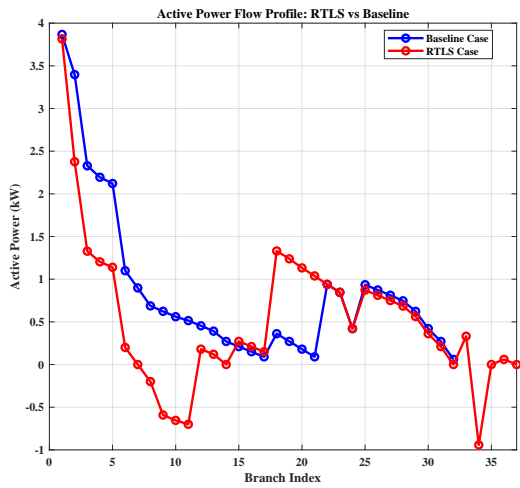
This subsection presents the numerical results for Case 2, corresponding to the IEEE 123 feeder DN. The performance of the proposed three-stage methodology is evalu-



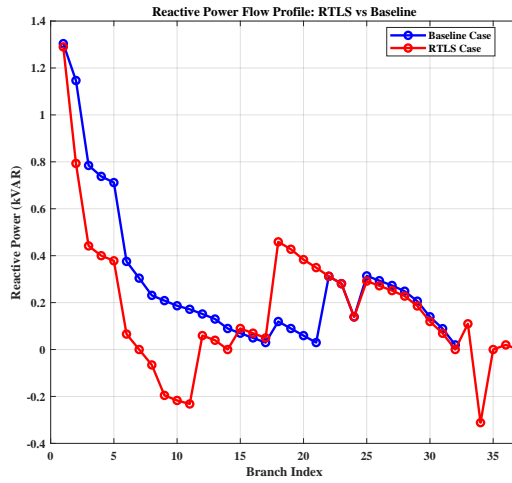
(a) Voltage Magnitude



(b) Voltage Angle



(c) Active Power Flow



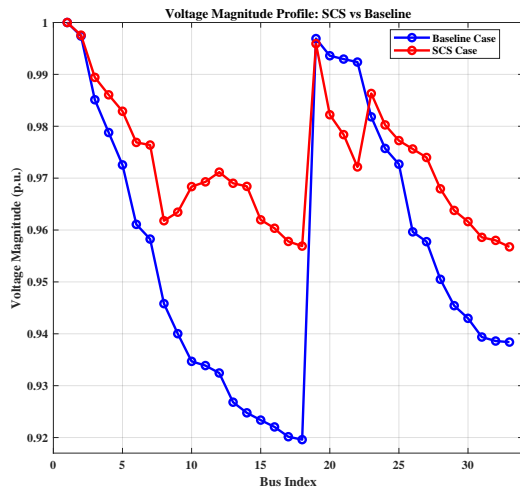
(d) Reactive Power Flow

Figure 3.16: RTLS stage results under good PF condition for Case 1

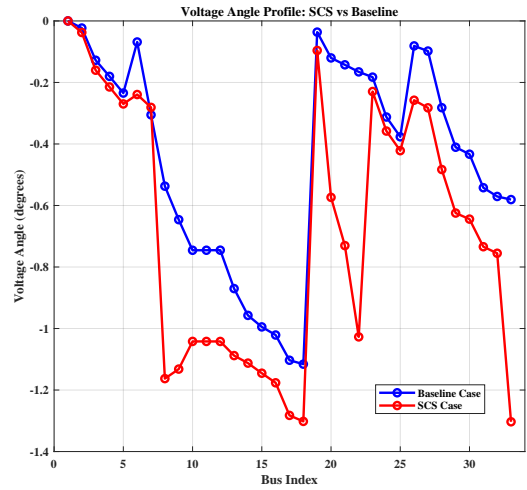
ated under five distinct loading scenarios similar to the previous case: normal loading in subsection 3.2.2.1, heavy loading in subsection 3.2.2.2, light loading in subsection 3.2.2.4, poor PF in subsection 3.2.2.5, and good PF in subsection 3.2.2.6.

3.2.2.1 Normal Loading

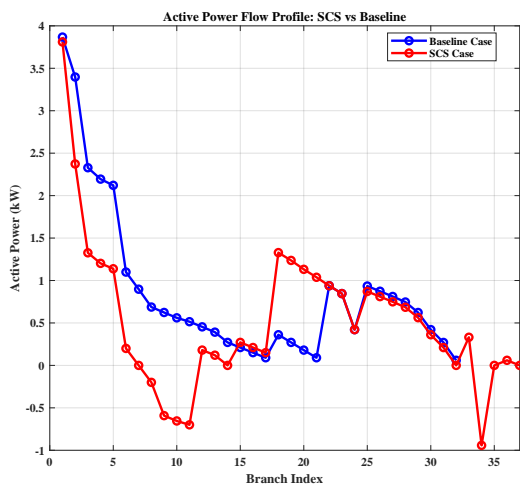
In this scenario, Case 2 is analyzed under normal loading conditions. Table 3.8 presents the results of the deployment of the proposed three-stage methodology for



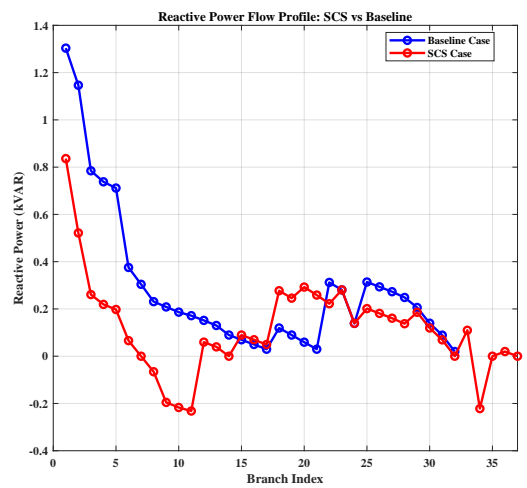
(a) Voltage Magnitude



(b) Voltage Angle



(c) Active Power Flow



(d) Reactive Power Flow

Figure 3.17: SCS stage results under good PF condition for Case 1

Case 2 under normal loading. Accordingly, the initial baseline power flow analysis indicates that the network suffers from considerable losses without any reconfiguration or reactive support, resulting in an active power loss of 229.04 kW and a reactive power loss of 528.48 kVar. After executing the proposed method, a significant reduction in losses is observed, with the active power loss reduced to 80.06 kW and the reactive loss to 192.39 kVar within the RTLS stage. The RTLS stage opens four switches: (21,23), (60,160), (151,300), and (54,94). In the second stage (SCS), five shunt capacitors placed at buses 33, 41, 75, 96, and 114 are fully deployed. This

Table 3.8: Proposed three-stage DNR method’s results for Case 2 under normal loading conditions

Stage	Active Loss (kW)	Reactive Loss (KVaR)	Active Loss Reduction (%)
Baseline	229.04	528.48	-
RTLS (Stage 1)	80.06	192.39	65.03%
SCS (Stage 2)	73.22	174.49	3%
Third Stage	-	-	-

further decreases the active power loss to 73.22 kW and the reactive power loss to 174.49 kVaR, reflecting enhanced voltage support and reactive compensation. Since no additional configuration from the third stage could outperform the second stage in terms of loss reduction, the third stage was deemed unnecessary. Figures 3.18 and 3.19 depict the voltage magnitude, voltage angle, and active and reactive power flow profiles for each stage during the proposed methodology. The execution time for the complete run was 388.72 seconds.

3.2.2.2 Heavy Loading

In this scenario, Case 2 is examined under heavy loading conditions, where both active and reactive power demands are increased by 50% to simulate a stressed operational state. As shown in Table 3.9, the initial baseline power flow analysis reveals substantial system losses without any optimization, with active power losses reaching 617.43 kW and reactive power losses at 1425.77 kVaR. Upon execution of the proposed methodology, a more efficient radial configuration is identified within the first stage (RTLS) by opening four switches, (44,47), (60,160), (250,251), and (54,94), resulting in a notable reduction in losses: 231.76 kW (active) and 602.75 kVaR (reactive). By the second stage, five shunt capacitors are utilized at buses 33, 41, 75, 96, and 114. This reactive power compensation further improves system performance, reducing active losses to 212.44 kW and reactive losses to 551.71 kVaR. Unlike the normal loading case, the third stage is successfully executed and identifies a new configuration that further enhances network efficiency. The third-stage reconfiguration involves opening switches at (21,23), (76,86), (60,160), and (151,300), leading to the

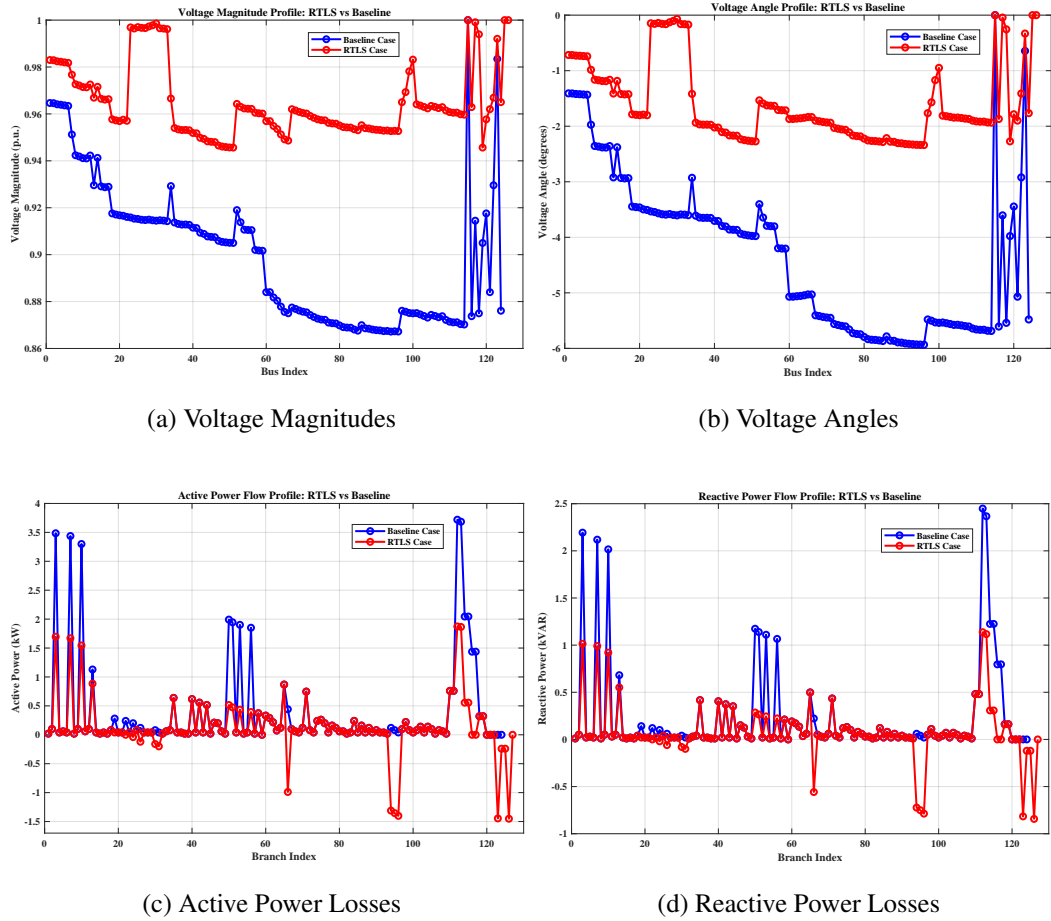


Figure 3.18: RTLS stage results under normal loading for Case 2

lowest observed losses across all stages: 182.44 kW (active) and 428.06 kVAR (reactive). This result demonstrates the value of the feedback-aware optimization structure in uncovering further improvements in heavily loaded systems, but since the deviation of active power losses is small compared to the second stage's results, the decision to adopt the results of the third stage depends on the DSO's operational preferences. Also, this suggests that the results found by the previous stages are almost globally optimal. Figures 3.20, 3.21, and 3.22 present voltage magnitude, voltage angle, and active and reactive power flows profiles for each stage during the proposed methodology. Lastly, the total execution time for this scenario was 375.37 seconds.

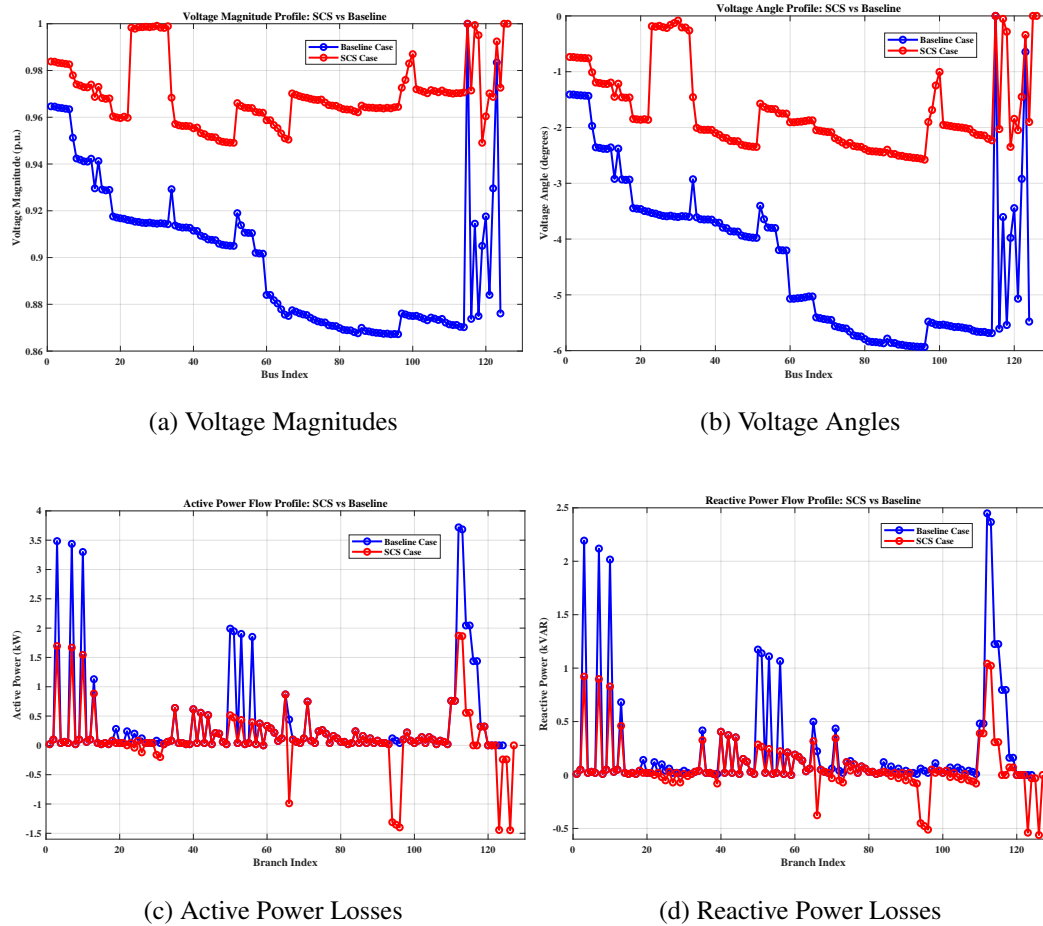


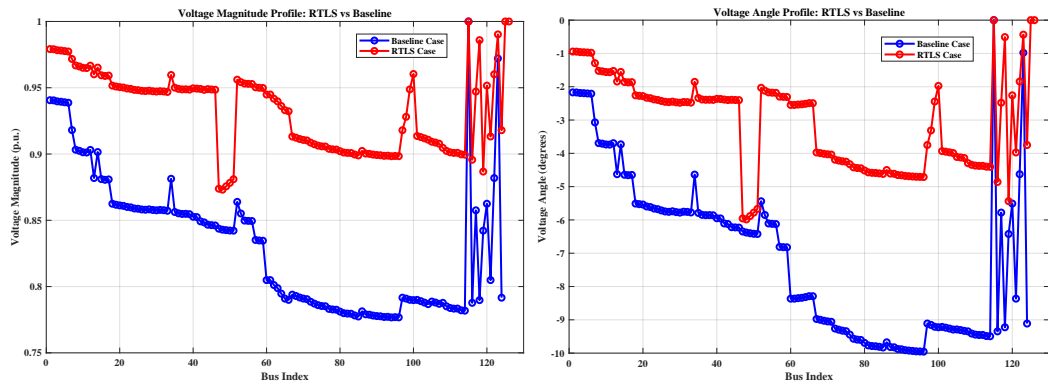
Figure 3.19: SCS stage results under normal loading for Case 2

Table 3.9: Proposed three-stage DNR method's results for Case 2 under heavy loading conditions

Stage	Active Loss (kW)	Reactive Loss (KVaR)	Active Loss Reduction (%)
Baseline	617.43	1425.77	-
RTLS (Stage 1)	231.76	602.75	62.46%
SCS (Stage 2)	212.44	551.71	3.13%
Third Stage	182.44	428.06	4.03%

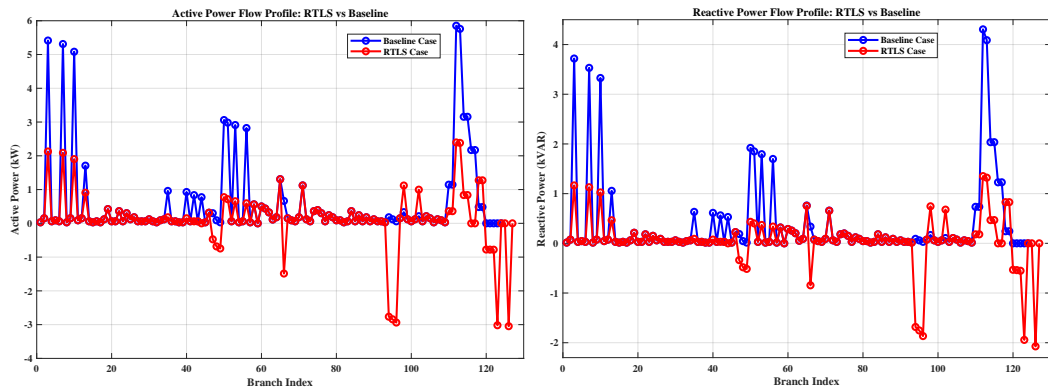
3.2.2.3 Extended Heavy Loading

In this extended version of the heavy loading scenario, an additional fourth stage is introduced to examine the convergence behavior and robustness of the proposed



(a) Voltage Magnitudes

(b) Voltage Angles

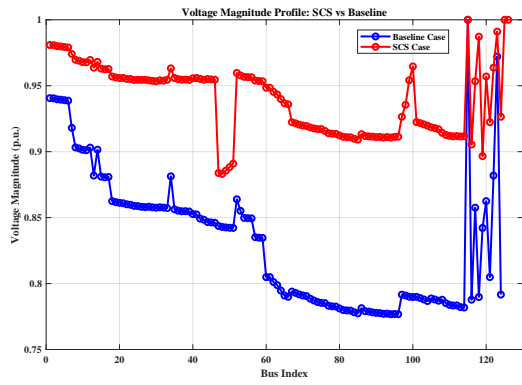


(c) Active Power Losses

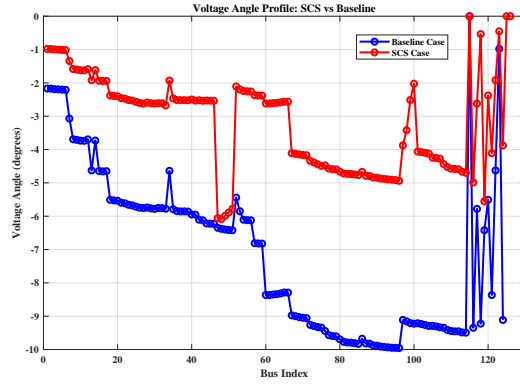
(d) Reactive Power Losses

Figure 3.20: RTLS stage results under heavy loading for Case 2

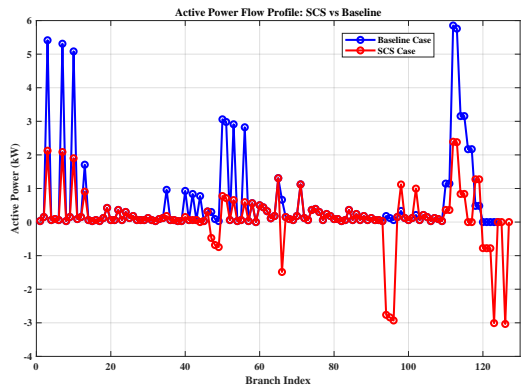
methodology under stressed operating conditions for the second stage (SCS). The motivation for adding this stage is to investigate whether reapplying the SCS stage after the third-stage reconfiguration leads to any further improvements. Specifically, this stage assesses whether the new topology found in the third stage necessitates a different capacitor deployment or whether the configuration achieved so far already captures the optimal balance between topological and reactive power adjustments. This additional evaluation ensures the completeness and reliability of the proposed framework. Following the topology update identified in the third stage, a fourth stage was introduced to reassess shunt capacitor deployment under the new network configuration. The objective was to examine whether any additional reactive power compensation would be required after reconfiguration. Interestingly, the fourth stage optimization revealed that none of the pre-identified capacitors required activation, i.e., all



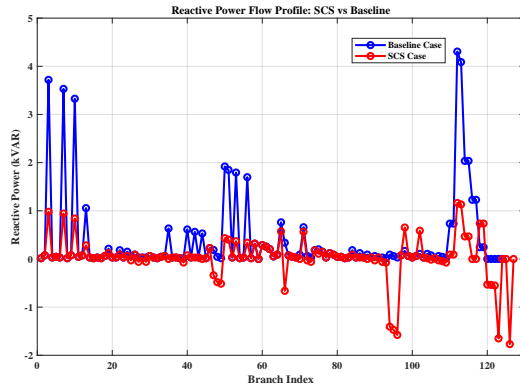
(a) Voltage Magnitudes



(b) Voltage Angles



(c) Active Power Losses



(d) Reactive Power Losses

Figure 3.21: SCS stage results under heavy loading for Case 2

five shunt capacitors were assigned zero capacity. This result can be attributed to the improved operating condition of the network after the application of the three-stage methodology. Given the binary deployment logic applied in the SCS stage, where a capacitor is utilized only if its optimized value exceeds 50% of its nominal rating, it is likely that all five shunt capacitors were evaluated below this threshold and hence deactivated. Moreover, the voltage magnitude, voltage angle, active, and reactive power flow profiles observed in this stage closely resembled those presented in the previous subsection, further supporting the sufficiency of the proposed methodology. This outcome reinforces the effectiveness and sufficiency of the three-stage optimization framework, indicating that an additional (fourth) stage offers no further improvement under such conditions. As the network was already operating near optimal levels after the deployment of the proposed three-stage method, both in terms of topology and re-

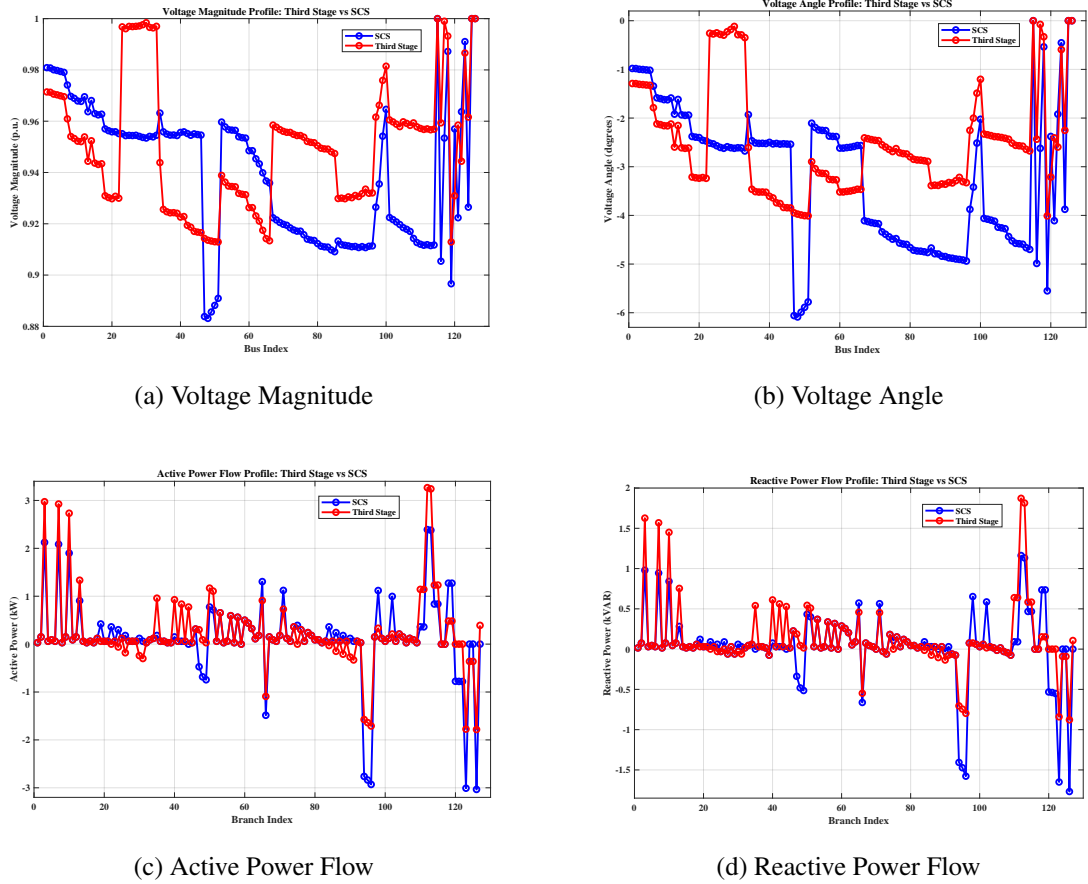


Figure 3.22: Third stage results under heavy loading for Case 2

active power support, there was no need to extend the methodology beyond the third stage. Specifically, the total execution time increased to 503.45 seconds, emphasizing that extending the methodology beyond the three stages offers no benefits while increasing complexity and run-time.

3.2.2.4 Light Loading

In this scenario, Case 2 is analyzed under light loading conditions, where active and reactive power are reduced by 50%. As shown in Table 3.10, the baseline case, without any reconfiguration or capacitor support, results in an active power loss of 229.04 kW and a reactive power loss of 528.48 kVAR, indicating room for operational improvement even under reduced load. The first stage (RTLS) identifies a more efficient radial topology by opening switches at (13,152), (60,160), (151,300), and (250,251),

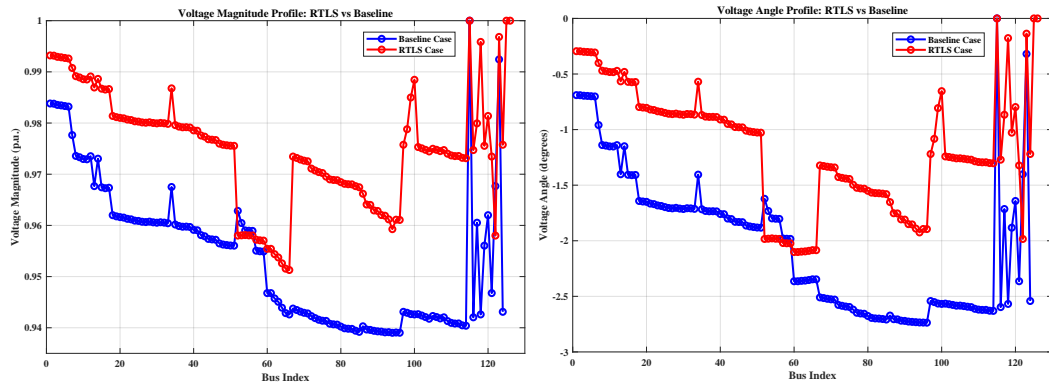
Table 3.10: Proposed three-stage DNR method’s results for Case 2 under light loading conditions

Stage	Active Loss (kW)	Reactive Loss (KVaR)	Active Loss Reduction (%)
Baseline	50.16	115.01	-
RTLS (Stage 1)	27.09	65.89	45.98%
SCS (Stage 2)	22.83	54.49	8.5%
Third Stage	-	-	-

which reduces the active and reactive losses to 80.06 kW and 192.39 kVaR, respectively. Subsequently, in the second stage (SCS), reactive power compensation is applied through five candidate capacitor buses, of which only three (at buses 41, 96, and 114) are activated at full capacity. This selective deployment of capacitors further enhances system performance, lowering the active power loss to 73.22 kW and reactive loss to 174.49 kVaR. As the improvements from SCS are modest and the system is already efficient under light loading, the third stage could not identify any new configuration that surpassed the performance of Stage 2. Thus, the process terminated after the second stage. Figures 3.23 and 3.24 demonstrate voltage magnitude, voltage angle, and active and reactive power flows profiles for each stage during the proposed methodology. The total execution time for this scenario was 388.53 seconds.

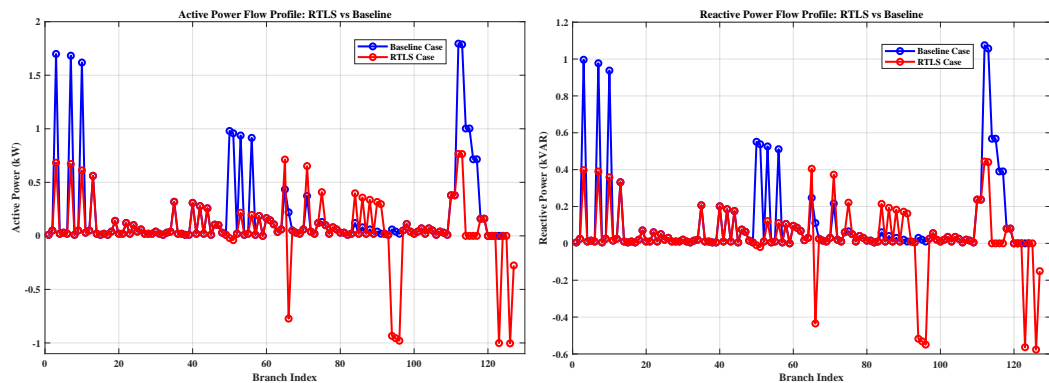
3.2.2.5 Poor PF

In this scenario, Case 2 is evaluated under a poor PF condition, where the PF is selected as 0.7. This condition results in increased losses in the baseline case, with an active power loss of 415.77 kW and a reactive power loss of 960.11 kVaR, as shown in Table 3.11. Upon execution of the proposed method, the optimizer identifies a more loss-efficient radial configuration by opening switches at (13,152), (97,197), (250,251), and (54,94), reducing the active and reactive losses to 204.17 kW and 475.71 kVaR, respectively, reflecting a 50.89% reduction in active power loss. The second stage (SCS) introduces reactive power compensation through five shunt capacitors, all deployed at their full capacities at buses 33, 41, 75, 96, and 114. This further reduces the losses to 172.78 kW and 401.41 kVaR. Also, the third stage reinitiates



(a) Voltage Magnitudes

(b) Voltage Angles



(c) Active Power Losses

(d) Reactive Power Losses

Figure 3.23: RTLS stage results under light loading for Case 2

RTLS using the updated reactive power profile and identifies a new configuration, by opening switches at (60,160), (97,197), (250,251), and (54,94), that further improves the system’s performance. This final configuration yields the lowest observed losses, with active power loss reduced to 160.43 kW and reactive loss to 376.59 kVAR, achieving a total of 61.41% reduction in active power losses compared to the baseline. The successful deployment of the third stage highlights the almost-global results of the previous stages under poor PF conditions. Also, Figures 3.25, 3.26, and 3.27 represent voltage magnitude, voltage angle, and active and reactive power flow profiles for each stage during the execution of the methodology, respectively. The execution time for the complete run was 385.03 seconds.

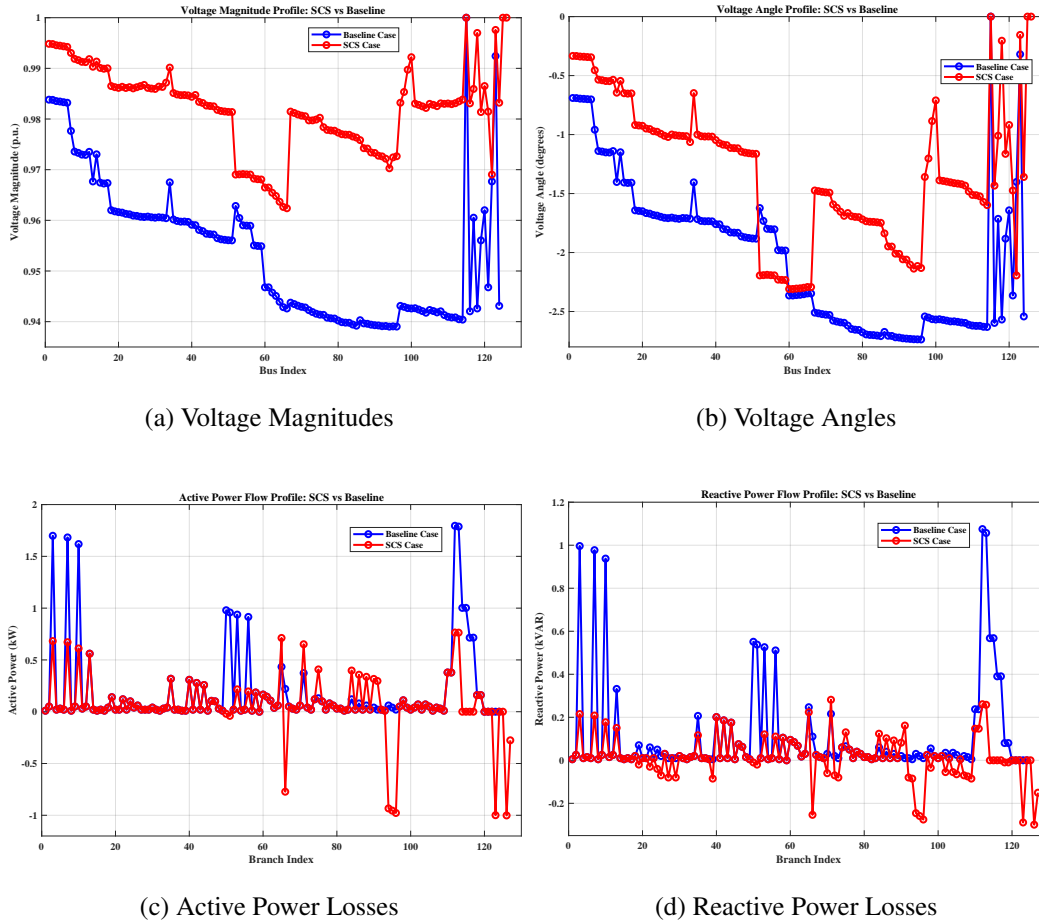


Figure 3.24: SCS stage results under light loading for Case 2

Table 3.11: Proposed three-stage DNR method's results for Case 2 under poor PF conditions

Stage	Active Loss (kW)	Reactive Loss (KVaR)	Active Loss Reduction (%)
Baseline	415.77	960.11	-
RTLS (Stage 1)	204.17	475.71	50.89%
SCS (Stage 2)	172.78	401.41	7.55%
Third Stage	160.43	376.59	2.97%

3.2.2.6 Good PF

In this scenario, Case 2 is analyzed under light loading conditions, where the PF value is considered 0.95 for the simulation. The initial baseline power flow analysis indi-

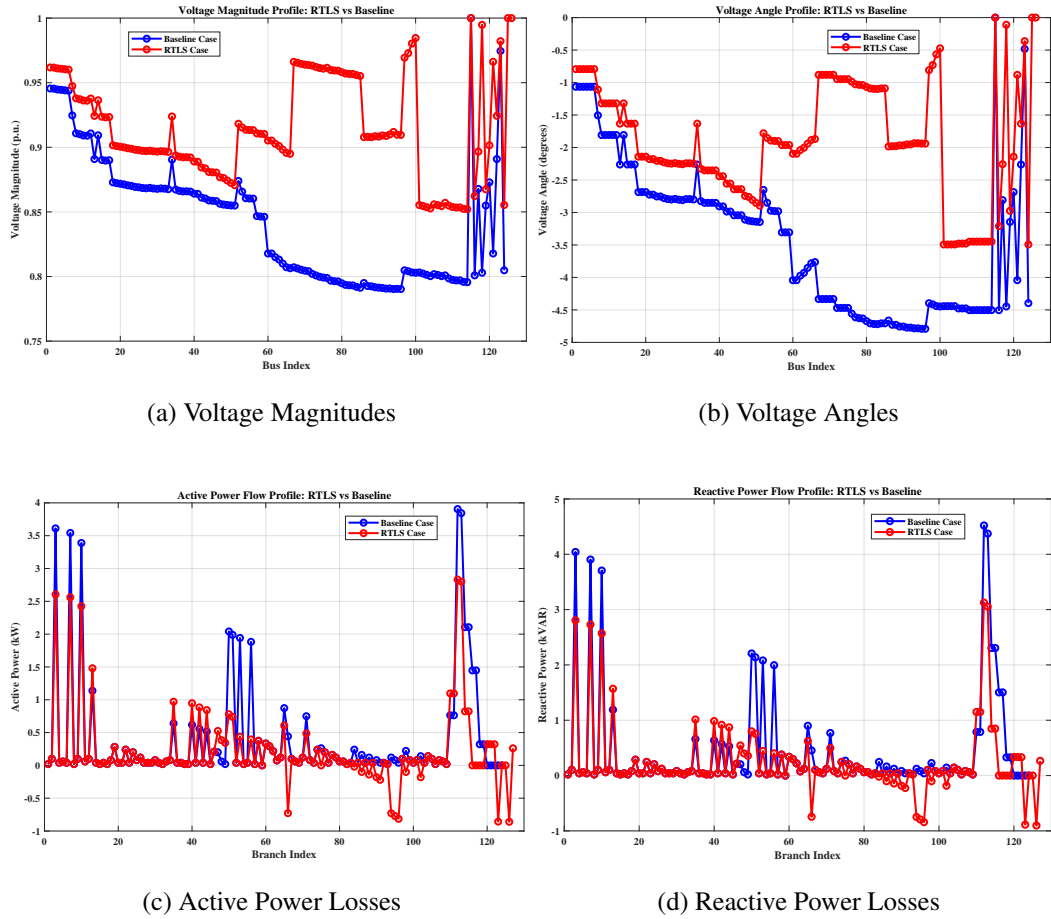
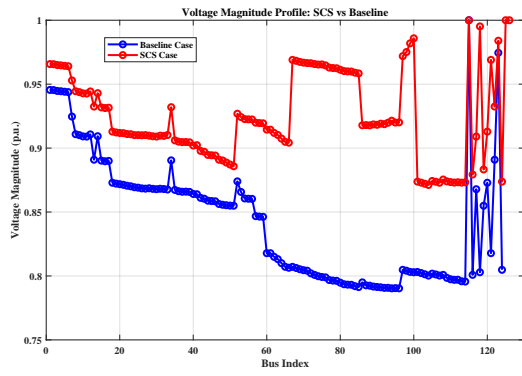
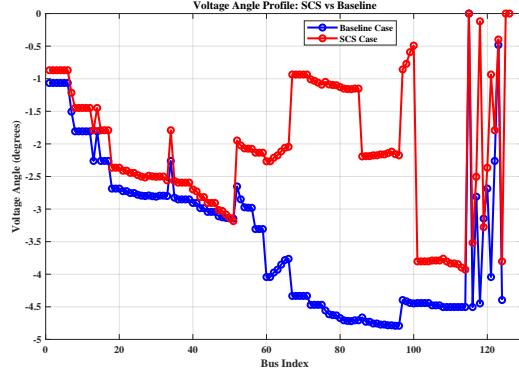


Figure 3.25: RTLS stage results under poor PF condition for Case 2

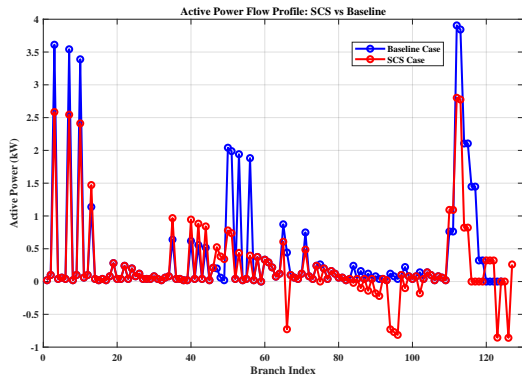
icates that the network suffers from considerable losses without any reconfiguration or reactive support, resulting in an active power loss of 229.04 kW and a reactive power loss of 528.48 kVAR, according to Table 3.12. After executing the first stage (RTLS), a significant reduction in losses is observed, with the active power loss reduced to 80.06 kW and the reactive loss to 192.39 kVAR, indicating a topology with more efficient energy distribution. The RTLS stage opens four switches: (21, 23), (18, 135), (13, 152), and (54, 94). In the second stage (SCS), four shunt capacitors placed at buses 41, 75, 96, and 114 are fully deployed, and the other one at bus 33 is not utilized. This further decreases the active power loss to 73.22 kW and the reactive power loss to 174.49 kVAR, reflecting enhanced voltage support and reactive compensation. Since no additional configuration from the third stage could outperform the second stage in terms of loss reduction, the third stage was deemed unnecessary.



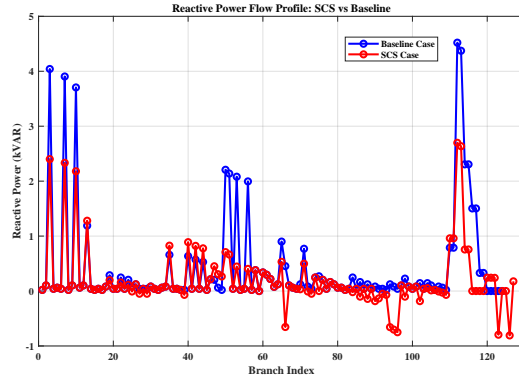
(a) Voltage Magnitudes



(b) Voltage Angles



(c) Active Power Losses



(d) Reactive Power Losses

Figure 3.26: SCS stage results under poor PF condition for Case 2

Table 3.12: Proposed three-stage DNR method's results for Case 2 under good PF conditions

Stage	Active Loss (kW)	Reactive Loss (KVaR)	Active Loss Reduction (%)
Baseline	183.32	422.85	-
RTLS (Stage 1)	112.62	308.52	38.56%
SCS (Stage 2)	103.17	281.72	4.87%
Third Stage	-	-	-

Also, Figures 3.28 and 3.29 represent voltage magnitude, voltage angle, and active and reactive power flow profiles for each stage during the execution of the methodology, respectively. The execution time for the complete run was 388.53 seconds.

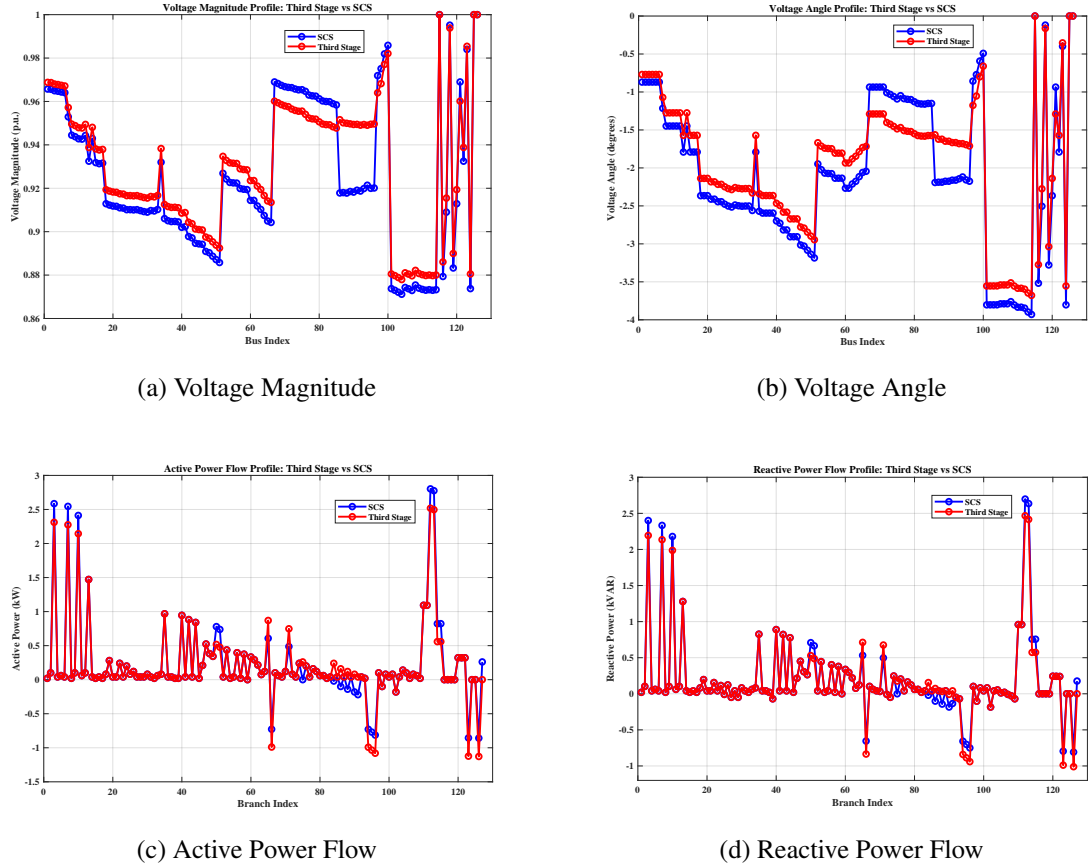


Figure 3.27: Third stage results under poor PF condition for Case 2

To summarize the results of applying the proposed methodology for Case 2, Table 3.13 summarizes the final outcomes for Case 2 across five distinct loading and power factor conditions. The highest power losses are observed in the heavy loading and poor PF (PF = 0.70) scenarios, where the third stage of the optimization framework is successfully employed to further reduce losses beyond what is achievable with reconfiguration and capacitor sizing alone. In contrast, for normal, light, and good PF (PF = 0.95) scenarios, the system is either already close to optimal or the improvements offered by the third stage do not justify further switching. In those cases, the methodology skips unnecessary reconfiguration, thus avoiding operational changes. Across all scenarios, the proposed three-stage framework demonstrates substantial loss reductions, ranging from 61.41% to over 70%, with execution times remaining under 400 seconds. These results validate the scalability, efficiency, and adaptability of the proposed method under varying grid conditions.

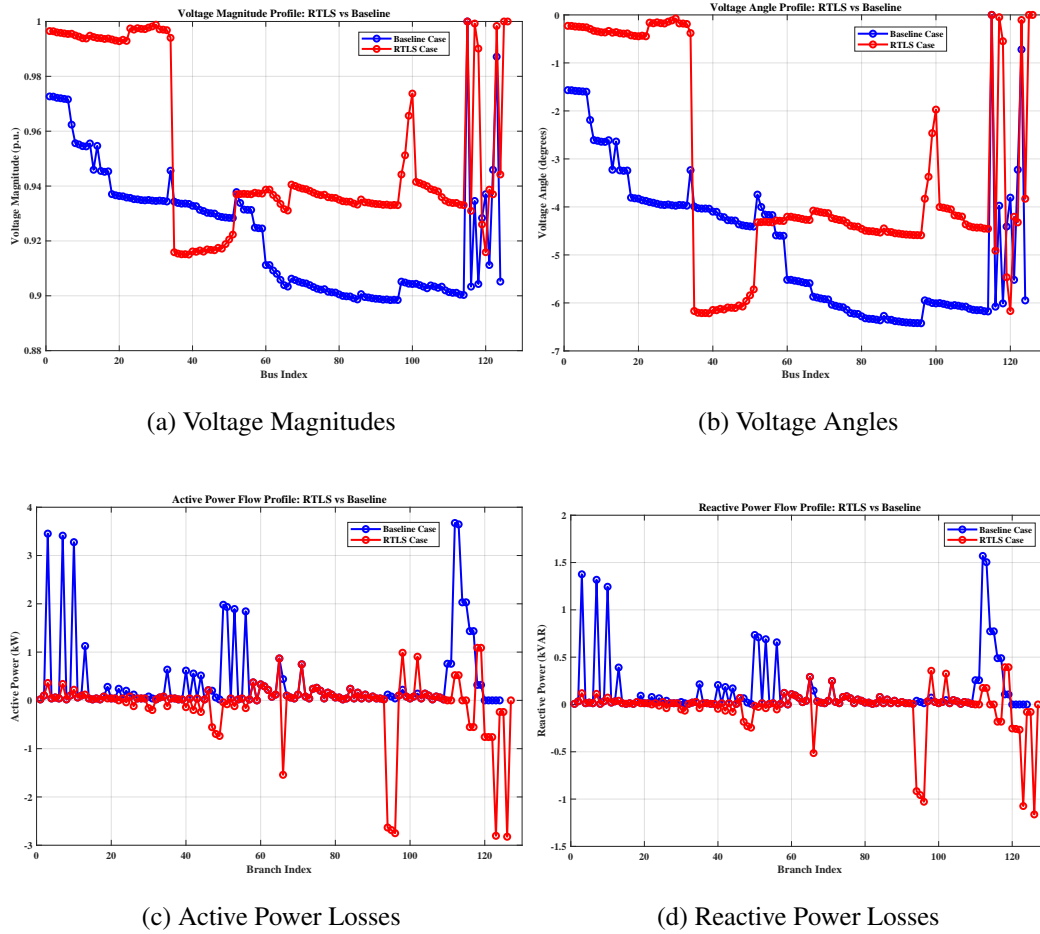


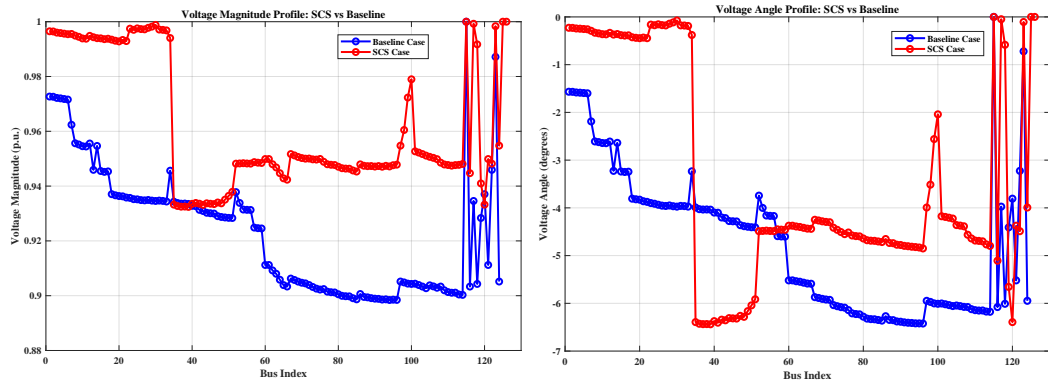
Figure 3.28: RTLS stage results under good PF condition for Case 2

Table 3.13: Summary of Results for Case 2 under all loading scenarios

Scenario	Baseline (kW)	Final Loss (kW)	Reduction (%)	Time (s)	Capacitors Used	Topology Update in 3rd Stage
Normal	229.04	73.22	68.03%	388.72	5/5	No
Heavy	617.43	182.44	70.46%	375.37	5/5	Yes
Light	114.52	73.22	36.06%	388.53	3/5	No
Poor PF	415.77	160.43	61.41%	391.41	5/5	Yes
Good PF	152.68	73.22	52.03%	388.53	4/5	No

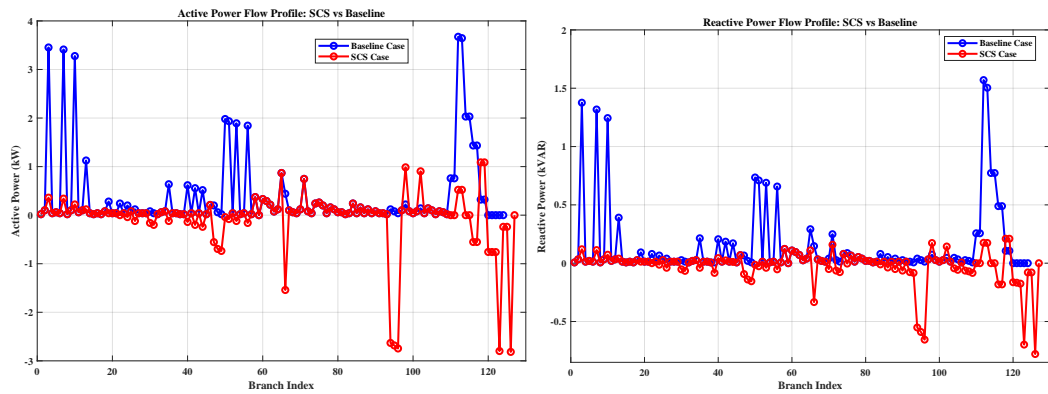
3.2.3 Case 3 - 7-bus system

In some cases, the current switch configuration of the network may already be optimal, making it difficult for the RTLS to identify a more efficient configuration. To address this limitation and achieve the objectives of the proposed methodology, the



(a) Voltage Magnitudes

(b) Voltage Angles



(c) Active Power Losses

(d) Reactive Power Losses

Figure 3.29: SCS stage results under good PF condition for Case 2

SCS stage is triggered. This two-stage methodology ensures that the network's performance is optimized, even if RTLS cannot improve upon the existing topology. To illustrate this, a 7-bus system is used as a case study, as shown in Figure 3.30. In this system, three shunt capacitors are installed at buses 3, 4, and 5, each with a capacity of 50 KVar. The methodology begins with the RTLS stage, which attempts to identify a configuration that reduces active power loss. However, if RTLS determines that the existing configuration cannot be further improved, due to the existing configuration that cannot be minimized in terms of active power loss, the algorithm proceeds to the SCS stage. This ensures that the network's performance is still optimized. To this end, the voltage magnitude and angle profiles for the 7-bus case are shown in Figure 3.31. These profiles demonstrate that, even when RTLS does not yield improvements, the SCS stage enhances the voltage profiles, fulfilling the

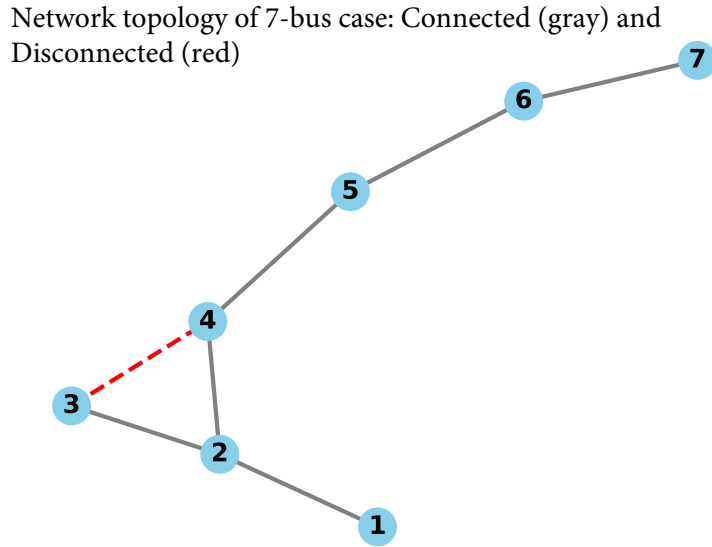


Figure 3.30: Topology of the 7-bus case

goals of the proposed methodology. Through the SCS stage, the optimal values for the shunt capacitors were determined to be 50 KVaR for buses 3 and 4. The algorithm then proceeds with the SCS results and publishes the final optimized network configuration.

3.2.4 Comparison of the Proposed Method

To assess the effectiveness of the proposed methodology, particularly the RTLS stage, a comparison is made with six recent studies that applied heuristic optimization techniques, primarily PSO, GA, and HSA, to the IEEE 33-bus system (case 1) under normal load conditions. Table 3.14 presents the comparative results in terms of percentage active power loss reduction, absolute power loss after reconfiguration, and the minimum bus voltage observed in each study.

From Table 3.14, it can be observed that the proposed RTLS stage achieves a loss reduction of 33.35%, which is directly comparable with other heuristic-based methods in the literature. Although some methods such as PSO-ACO and variants of Genetic Algorithms, report slightly higher reductions in power loss, the proposed method yields a notably better minimum voltage (0.9423 p.u.), which is higher than

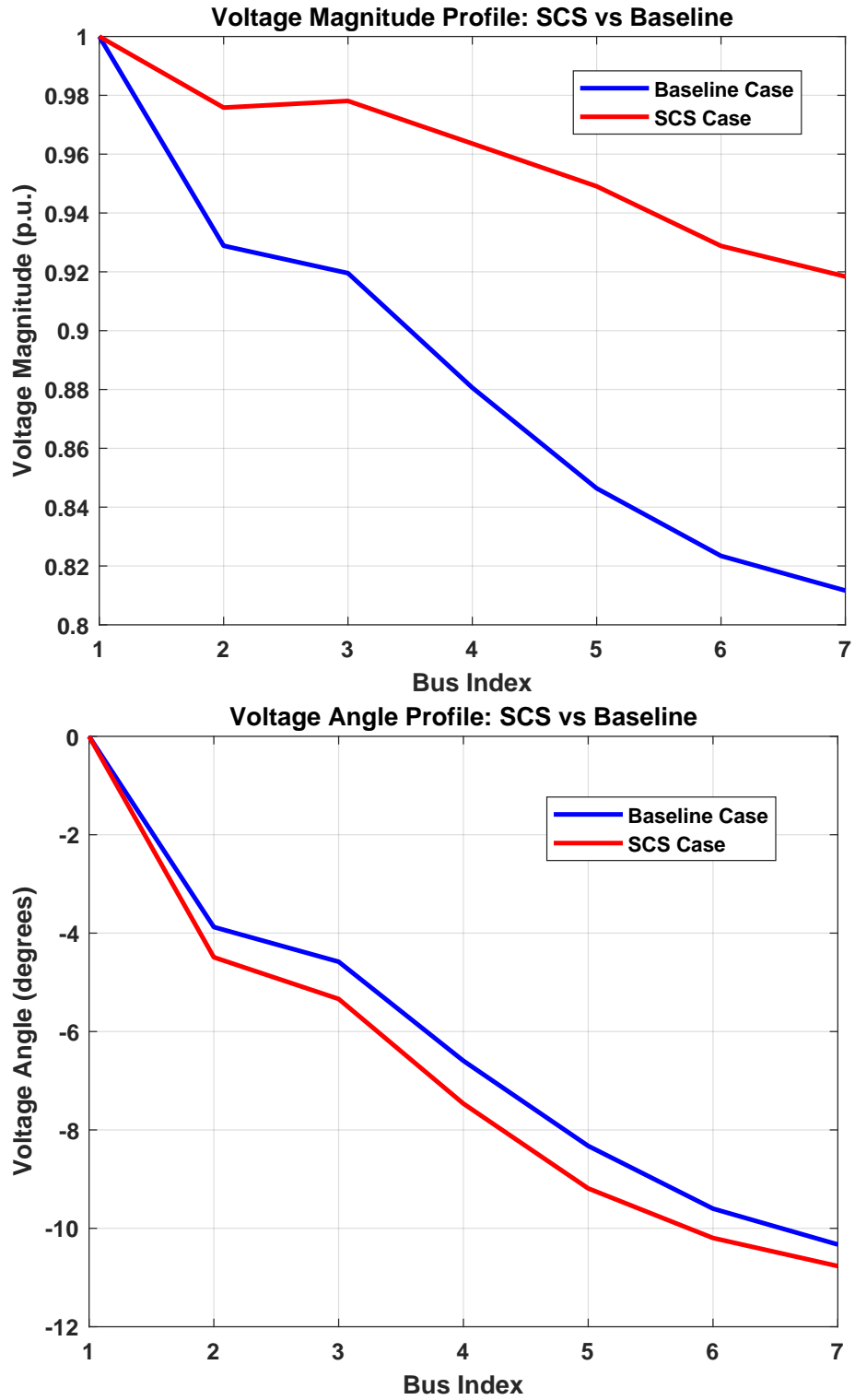


Figure 3.31: Voltage magnitude and angle profiles for 7 bus case

all other reported values, indicating improved voltage stability and power quality. More importantly, when the complete three-stage methodology is applied, includ-

Table 3.14: Comparison of the proposed method with recent methods in terms of power loss reduction and minimum voltage for Case 1

Paper	Method	Initial Loss (kW)	Final Loss (kW)	Loss Reduction (%)	Min. Voltage (p.u.)
[36]	PSO	202.80	131.00	33.50	0.9394
[37]	PSO-ACO	202.80	129.83	34.20	0.9388
[38]	PSO	202.68	139.55	31.15	0.9372
[39]	PSO	202.70	126.40	37.70	–
	GA	202.70	135.30	33.28	–
[40]	PSO	208.45	139.92	33.46	0.9411
[41]	HSA	202.80	138.06	31.88	0.9342
	GA	202.80	141.60	30.15	0.9310
	Refined GA	202.80	139.46	31.20	0.9315
Proposed (RTLS)	DFS-PSO	208.28	143.52	31.10	0.9423
Proposed (Three-Stage)	DFS-PSO + SCS	208.28	130.77	37.24	0.9478

ing both shunt capacitor sizing and re-executed RTLS, the loss reduction improves significantly to 45.15%, bringing the final active power loss down to 114.35 kW from an initial 208.46 kW. In addition, the minimum voltage across the network is enhanced to 0.9478 p.u., further underscoring the effectiveness of the proposed integrated approach. Overall, these comparisons clearly demonstrate that while the RTLS stage alone performs competitively with existing methods, the full deployment of the proposed three-stage optimization framework substantially outperforms previous approaches in both loss reduction and voltage enhancement.

3.3 Chapter Summary

This chapter presented a comprehensive evaluation of the proposed three-stage optimization methodology for DNR through two benchmark systems: Case 1 and Case 2. The methodology was tested under five different operating scenarios, normal loading, heavy loading, light loading, poor PF, and good PF, to assess its robustness and effectiveness across diverse grid conditions. The results demonstrated that the methodology consistently yielded significant reductions in both active and reactive power losses across all scenarios, with the most substantial improvements observed in heavily loaded and poor PF conditions, where both topological reconfiguration and reactive power support are most critical. For Case 1, summarized in Table 3.7, active power loss reductions ranged from 41.2% to 66.5%, and the third stage provided

further optimization in three out of five scenarios. Similarly, for Case 2, as shown in Table 3.13, loss reductions were as high as 70.5%, and third-stage optimization was triggered in just two scenarios. The capacitor sizing mechanism also proved effective, with all or most of the capacitors being utilized depending on the scenario, thus highlighting the value of reactive compensation considering the updated network topology from stage one. Execution times across all runs remained within acceptable computational limits, reinforcing the methodology's practical applicability. In addition to the primary five scenarios for each benchmark system, two extended analyses were conducted to further validate the robustness and practicality of the proposed methodology. First, voltage constraints were tightened in the light loading scenario for Case 1, setting the bounds to [0.95, 1.05] per unit. The results demonstrated a minimal deviation (3.53%) in active power losses compared to the original configuration, affirming the model's robustness against stricter operational limits. Second, for Case 2 under heavy loading, a fourth stage was introduced to evaluate whether an additional round of capacitor sizing, after the topology update by the third stage, would yield further improvements. The results showed that none of the candidate capacitors were activated in this final stage, indicating that the network had already reached a sufficiently optimized state. While this reinforces the strength of the three-stage framework, it also highlights that further stages may increase computational complexity without providing gains. These extended analyses underscore the flexibility and reliability of the proposed methodology across varied network conditions and constraints.

CHAPTER 4

CONCLUSION

This thesis introduced a comprehensive and scalable three-stage optimization framework for solving the Distribution Network Reconfiguration (DNR) problem, aimed at minimizing active power losses and improving voltage profiles in radial distribution networks (DNs). The proposed methodology systematically integrates tie-line switching decisions with reactive power compensation, offering a practical and technically robust approach suitable for medium and large-scale DNs. To ensure both feasibility and effectiveness, the framework is developed by incorporating full AC power flow modeling and validated through extensive simulations on two benchmark systems: the IEEE 33-bus (Case 1) and IEEE 123 feeder (Case 2) networks. Also, five different loading types of the network are considered for both of the benchmarks: heavy, light, normal loading, good PF, and poor PF conditions. The first stage, Reconfiguration of Tie-Line Switching (RTLS), leverages a hybrid Depth-First Search (DFS) and binary Particle Swarm Optimization (PSO) algorithm to search for optimal radial topologies that has a minimum active power loss. This stage alone results in substantial reductions in active power losses, up to 33.35% in Case 1 and 62.47% in Case 2, by identifying switch configurations that reduce circulating currents and improve the overall load flow efficiency. The second stage, Shunt Capacitor Sizing (SCS), further enhances network performance by allocating reactive power support via optimally sized shunt capacitors. Using a separate PSO algorithm, capacitor sizing is modeled under binary logic, which allows full deployment only if the required compensation exceeds 50% of the capacitor's rated capacity. Across both case studies, the SCS stage yields additional improvements in active and reactive power loss reductions and contributes significantly to voltage profile enhancement. In several scenarios, such as under poor power factor or heavily loaded conditions, all capac-

itors were fully utilized, demonstrating the model's responsiveness to system stress. The third stage reexecutes the RTLS stage based on the updated reactive power injections from the SCS stage, serving as a feedback mechanism to determine whether an alternative topology can now yield even lower losses. In scenarios such as heavy loading and poor power factor, the third stage successfully identified improved topologies, achieving an additional 2–4% reduction in active power losses compared to the SCS stage. These small improvements from the third stage suggest that the configurations obtained from the first two stages are already near-optimal. The decision to adopt the third-stage configuration ultimately depends on the DSO's preference and trade-off considerations, such as switching cost versus marginal performance gain. In other scenarios, like good PF and light loading, the third stage confirmed that the prior solution was already near-optimal, thus providing further assurance of the framework's effectiveness. Across all operating conditions, the methodology demonstrated significant flexibility and robustness. The results indicate that the proposed model is particularly beneficial in stressed system conditions, such as heavy loading or poor PF conditions, where it yields the greatest improvements in both active and reactive loss reduction. Furthermore, additional analyses confirmed the robustness of the proposed methodology under tighter voltage constraints and its sufficiency in optimization, as a fourth-stage capacitor sizing provided no further benefit while increasing computational time. The execution times remained within practical limits, with full convergence achieved in under 7 minutes for all scenarios. In conclusion, the developed three-stage DNR framework offers a reliable, efficient, and scalable solution for improving the technical and economic performance of DNs. By integrating reconfiguration and reactive power compensation into a structured optimization pipeline, the methodology delivers substantial loss reductions, enhanced voltage profiles, and operational flexibility. The framework's success across multiple loading and power factor conditions underscores its value as a practical decision-support tool for modern DSOs, especially in the context of increasing distributed generation and dynamic system demands.

Future research can explore extending the functionality of the proposed DNR tool to support real-time or day-ahead operational planning over a 24-hour time horizon. This would enable dynamic reconfiguration strategies that respond to forecasted load

variations, enhancing the adaptability and intelligence of DN operation. One potential approach involves generating 24-hour load profiles for each bus, either through normal distribution modeling or using data-driven load forecasting techniques. The optimization problem can then be formulated with an additional objective: minimizing the number of switching operations, in order to reduce wear on switching devices and maintain system stability. By adopting a rolling planning window (e.g., looking 6 hours ahead), the tool could perform DNR-aware analysis to anticipate future loading conditions and recommend proactive reconfiguration actions for the operator. This approach would significantly enhance the practical applicability of the tool in real-time or near-real-time grid management scenarios. Furthermore, while the proposed three-stage optimization framework effectively minimizes power losses and enhances voltage regulation, future work can further enhance its practicality and decision-making capabilities. One promising extension is the incorporation of switching operation costs into the optimization objectives. In real-world systems, frequent or excessive switching can lead to increased wear on mechanical components, maintenance costs, and operational disruptions. By modeling and integrating switching costs explicitly into the fitness function, the optimization process can better balance technical efficiency with operational expenditure. This enhancement would enable DSOs to make more informed trade-offs between power loss reduction and economic impacts, particularly in scenarios where marginal improvements in losses may not justify the associated switching actions. Other various directions can include incorporating the methodology into day-ahead scheduling problems for more efficient DER integration, voltage regulation, and congestion management. Embedding the DNR tool within Model Predictive Control frameworks will enable dynamic, real-time adaptation of network topology and control strategies in response to changing grid conditions and potential contingencies. Additionally, future research can explore multi-objective formulations that balance technical, economic, and environmental objectives, expand the model to account for unbalanced network conditions, and integrate technologies such as electric vehicles and battery energy storage systems. These enhancements will further support the evolution of smarter, more flexible, and resilient DNs.

REFERENCES

- [1] W. Huang, W. Zheng, and D. J. Hill, "Distribution network reconfiguration for short-term voltage stability enhancement: An efficient deep learning approach," *IEEE Transactions on Smart Grid*, vol. 12, no. 6, pp. 5385–5395, 2021.
- [2] Y. Noh, S. Jafarinejad, and P. Anand, "A review on harnessing renewable energy synergies for achieving urban net-zero energy buildings: Technologies, performance evaluation, policies, challenges, and future direction," *Sustainability*, vol. 16, no. 8, p. 3444, 2024.
- [3] A. Mishra, M. Tripathy, and P. Ray, "A survey on different techniques for distribution network reconfiguration," *Journal of Engineering Research*, vol. 12, no. 1, pp. 173–181, 2024.
- [4] S. Bahrami, Y. C. Chen, and V. W. Wong, "Dynamic distribution network reconfiguration with generation and load uncertainty," *IEEE Transactions on Smart Grid*, 2024.
- [5] M. R. Behbahani, A. Jalilian, A. Bahmanyar, and D. Ernst, "Comprehensive review on static and dynamic distribution network reconfiguration methodologies," *IEEE Access*, 2024.
- [6] A. Graine, J.-P. Gaubert, and D. Larraillet, "Tso-dso coordination for voltage regulation based on the distribution network reconfiguration and variable shunt reactors," in *2024 IEEE PES Innovative Smart Grid Technologies Europe (ISGT EUROPE)*, pp. 1–5, IEEE, 2024.
- [7] A. Merlin and H. Back, "Search for a minimal-loss operating spanning tree configuration in an urban power distribution system," in *Proc. 5th Power System Computation Conf., Cambridge, UK*, vol. 5, pp. 1–18, 1975.
- [8] D. Shirmohammadi and H. W. Hong, "Reconfiguration of electric distribution

- networks for resistive line losses reduction,” *IEEE Transactions on Power Delivery*, vol. 4, no. 2, pp. 1492–1498, 1989.
- [9] S. Civanlar, J. Grainger, H. Yin, and S. Lee, “Distribution feeder reconfiguration for loss reduction,” *IEEE Transactions on Power Delivery*, vol. 3, no. 3, pp. 1217–1223, 1988.
- [10] M. E. Baran and F. F. Wu, “Network reconfiguration in distribution systems for loss reduction and load balancing,” *IEEE Transactions on Power delivery*, vol. 4, no. 2, pp. 1401–1407, 1989.
- [11] K. Nara, A. Shiose, M. Kitagawa, and T. Ishihara, “Implementation of genetic algorithm for distribution systems loss minimum re-configuration,” *IEEE Transactions on Power systems*, vol. 7, no. 3, pp. 1044–1051, 1992.
- [12] H.-C. Chang and C.-C. Kuo, “Network reconfiguration in distribution systems using simulated annealing,” *Electric Power Systems Research*, vol. 29, no. 3, pp. 227–238, 1994.
- [13] D. Otuo-Acheampong, G. I. Rashed, A. M. Akwasi, and H. Haider, “Application of optimal network reconfiguration for loss minimization and voltage profile enhancement of distribution system using heap-based optimizer,” *International Transactions on Electrical Energy Systems*, vol. 2023, no. 1, p. 9930954, 2023.
- [14] D. Anteneh, B. Khan, O. P. Mahela, H. H. Alhelou, and J. M. Guerrero, “Distribution network reliability enhancement and power loss reduction by optimal network reconfiguration,” *Computers & Electrical Engineering*, vol. 96, p. 107518, 2021.
- [15] Q. Peng, Y. Tang, and S. H. Low, “Feeder reconfiguration in distribution networks based on convex relaxation of opf,” *IEEE Transactions on Power Systems*, vol. 30, no. 4, pp. 1793–1804, 2014.
- [16] J. A. Taylor and F. S. Hover, “Convex models of distribution system reconfiguration,” *IEEE Transactions on Power Systems*, vol. 27, no. 3, pp. 1407–1413, 2012.

- [17] Y. Liu, J. Li, and L. Wu, "Coordinated optimal network reconfiguration and voltage regulator/der control for unbalanced distribution systems," *IEEE Transactions on Smart Grid*, vol. 10, no. 3, pp. 2912–2922, 2018.
- [18] A. Akrami, M. Doostizadeh, and F. Aminifar, "Optimal reconfiguration of distribution network using pmu measurements: a data-driven stochastic robust optimization," *IEEE Transactions on Smart Grid*, vol. 11, no. 1, pp. 420–428, 2019.
- [19] A. Azizivahed, A. Arefi, S. Ghavidel, M. Shafie-Khah, L. Li, J. Zhang, and J. P. Catalão, "Energy management strategy in dynamic distribution network reconfiguration considering renewable energy resources and storage," *IEEE Transactions on Sustainable Energy*, vol. 11, no. 2, pp. 662–673, 2019.
- [20] M. R. Dorostkar-Ghamsari, M. Fotuhi-Firuzabad, M. Lehtonen, and A. Safdar-ian, "Value of distribution network reconfiguration in presence of renewable energy resources," *IEEE Transactions on Power Systems*, vol. 31, no. 3, pp. 1879–1888, 2015.
- [21] X. Cao, J. Wang, J. Wang, and B. Zeng, "A risk-averse conic model for networked microgrids planning with reconfiguration and reorganizations," *IEEE Transactions on Smart Grid*, vol. 11, no. 1, pp. 696–709, 2019.
- [22] W. Zheng, W. Huang, D. J. Hill, and Y. Hou, "An adaptive distributionally robust model for three-phase distribution network reconfiguration," *IEEE Transactions on Smart Grid*, vol. 12, no. 2, pp. 1224–1237, 2020.
- [23] S. Huang, Q. Wu, L. Cheng, and Z. Liu, "Optimal reconfiguration-based dynamic tariff for congestion management and line loss reduction in distribution networks," *IEEE Transactions on Smart Grid*, vol. 7, no. 3, pp. 1295–1303, 2015.
- [24] M. Rahmani-Andebili and M. Fotuhi-Firuzabad, "An adaptive approach for pevs charging management and reconfiguration of electrical distribution system penetrated by renewables," *IEEE Transactions on Industrial Informatics*, vol. 14, no. 5, pp. 2001–2010, 2017.

- [25] A. Asrari, S. Lotfifard, and M. Ansari, "Reconfiguration of smart distribution systems with time varying loads using parallel computing," *IEEE Transactions on Smart Grid*, vol. 7, no. 6, pp. 2713–2723, 2016.
- [26] H. Wu, P. Dong, and M. Liu, "Distribution network reconfiguration for loss reduction and voltage stability with random fuzzy uncertainties of renewable energy generation and load," *IEEE Transactions on Industrial Informatics*, vol. 16, no. 9, pp. 5655–5666, 2018.
- [27] A. Kavousi-Fard, T. Niknam, and M. Fotuhi-Firuzabad, "A novel stochastic framework based on cloud theory and bat algorithm to solve the distribution feeder reconfiguration," *IEEE Transactions on Smart Grid*, vol. 7, no. 2, pp. 740–750, 2015.
- [28] P. Harsh and D. Das, "A simple and fast heuristic approach for the reconfiguration of radial distribution networks," *IEEE Transactions on Power Systems*, vol. 38, no. 3, pp. 2939–2942, 2023.
- [29] M. Naguib, W. A. Omran, and H. E. Talaat, "Performance enhancement of distribution systems via distribution network reconfiguration and distributed generator allocation considering uncertain environment," *Journal of Modern Power Systems and Clean Energy*, vol. 10, no. 3, pp. 647–655, 2021.
- [30] M. Amini, A. Jalilian, and M. R. P. Behbahani, "Fast network reconfiguration in harmonic polluted distribution network based on developed backward/forward sweep harmonic load flow," *Electric Power Systems Research*, vol. 168, pp. 295–304, 2019.
- [31] M. Rahimipour Behbahani and A. Jalilian, "Reconfiguration of harmonic polluted distribution network using modified discrete particle swarm optimization equipped with smart radial method," *IET Generation, Transmission & Distribution*, vol. 17, no. 11, pp. 2563–2575, 2023.
- [32] M. Rahimi Pour Behbahani, A. Jalilian, and M. Amini, "Reconfiguration of distribution network using discrete particle swarm optimization to reduce voltage fluctuations," *International Transactions on Electrical Energy Systems*, vol. 30, no. 9, p. e12501, 2020.

- [33] S. R. Salkuti, “Feeder reconfiguration in unbalanced distribution system with wind and solar generation using ant lion optimization,” *International Journal of Advanced Computer Science and Applications*, vol. 12, no. 3, 2021.
- [34] C. Gerez, E. Coelho Marques Costa, and A. J. Sguarezi Filho, “Distribution network reconfiguration considering voltage and current unbalance indexes and variable demand solved through a selective bio-inspired metaheuristic,” *Energies*, vol. 15, no. 5, p. 1686, 2022.
- [35] H. Lotfi and A. A. Shojaei, “A dynamic model for multi-objective feeder reconfiguration in distribution network considering demand response program,” *Energy Systems*, vol. 14, no. 4, pp. 1051–1080, 2023.
- [36] S. Essallah and A. Khedher, “Optimization of distribution system operation by network reconfiguration and dg integration using mpso algorithm,” *Renewable Energy Focus*, vol. 34, pp. 37–46, 2020.
- [37] M. Amin Heidari, “Optimal network reconfiguration in distribution system for loss reduction and voltage-profile improvement using hybrid algorithm of pso and aco,” *CIREN 24*, vol. 2017, no. 1, pp. 2458–2461, 2017.
- [38] O. Kahouli, H. Alsaif, Y. Bouteraa, N. Ben Ali, and M. Chaabene, “Power system reconfiguration in distribution network for improving reliability using genetic algorithm and particle swarm optimization,” *Applied Sciences*, vol. 11, no. 7, p. 3092, 2021.
- [39] W. M. Dahalan and H. Mokhlis, “Network reconfiguration for loss reduction with distributed generations using pso,” in *2012 IEEE international conference on power and energy (PECon)*, pp. 823–828, IEEE, 2012.
- [40] Y. Merzoug, B. Abdelkrim, and B. Larbi, “Distribution network reconfiguration for loss reduction using pso method,” *International Journal of Electrical and Computer Engineering*, vol. 10, no. 5, p. 5009, 2020.
- [41] R. S. Rao, K. Ravindra, K. Satish, and S. Narasimham, “Power loss minimization in distribution system using network reconfiguration in the presence of distributed generation,” *IEEE transactions on power systems*, vol. 28, no. 1, pp. 317–325, 2012.

- [42] M. Khajevand, A. Fakharian, and M. Sedighzadeh, "Stochastic joint optimal distributed generation scheduling and distribution feeder reconfiguration of microgrids considering uncertainties modeled by copula-based method," *Iranian Journal of Electrical and Electronic Engineering*, vol. 16, no. 3, pp. 371–392, 2020.
- [43] R. Khorram-Nia, B. Bahmani-Firouzi, and M. Simab, "Optimal scheduling of reconfigurable microgrids incorporating the pevs and uncertainty effects," *IET Renewable Power Generation*, vol. 16, no. 16, pp. 3531–3543, 2022.
- [44] S. Esmaeili, A. Anvari-Moghaddam, S. Jadid, and J. M. Guerrero, "Optimal simultaneous day-ahead scheduling and hourly reconfiguration of distribution systems considering responsive loads," *International Journal of Electrical Power & Energy Systems*, vol. 104, pp. 537–548, 2019.
- [45] Z. Li, S. Jazebi, and F. De Leon, "Determination of the optimal switching frequency for distribution system reconfiguration," *IEEE Transactions on Power Delivery*, vol. 32, no. 4, pp. 2060–2069, 2016.
- [46] I. M. Diaaeldin, S. H. Abdel Aleem, A. El-Rafei, A. Y. Abdelaziz, and A. F. Zobaa, "Enhancement of hosting capacity with soft open points and distribution system reconfiguration: Multi-objective bilevel stochastic optimization," *Energies*, vol. 13, no. 20, p. 5446, 2020.
- [47] A. S. Abbas, A. A. Abou El-Ela, and R. A. El-Sehiemy, "Maximization approach of hosting capacity based on uncertain renewable energy resources using network reconfiguration and soft open points," *International Transactions on Electrical Energy Systems*, vol. 2022, no. 1, p. 2947965, 2022.
- [48] R. Čađenović and D. Jakus, "Maximization of distribution network hosting capacity through optimal grid reconfiguration and distributed generation capacity allocation/control," *Energies*, vol. 13, no. 20, p. 5315, 2020.
- [49] N. N. Cikan and M. Cikan, "Reconfiguration of 123-bus unbalanced power distribution network analysis by considering minimization of current & voltage unbalanced indexes and power loss," *International Journal of Electrical Power & Energy Systems*, vol. 157, p. 109796, 2024.

- [50] P. Gangwar, S. Singh, and S. Chakrabarti, "Network reconfiguration for unbalanced distribution systems," in *TENCON 2017-2017 IEEE Region 10 Conference*, pp. 3028–3032, IEEE, 2017.
- [51] A. T. Hachemi, F. Sadaoui, A. Saim, M. Ebeed, and S. Arif, "Dynamic operation of distribution grids with the integration of photovoltaic systems and distribution static compensators considering network reconfiguration," *Energy Reports*, vol. 12, pp. 1623–1637, 2024.
- [52] S. Yang, B. Vaagensmith, and D. Patra, "Power grid contingency analysis with machine learning: A brief survey and prospects," *2020 Resilience Week (RWS)*, pp. 119–125, 2020.
- [53] B. Liu and J. H. Braslavsky, "Robust dynamic operating envelopes for der integration in unbalanced distribution networks," *IEEE Transactions on Power Systems*, 2023.
- [54] A. Kumar, Y. Deng, X. He, A. R. Singh, P. Kumar, R. C. Bansal, M. Bettayeb, C. Ghenai, and R. Naidoo, "Impact of demand side management approaches for the enhancement of voltage stability loadability and customer satisfaction index," *Applied Energy*, vol. 339, p. 120949, 2023.
- [55] W. Fadel, "A review of distributed generation optimization with shunt capacitors in reconfigured distribution networks," *Wireless Personal Communications*, pp. 1–33, 2024.
- [56] H. Soleimani, D. Habibi, M. Ghahramani, and A. Aziz, "Strengthening power systems for net zero: A review of the role of synchronous condensers and emerging challenges," *Energies*, vol. 17, no. 13, p. 3291, 2024.
- [57] A. A. Abou El-Ela, R. A. El-Sehiemy, A. M. Shaheen, and I. A. Eissa, "Optimal coordination of static var compensators, fixed capacitors, and distributed energy resources in egyptian distribution networks," *International Transactions on Electrical Energy Systems*, vol. 30, no. 11, p. e12609, 2020.
- [58] P. Yuan, Q. Zhang, T. Zhang, C. Chi, X. Zhang, P. Li, and X. Gong, "Analysis and enlightenment of the blackouts in argentina and new york," in *2019 Chinese Automation Congress (CAC)*, pp. 5879–5884, IEEE, 2019.

- [59] N. M. Flores, H. McBrien, V. Do, M. V. Kiang, J. Schlegelmilch, and J. A. Casey, “The 2021 texas power crisis: distribution, duration, and disparities,” *Journal of exposure science & environmental epidemiology*, vol. 33, no. 1, pp. 21–31, 2023.
- [60] M. Gaeta, C. Nsangwe Businge, and A. Gelmini, “Achieving net zero emissions in italy by 2050: challenges and opportunities,” *Energies*, vol. 15, no. 1, p. 46, 2021.
- [61] H. L. Willis, *Power distribution planning reference book*. CRC press, 1997.
- [62] Siemens, “Smart grid electric power utilities - distribution automation.” <https://www.siemens.com/global/en/products/automation/industrial-communication/smart-grid-electric-power-utilities/distribution-automation>. [Online].
- [63] S. E. Company, “Scada-mate switching systems.” <https://www.sandc.com/en/products--services/products/scada-mate-switching-systems>. [Online].
- [64] S. Electric, “Remote control and monitoring.” <https://www.se.com/ca/en/product-subcategory/1950-remote-control-and-monitoring>. [Online].
- [65] H. P. Systems, “Advanced distribution automation.” <https://www.hubbell.com/hubbellpowersystems/en/solutions/advanced-distribution-automation>. [Online].
- [66] G. Electric, “Distribution reclosers and overhead switches.” <https://www.gwelectric.com/products/distribution-reclosers-and-overhead-switches>. [Online].
- [67] S. source, “Distribution reclosers and overhead switches.” <https://www.switchedsources.com/tie-controller>. [Online].
- [68] I. Aravena, D. K. Molzahn, S. Zhang, C. G. Petra, F. E. Curtis, S. Tu, A. Wächter, E. Wei, E. Wong, A. Gholami, *et al.*, “Recent developments in security-constrained ac optimal power flow: Overview of challenge 1 in the

- arpa-e grid optimization competition,” *Operations research*, vol. 71, no. 6, pp. 1997–2014, 2023.
- [69] M. Bayat, M. M. Koushki, A. A. Ghadimi, M. Tostado-Véliz, and F. Jurado, “Comprehensive enhanced newton raphson approach for power flow analysis in droop-controlled islanded ac microgrids,” *International Journal of Electrical Power & Energy Systems*, vol. 143, p. 108493, 2022.
- [70] A. Nur and A. Kaygusuz, “Load flow analysis with newton–raphson and gauss–seidel methods in a hybrid ac/dc system,” *IEEE Canadian Journal of Electrical and Computer Engineering*, vol. 44, no. 4, pp. 529–536, 2021.
- [71] A. K. Roy and S. K. Jain, “Improved transmission line contingency analysis in power system using fast decoupled load flow,” *International Journal of Advances in Engineering & Technology*, vol. 6, no. 5, p. 2159, 2013.
- [72] S. Park, W. Chen, T. W. Mak, and P. Van Hentenryck, “Compact optimization learning for ac optimal power flow,” *IEEE Transactions on Power Systems*, 2023.
- [73] M. Usman and F. Capitanescu, “Three solution approaches to stochastic multi-period ac optimal power flow in active distribution systems,” *IEEE Transactions on Sustainable Energy*, vol. 14, no. 1, pp. 178–192, 2022.

APPENDICES

A Branch Index for Case 1

Table A.1: Branch indexing table for Case 1

Branch Index	From Bus	To Bus	Branch Index	From Bus	To Bus	Branch Index	From Bus	To Bus
1	1	2	14	14	15	27	27	28
2	2	3	15	15	16	28	28	29
3	3	4	16	16	17	29	29	30
4	4	5	17	17	18	30	30	31
5	5	6	18	2	19	31	31	32
6	6	7	19	19	20	32	32	33
7	7	8	20	20	21	33	21	8
8	8	9	21	21	22	34	9	15
9	9	10	22	3	23	35	12	22
10	10	11	23	23	24	36	18	33
11	11	12	24	24	25	37	25	29
12	12	13	25	6	26			
13	13	14	26	26	27			

B Branch Index for Case 2

Table B.1: Branch indexing table for Case 2

Branch Index	From Bus	To Bus	Branch Index	From Bus	To Bus	Branch Index	From Bus	To Bus	Branch Index	From Bus	To Bus
1	1	2	41	42	43	81	81	82	121	151	300
2	1	3	42	42	44	82	82	83	122	300	108
3	1	7	43	44	45	83	83	84	123	100	450
4	3	4	44	45	46	84	84	85	124	30	250
5	3	5	45	46	47	85	86	87	125	250	251
6	5	6	46	47	48	86	87	88	126	450	451
7	7	8	47	47	49	87	87	89	127	54	94
8	8	12	48	49	50	88	89	90			
9	8	9	49	50	51	89	89	91			
10	8	13	50	52	53	90	91	92			
11	9	14	51	53	54	91	91	93			
12	13	34	52	54	55	92	93	94			
13	13	18	53	54	57	93	93	95			
14	14	11	54	55	56	94	97	98			
15	14	10	55	57	58	95	98	99			
16	15	16	56	57	60	96	99	100			
17	15	17	57	58	59	97	101	102			
18	18	19	58	59	60	98	101	105			
19	18	21	59	60	61	99	102	103			
20	19	20	60	62	63	100	103	104			
21	21	22	61	63	64	101	105	106			
22	21	23	62	64	65	102	105	108			
23	23	24	63	65	66	103	106	107			
24	23	25	64	67	68	104	108	109			
25	25	26	65	67	97	105	109	110			
26	25	28	66	68	69	106	110	111			
27	26	27	67	69	70	107	110	112			
28	26	31	68	70	71	108	112	113			
29	27	33	69	71	72	109	113	114			
30	28	29	70	72	73	110	18	135			
31	29	30	71	72	76	111	135	35			
32	31	32	72	73	74	112	150	149			
33	34	15	73	74	75	113	149	1			
34	35	36	74	75	76	114	13	152			
35	35	40	75	76	86	115	152	52			
36	36	37	76	77	78	116	60	160			
37	36	38	77	78	79	117	160	67			
38	38	39	78	78	80	118	97	197			
39	40	41	79	80	81	119	197	101			
40	40	42	80	81	82	120	51	151			